NOAA Contract Report NMFS-NWFSC-CR-2023-02

https://doi.org/10.25923/v2mt-nj66

Habitat Assessment and Restoration Planning (HARP) Model for the Snohomish and Stillaguamish River Basins

Contracts **Snohomish County ILA-NOAA-001** and **Tulalip Tribes TT-2021-0001**

February 2023

U.S. DEPARTMENT OF COMMERCE

National Oceanic and Atmospheric Administration
National Marine Fisheries Service
Northwest Fisheries Science Center

NOAA Contract Report Series NMFS-NWFSC-CR

Recommended citation:

(Beechie et al. 2023)[1]

[1] Beechie, T. J., A. Goodman, O. Stefankiv, B. Timpane-Padgham, and M. Lowe. 2023. Habitat Assessment and Restoration Planning (HARP) Model for the Snohomish and Stillaguamish River Basins. U.S. Department of Commerce, NOAA Contract Report NMFS-NWFSC-CR-2023-02.

https://doi.org/10.25923/v2mt-nj66

NOAA FISHERIES

Habitat Assessment and Restoration Planning (HARP) Model for the Snohomish and Stillaguamish River Basins

Timothy J. Beechie,[1] Arianna Goodman,[1] Oleksandr Stefankiv,[1] Britta Timpane-Padgham,[1] and Michaela Lowe[2]

https://doi.org/10.25923/v2mt-nj66

February 2023

[1]Fish Ecology Division
Northwest Fisheries Science Center
2725 Montlake Boulevard East
Seattle, Washington 98112

[2]Washington Department of Fish and Wildlife
1111 Washington Street Southeast
Olympia, Washington 98501

U.S. DEPARTMENT OF COMMERCE

National Oceanic and Atmospheric Administration
National Marine Fisheries Service
Northwest Fisheries Science Center

Table of Contents

Acknowledgments

The HARP Model implementation in the Snohomish and Stillaguamish River basins relied on the Life-cycle Model Workgroup, including Steve Hinton (Tulalip Tribes), Frank Leonetti (Snohomish County), Josh Kubo (King County), and Neala Kendall (Washington Department of Fish and Wildlife). We were also assisted by local scientists and stakeholders who provided data or recommendations on model options (Mike Crewson, Jason Griffith, Diego Holmgren, Kate Konoski, Erin Lowery, Kurt Nelson, and Peter Verhey). Jeff Jorgensen, Peter Kiffney, and Aimee Fullerton of NOAA Northwest Fisheries Science Center also assisted with the life-cycle modeling and spatial analyses.

Chinook salmon juvenile density data were provided by King County's Science and Technical Support Section, Ecological Restoration and Engineering Services Unit, and the River and Floodplain Management Section (referred to as "King County, unpublished data" in the report). Chinook salmon density data were also provided by Erin Lowery, Seattle City Light (referred to as "E. Lowery, unpublished data" in the report).

This work was supported by Snohomish County under agreement #ILA-NOAA-001, and by The Tulalip Tribes under agreement #TT-2021-0001.

This project has been funded wholly or in part by the United States Environmental Protection Agency under assistance agreement PC-01J22301 through the Washington Department of Fish and Wildlife. The contents of this document do not necessarily reflect the views and policies of the Environmental Protection Agency or the Washington Department of Fish and Wildlife, nor does mention of trade names or commercial products constitute endorsement or recommendation for use.

Executive Summary

We applied the Habitat Assessment and Restoration Planning (HARP) Model in the Stillaguamish and Snohomish River basins to help guide habitat restoration planning. The habitat and salmon population assessments are based on a process-based conceptual model that links landscape processes to habitat conditions, and then habitat conditions to salmon populations (Figure ES-1). The analysis evaluates how habitat-forming processes, habitats and salmon populations have changed from historical to current conditions.

The main objectives of this project were to:

1. Assess current habitat conditions and parameterize the life-cycle models for current habitat conditions,

2. Estimate historical habitat conditions, and

3. Construct diagnostic scenarios that evaluate the restoration potential for each restoration action type individually.

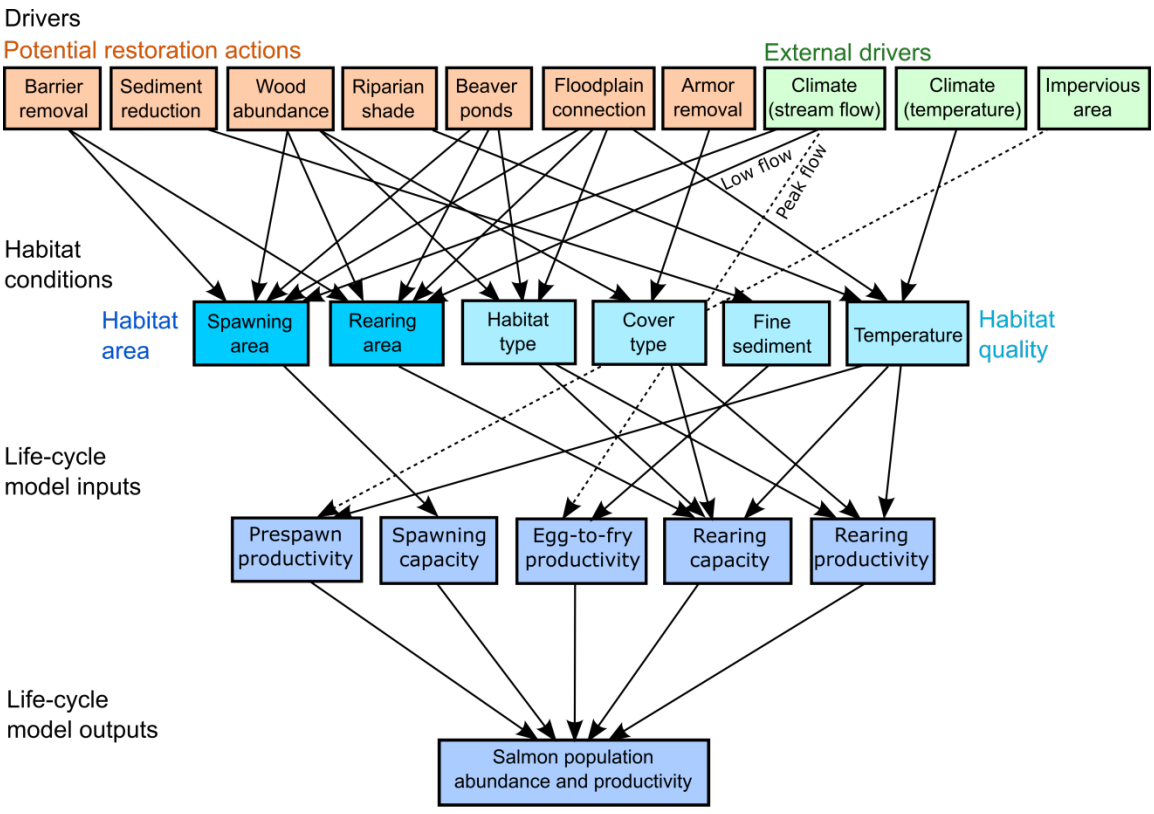

Figure ES-1. Schematic diagram of process linkages represented in the Habitat Assessment and Restoration Planning (HARP) Model.

Each diagnostic scenario helps managers understand the potential effect of each restoration action type modeled, which can inform setting restoration priorities in each river basin.

The model analysis sequence includes a spatial analysis, a habitat analysis, and the life-cycle models. The spatial analyses use raw geospatial data layers to produce a set of habitat data layers that become the inputs to the habitat analysis. The habitat analysis uses the habitat data layers and other information to produce estimates of historical and current habitat conditions for each reach in the basin, which are then used to produce the diagnostic habitat scenarios. Finally, the life-cycle models run each diagnostic scenario to identify habitat restoration actions that are most likely to increase spawner abundance for each modeled species (coho salmon, summer- and fall-run Chinook salmon, and winter- and summer-run steelhead).

Habitat Change Results

Estimated loss of floodplain habitats and beaver ponds were very high in both basins. In the Stillaguamish basin, there has been a 90 to 95% decrease in beaver ponds, a 59% decrease in side channel length, and an ~80% decrease in floodplain marshes and ponds (Table ES-1). In the Snohomish basin, there has been a 90 to 95% decrease in beaver ponds, a 63% decrease in side channel length, and an ~80% decrease in floodplain marshes and ponds. Estuary habitat losses are also large in both basins, with estimated decreases in rearing habitat area of 44% in the Stillaguamish basin and 90% in the Snohomish basin.

Migration barrier effects vary among species because their spawning ranges differ. Only 1% of Chinook salmon habitat length and 3% of summer-run steelhead habitat length is above full or partial barriers in the Stillaguamish basin, and 9% and 7% of Chinook and summer steelhead habitat length, respectively, is above full or partial barriers in the Snohomish basin. By contrast, 20% and 22% of coho salmon habitat length and 10% and 13% of winter-run steelhead habitat length is above full or partial barriers in the Stillaguamish and Snohomish River basins, respectively

Shade levels have decreased significantly in agricultural and developed areas, resulting in significant increases in modeled stream temperature. According to the model, stream temperatures have increased more than 2°C in 23% of reaches in the Stillaguamish River basin and 28% of reaches in the Snohomish River basin. Substantial wood loss is assumed to be ubiquitous in both basins, and one indicator of the effect of wood loss is the estimated decrease in spawning and rearing capacity.

Impervious surfaces and roads produce a modeled increase in coho salmon prespawn mortality >20% in small streams in or near urban areas such as Arlington, Marysville, and Lake Stevens. Most other locations have predicted coho salmon prespawn mortality much lower than 20%. Bank armor is documented only in the large rivers (>20m bankfull width), with 9% of bank length armored in the Stillaguamish basin and 13% of bank length armored in the Snohomish basin.

Table ES-1. Summary of estimated habitat changes in the Stillaguamish and Snohomish River basins.

Habitat type	Habitat Change	
	Stillaguamish	**Snohomish**
Beaver ponds	Decrease of 90-95%	Decrease of 90-95%
Side channels	Decrease of 59%	Decrease of 63%
Floodplain marshes, ponds	Decrease of ~80%	Decrease of ~80%
Estuary rearing habitat area	Decrease of 44%	Decrease of 90%
Percent of habitat length above migration barriers	Coho: 20% Chinook: 1% Winter Steelhead: 10% Summer Steelhead: 3%	Coho: 22% Chinook: 9% Winter Steelhead: 13% Summer Steelhead: 7%
Shade and Temperature	Temperature increase >2°C in 23% of reaches	Temperature increase >2°C in 28% of reaches
In-stream wood	Wood abundance reduced basin-wide, reducing spawning and rearing capacities for all species	Wood abundance reduced basin-wide, reducing spawning and rearing capacities for all species
Bank armor	9% of bank habitat armored	13% of bank habitat armored
Impervious surface and roads	Predicted coho prespawn mortality >20% in small streams near Arlington	Predicted coho prespawn mortality >20% in small streams near Marysville and Lake Stevens
Fine sediment	Modest increase in fine sediment levels in small streams in developed or agricultural lands	Modest increase in fine sediment levels in small streams in developed or agricultural lands

Life-cycle Model Results

We quantified restoration potential as the modeled percent change in spawner abundance when a habitat attribute was changed from its current condition to natural potential (historical) condition, and each habitat attribute was modeled as a separate diagnostic scenario so that we could compare restoration potentials across restoration action types.

The diagnostic scenarios suggest that restoration actions to improve coho salmon populations should focus on restoration of beaver pond and floodplain habitats in both River basins (Figure ES-2), which have predicted restoration potentials of +43 to +87% in both basins. Restoring wood abundance has a relatively smaller predicted effect (+25% and +30% in the Stillaguamish and Snohomish basins, respectively), and removing migration barriers is relatively minor (+13% and +14%, respectively). Restoration potentials for the remaining restoration actions are less than +7%.

Summer- and fall-run Chinook salmon are much less responsive to restoration actions in the model. Restoration potentials are highest for wood augmentation, bank armor removal, and floodplain reconnection in both basins (restoration potentials of +13% or more). Other freshwater restoration actions will likely produce a smaller response than those three action types. However, estuary restoration could increase number of spawners by 45% in the Snohomish basin and 4% in Stillaguamish basin. Estuary restoration potential is smaller in the Stillaguamish basin than the Snohomish basin due to the relatively low numbers of fry-sized Chinook juveniles currently reaching the Stillaguamish delta.

Steelhead will likely be most responsive to wood augmentation in both basins, although shade restoration and floodplain reconnection also benefit steelhead. All other action types produced a very small (≤+3%) modeled restoration potential for steelhead.

The sensitivity analysis results generally support the diagnostic scenario results. For coho salmon, winter rearing capacity is the most sensitive parameter, and winter rearing capacity is most increased by restoration of slow water habitats (beaver ponds and floodplain marshes and ponds). For Chinook salmon, estuary rearing and subyearling rearing are sensitive parameters, and those parameters are most increased by restoration actions to increase rearing habitat in large rivers and the estuary. Steelhead are most sensitive to the summer and winter rearing productivity parameters, which are most influenced by wood augmentation, floodplain reconnection, and increasing shade levels.

Perhaps the most important uncertainty in the model is the productivity parameter for the estuary Beverton-Holt function for Chinook fry, which has a significant effect on the modeled response of Chinook populations to estuary restoration. There are very few data on Chinook fry survival in deltas to constrain this parameter estimate, so we conducted a simple sensitivity analysis evaluate how much the productivity parameter changes the modeled response in spawner abundance. We found that at a low productivity value of 0.10, the model predicts a minimal response of Chinook to restoring the full delta (~5% increase in spawner abundance in the Snohomish delta), but at high productivity value of 0.50, the model predicts a very large response (~80% increase in spawner abundance in the Snohomish delta). However, at all productivity values in both basins, the response increases as more Chinook fry enter the delta, suggesting that the response of the Chinook population to estuary restoration will increase as freshwater restoration produces more fry migrants.

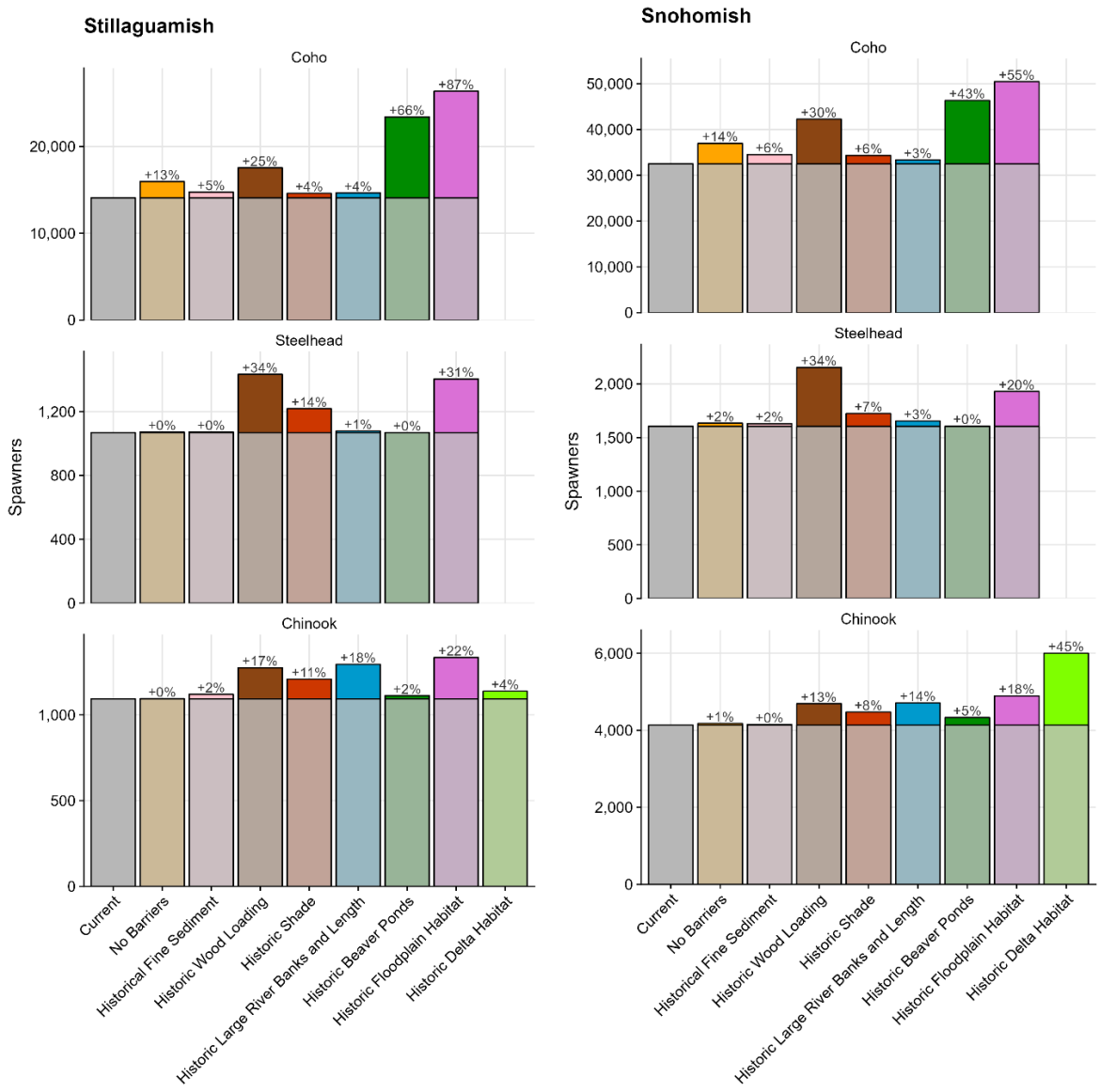

Figure ES-2. Spawner abundances for each basin and species under each diagnostic scenario. Steelhead is the total of summer and winter steelhead combined.

1. Introduction

The Habitat Assessment and Restoration Planning (HARP) Model was developed in the Chehalis River basin to assess habitat changes from historical potential to current conditions, use salmon life-cycle models to compare restoration alternatives (diagnostic scenarios), and model alternative future restoration scenarios including climate change (Jorgensen et al. 2021, Beechie et al. 2021a, 2023, Nicol et al. 2022, Fogel et al. 2022). In this project we apply this modeling approach to the Stillaguamish and Snohomish River basins, with the goal of modeling the diagnostic scenarios using available datasets. We model potential effects of eight restoration action types for coho salmon, Chinook salmon, and steelhead.

1.1 Project Objectives

The main objectives of this habitat assessment and life-cycle modeling effort are to

4. Assess current habitat conditions and parameterize the life-cycle models for current habitat conditions,

5. Estimate historical habitat conditions, and

6. Run diagnostic scenarios that evaluate the restoration potential for each restoration action type individually.

Each diagnostic scenario helps managers understand the potential effect of each restoration action type modeled, which can inform setting restoration priorities in each river basin. While the HARP Model has the capability of modeling future climate and restoration scenarios, modeling alternative futures was outside the scope of this project.

1.2 Overview of Modeling Process

To implement the HARP Model in the Stillaguamish and Snohomish River basins, we first assembled and processed the geospatial data sets necessary for the habitat assessment. The project scope did not include collection of new habitat data (historical or current), although in some cases we were able to develop new data sets for this effort (e.g., we digitized large river edge habitats and created canopy-opening angle data). Once we had all of the geospatial data sets in order, we calculated current and historical habitat conditions for each 200-m segment in the stream network used by Chinook, steelhead, or coho, and translated habitat conditions into the life-stage capacities and productivities for the life-cycle models. Finally, we tuned each life-cycle model to local biological data (e.g., adjusted maturation rates to produce an age structure consistent with the local populations), and ran the diagnostic scenarios in the life-cycle models to produce final results.

Throughout the modeling effort, we were advised by the HARP Work Group, which was composed of Steve Hinton, Kurt Nelson, and Diego Holmgren (Tulalip Tribes), Frank Leonetti (Snohomish County), Neala Kendall (Washington Department of Fish and

Wildlife), and Josh Kubo (King County). The Work Group reviewed many of the modeling decisions made (e.g., which fine sediment model to use), as well as which input data sets were most appropriate (e.g., which stream network to use). The Work Group also assisted in acquiring necessary data sets from their agencies or other state and local entities.

2. The Habitat Assessment and Restoration Planning (HARP) Model

In the HARP Model, the habitat and salmon population assessments are based on a process-based conceptual model that links landscape processes to habitat conditions, and then habitat conditions to salmon populations (Figure 2-1). The analysis itself evaluates how habitat-forming processes, habitats and salmon populations have changed from historical to current conditions, and how habitat restoration may influence salmon populations in the future. The key question we address in this project with the HARP approach is "Which habitat restoration actions have the greatest potential to benefit salmon populations under current climate conditions?"

Habitat data underlying the life-cycle models are at the resolution of 200-m reaches, and all habitat attributes (e.g., pool area, spawning gravel area, stream temperature) are assigned to each reach within the spawning and rearing ranges of coho salmon, Chinook salmon, winter-run steelhead, and summer run steelhead. Spawning and rearing ranges used in the model were reviewed by local biologists and all suggested edits incorporated into the final distributions (Appendix A). The life-cycle models are run at the subbasin scale, with each subbasin modeled as a separate subpopulation. Subbasin delineations are also shown in Appendix A.

In practical terms, the model analysis sequence includes a spatial analysis, a habitat analysis, and the life-cycle models (Figure 2-2). The spatial analyses include geospatial analyses that import raw data layers and produce a set of habitat data layers that become the inputs to the habitat analysis. The habitat analysis uses the habitat data layers and other information to produce historical and current habitat conditions for each reach in the basin, which are then used to produce the life-cycle model input parameters for the diagnostic habitat scenarios. (Future climate change and restoration scenarios can also be created in the habitat analysis.) Finally, the life-cycle models run each diagnostic scenario to identify habitat restoration actions that are most likely to increase spawner abundance for each modeled species (for these projects: coho salmon, summer- and fall-run Chinook salmon, and summer- and winter-run steelhead). Details of the model concept and structure are contained in two publications describing the HARP Model for the Chehalis basin (Jorgensen et al. 2021, Beechie et al. 2021a), as well as in the Chehalis Phase 1 contract report (Beechie et al. 2021b).

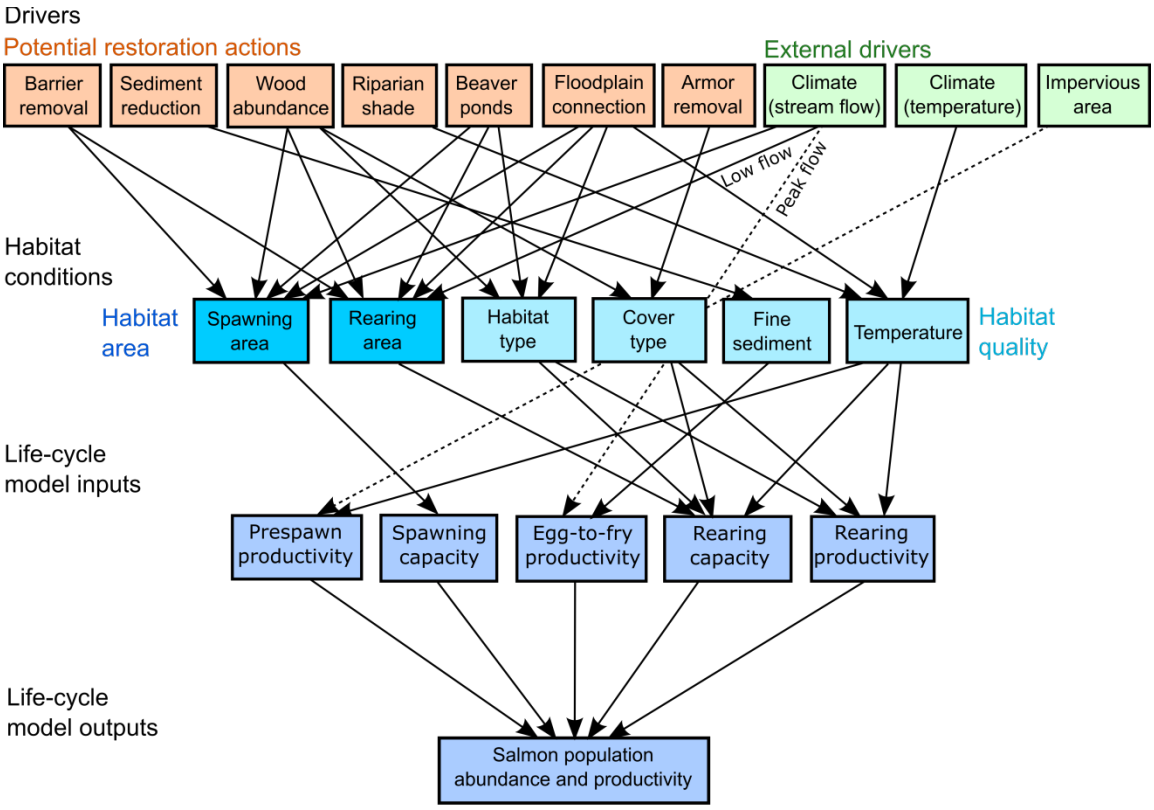

Figure 2-1. Schematic diagram of process linkages represented in the Habitat Assessment and Restoration Planning (HARP) Model.

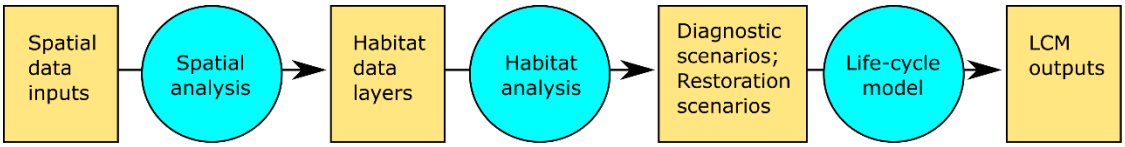

Raw data layers:
USGS 10-m DEM
C-CAP land cover raster
PRISM mean annual precip
Washington roads
Hydrography (1:24k)
WDFW Migration barriers
Local temperature data
Riparian data
Floodplain habitat polygons
Large river edge habitat
Large river backwaters
Spawning riffles

Final habitat layers:
Large river edge habitat
Large river backwaters
Large river spawning riffles
Floodplain habitats
Attributed streamline

Diagnostic scenarios:
Migration barriers
Fine sediment
Wood loading
Shade (temperature)
Bank armor/ straightening
Beaver ponds
Floodplain habitats
Estuary habitats

Restoration scenarios:
Restoration actions
Climate change effects
Future development

LCM results
-Coho
-Chinook
-Winter steelhead
-Summer steelhead

Figure 2-2. Illustration of the analysis steps, proceeding from the raw data layers, to habitat data layers, to habitat scenarios, and finally to the life-cycle model (LCM) outputs. C-CAP is NOAA's Coastal Change Analysis Program.

2.1 Habitat Change Analyses

In the HARP Model, the habitat change analysis that produces input files for the life-cycle models includes the spatial analysis and the habitat analysis (Figure 2-2). The spatial analysis calculates changes in habitat areas and qualities from historical conditions to current conditions for those attributes that have geospatial data for both historical and current conditions (e.g., floodplain habitat). The habitat analysis uses the spatial analysis outputs and other data to estimate historical and current life-stage capacities and productivities for each reach, species, and diagnostic scenario (summarized in Section 2.1.1). The final step of the habitat analysis is to aggregate all habitat changes to the subbasin level and produce estimates of life-stage capacities and productivities for each subbasin, species, and scenario (Section 2.1.2).

2.1.1 Stream Reaches and Geomorphic Attributes

The primary geospatial data sources for the Stillaguamish and Snohomish basin are listed in Tables 2-1 and 2-2. In the Stillaguamish River basin the HARP Work Group recommended using the Washington Department of Natural Resources (DNR) hydrography layer, and in the Snohomish River basin they recommended using the National Hydrography Dataset (NHD). We first segmented each stream network into 200-m reaches, and calculated geomorphic attributes for each reach. Drainage area upstream of each reach was calculated using flow accumulation with the 10-m National Elevation Dataset (NED). Mean annual precipitation upstream of each reach was then calculated using a weighted flow accumulation of the mean annual precipitation grid. Channel slope was calculated for each reach based on reach length and the difference between upstream and downstream elevations, with elevations being the lowest elevation within a 30-m radius of each endpoint to correct for misalignment between the stream line and the NED (Beechie and Imaki 2014). Subbasin designations and species presence were also assigned to each reach.

To model bankfull width and wetted width in the study basins, we utilized methods from Davies et al. (2007) based on drainage area (km^2) and mean annual precipitation (cm/yr) upstream of each reach. We used width measurements from aerial imagery collected during low flow conditions to create the predictions. In the Stillaguamish River basin, the R^2 values for bankfull and wetted width models were 0.79 and 0.78, respectively. While in the Snohomish River basin, bankfull and wetted width model R^2 values were 0.69 and 0.65, respectively.

In both basins, reaches were then designated as large river (≥20 m bankfull width) and small stream (<20m bankfull width). Large rivers and small streams have different habitat typing systems to account for the fact that preferred rearing depths and velocities are distributed differently in each (Table 2-3) (Bisson et al. 1988, Beechie et al. 2005). We also calculated the confinement ratio for each reach (floodplain width/bankfull width), and classified confined channels as those with ratio <4. Reaches that were unconfined or included within non-canyon floodplains were given the mixed species reference condition for the riparian analysis, and other reaches were given the conifer reference tree height.

Table 2-1. Input data layers for the spatial analysis in the Stillaguamish basin.

Input data layer	Source
National Elevation Dataset (NED)	United States Geological Survey (USGS) (https://lta.cr.usgs.gov/NED) (10-m resolution)
Lidar	Washington Department of Natural Resources (WDNR) (https://lidarportal.dnr.wa.gov/)
Hydrography	Washington Department of Natural Resources (from Snohomish County, includes modifications to the original WDNR layer).
Land cover raster	National Oceanic and Atmospheric Administration (NOAA) Coastal Change Analysis Program (C-CAP) land cover (https://coast.noaa.gov/digitalcoast/data/)
Land use raster	Washington State Land Use 2010 (https://ecology.wa.gov/Research-Data/Data-resources/Geographic-Information-Systems-GIS/Data#l)
Mean annual precipitation	PRISM (Oregon State University) (http://www.prism.oregonstate.edu/)
Unpaved roads	Washington Department of Natural Resources (http://geo.wa.gov/)
Subbasin boundaries	Endangered Species Act (ESA) subbasin boundaries acquired from Snohomish County, combined with floodplain reaches from NOAA (https://www.fisheries.noaa.gov/resource/map/salmon-habitat-status-and-trend-monitoring-program-data)
Spawning and rearing distributions for each species	Washington Conservation Commission Salmon Habitat Limiting Factors Analysis (LFA) reports, and updated by project partners (https://snohomishcountywa.gov/Archive/ViewFile/Item/2137)
Migration barriers	From WDFW barrier database, accessed 08/03/2021 (https://geodataservices.wdfw.wa.gov/hp/fishpassage/index.html)
Stream temperature	NorWeST (https://www.fs.fed.us/rm/boise/AWAE/projects/NorWeST.html)
Floodplain habitats	Hand mapped historical marshes and ponds from General Land Office surveys (Collins and Sheikh 2003) and National Hydrography Dataset waterbodies (https://www.usgs.gov/core-science-systems/ngp/national-hydrography/nhdplus-high-resolution). Field survey records from Snohomish County. Feature location within the floodplain based on the Puget Sound Ecosystem and Monitoring Floodplain Condition Assessment Level 2 dataset (https://wa-psp.maps.arcgis.com/apps/webappviewer/index.html?id=2f6f09bbb59f4b0b81d01440cb250bc0)
NOAA riparian condition dataset	Tree height and canopy opening angles from 2010-2019 lidar (historical, current)
NOAA large river edge habitats	Hand mapped from 2019 National Agriculture Imagery Program aerial imagery and 2004-2017 bank armor data from Snohomish County
NOAA large river backwaters	Hand mapped from 2019 National Agriculture Imagery Program aerial imagery
NOAA large river spawning riffles	Hand mapped from 2019 National Agriculture Imagery Program aerial imagery

Table 2-2. Input data layers for the spatial analysis in the Snohomish basin.

Input data layer	Source
National Elevation Dataset (NED)	United States Geological Survey (USGS), 10-m resolution (https://lta.cr.usgs.gov/NED)
Hydrography	National Hydrography Dataset High Resolution (NHDPlus HR) (https://www.usgs.gov/core-science-systems/ngp/national-hydrography/nhdplus-high-resolution)
Land cover raster	National Oceanic and Atmospheric Administration (NOAA) Coastal Change Analysis Program (C-CAP) land cover (https://coast.noaa.gov/digitalcoast/data/)
Land use raster	Washington State Land Use 2010 (https://ecology.wa.gov/Research-Data/Data-resources/Geographic-Information-Systems-GIS/Data#l)
Mean annual precipitation	PRISM (Oregon State University) (http://www.prism.oregonstate.edu/)
Unpaved roads	Washington Department of Natural Resources (http://geo.wa.gov/)
Subbasin boundaries (including Ecological Regions)	Endangered Species Act (ESA) subbasin boundaries acquired from Snohomish County, combined with floodplain reaches from NOAA (https://www.fisheries.noaa.gov/resource/map/salmon-habitat-status-and-trend-monitoring-program-data)
Spawning and rearing distributions for each species	Washington Conservation Commission Salmon Habitat Limiting Factors Analysis (LFA) reports updated by project partners (https://www2.clark.wa.gov/files/dept/community-planning/shoreline-master-program/proposal-comments-received/futurewise-cd-1/fish-&-wildlife-habitat/salmon-limiting-factors-summaries/wria07sum.pdf)
Migration barriers	From WDFW barrier database, accessed 08/03/2021 (https://geodataservices.wdfw.wa.gov/hp/fishpassage/index.html)
Stream temperature	Summarized temperature data from NorWeST (Isaak et al. 2017)
Floodplain habitats	Hand mapped historical marshes and ponds from General Land Office surveys (Collins and Sheikh 2003) and National Hydrography Dataset waterbodies (https://www.usgs.gov/core-science-systems/ngp/national-hydrography/nhdplus-high-resolution). Field survey records from Snohomish County. Feature location within the floodplain based on the Puget Sound Ecosystem and Monitoring Floodplain Condition Assessment Level 2 dataset (https://wa-psp.maps.arcgis.com/apps/webappviewer/index.html?id=2f6f09bbb59f4b0b81d01440cb250bc0)
NOAA riparian condition dataset	Tree height and canopy opening angles from 2003-2019 lidar and 2017 high-resolution digital aerial photogrammetry used to model stream temperature (historical, current)
Large river edge habitats	Manually digitized from 2021 National Agriculture Imagery Program aerial imagery and 2004-2018 bank armor data
Large river backwaters	Manually digitized from 2021 National Agriculture Imagery Program aerial imagery
NOAA large river spawning riffles	Digitized from DFW and King County redd surveys in Snoqualmie basin; for the Skykomish percent spawning area extrapolated from Stillaguamish basin.

Table 2-3. Definitions of rearing habitat types used to estimate rearing habitat capacity and productivity. Spawning gravel area is typed separately.

Macro habitat type	Habitat type	Definition
Small stream (<20 m bankfull width)	Riffle	Shallow, fast water (typically >0.45 m/sec)
	Pool	Deep, slow water (typically ≤0.45 m/sec)
	Beaver pond	Beaver pond with median size 500 m^2
Large river (≥20 m bankfull width)	Bank edge	Vertical or steeply sloping shore, velocity ≤0.45 m/sec, depth <1.0 m, no bank armor
	Armored bank edge	Vertical or steeply sloping shore, velocity ≤0.45 m/sec, depth <1.0 m, banks are classified as armored based on proximity to mapped rip-rap
	Bar edge	Gently sloping shore, velocity ≤0.45 m/sec, depth <1.0 m
	Backwater	Partially enclosed areas separated from the main river channel, velocity ≤0.45 m/sec
	Mid-channel	All habitat area not included in bank and backwater habitats, often >1 m deep or velocity >0.45 m/sec
Floodplain	Marsh	Partially vegetated, dry in summer and wet in winter
	Pond (small)	Open water, wet year-round, <500 m^2
	Pond (large)	Open water, wet year-round, 500 m^2 to 5 ha
	Lake	Open water, wet year-round, >5 ha
	Side-channel riffle	Shallow, fast water (typically >0.45 m/sec)
	Side-channel pool	Deep, slow water (typically ≤0.45 m/sec)
Estuary	Distributary	Channels that diverge from the mainstem and flow into the nearshore
	Tidal channel	Channel networks originating from the near shore; not connected to distributaries or mainstem

2.1.2 Migration Barriers

We used data from the WDFW migration barrier database (downloaded 08/31/2021). The most recent survey date from King County in the database was April 2020, but the database has been updated and the most recent survey dates from King County are now August 2021. Differences between the two versions are not accounted for in this analysis. Stream locations in both the DNR hydrography and NHD were often inaccurate, so barrier points were often not near a stream line. To associate barriers with streams, we searched for a stream within 25 m of each barrier point, and snapped each barrier to the nearest stream segment. Barrier locations and passage ratings were confirmed by local biologists. For WDFW database barriers located within King County, barriers with a passage rating of NA (102 barriers) were eliminated from the database because (a) there was no migration barrier at that location, (b) the potential barrier was not county owned, or (c) the potential barrier was not within the salmon distribution (E. Lewis, King County, personal communication). If the passage rating was "unknown", we assumed it was a complete barrier (E. Lewis, King County, personal communication). For barriers within Snohomish County, all barriers were reviewed and corrected by Snohomish County, Tulalip Tribes, and/or WDFW to assure that barrier passage ratings were correct.

Once all barriers within the ranges of the modeled species were confirmed (1039 in Snohomish basin, 440 in Stillaguamish basin), cumulative fish passage ratings for each reach were calculated based on the passability ratings assigned to each barrier (Beechie et al. 2021b). The passage rating reduces spawning capacity for all reaches above a barrier, and where there are multiple barriers in succession the passage ratings are multiplicative. That is, spawning capacity above a barrier with a passage rating of 0.33 is 0.33 × capacity, and spawning capacity in reaches above two barriers with passage ratings of 0.33 have spawning capacity that is 0.33^2 × capacity, or 0.11 × capacity.

2.1.3 Small Stream Habitats (Wood and Beaver Ponds)

We calculated spawning gravel area in small streams using:

$$Spawning\ Area = \#\ pools \times wetted\ width \times tail\ crest\ length$$

which assumes that spawning occurs on riffles at pool tail crests and that tail crest length is ½ the wetted width (Beechie et al. 2021a). The number of pools in a reach is calculated as:

$$\#\ pools = reach\ length\ /\ (pool\ spacing \times wetted\ width)$$

where pool spacing is in units of wetted widths/pool, and is a function of channel slope and wood abundance (Beechie et al. 2021a). Pool spacing values are given in Table 2-4 for current and natural potential wood abundance (Montgomery et al. 1995, Beechie and Sibley 1997). We did not have comprehensive current or historical wood data, so we assumed low wood abundance currently and high wood abundance historically. Because we were unable to see channels 20-30 m wide in aerial imagery, we could not digitize spawning gravels as we did for other large rivers. Therefore, we estimated spawning gravel areas in channels 20-30 m bankfull using the small stream method.

Table 2-4. Estimates of pool spacing in wetted widths per pool for slope ≤1% or >1% and low and high wood abundance (current and natural conditions, respectively). Note that bankfull widths per pool are 0.4 times these values (2-2.5 bankfull widths per pool at high wood abundance, 5-11 bankfull widths per pool at low wood abundance).

Slope class	Pool spacing (wetted widths/pool)	
	Current condition (low wood abundance)	Natural potential (high wood abundance)
< 1%	12.5	6.25
>1%	27.5	5

We estimated current percent rearing pool areas in small streams by extrapolating pool and riffle data from 555 surveyed reaches distributed across channel slope and land cover strata (Beechie et al. 1994, 2001) (data in file "Mean percent pool by stratum.xlsx"). We assumed that land cover classes were an indicator of wood abundance, with the lowest abundance in agriculture areas and the highest wood abundance in reference sites. We classified each surveyed reach by slope class and C-CAP land-cover class (30-m buffer on either side of each reach), and then calculated mean percent pool for each stratum (Table 2-5). We then extrapolated the mean values to all un-surveyed reaches of similar slope and land cover. To calculate current rearing pool area for each reach we multiplied percent pool by reach length and wetted width, and riffle area was the total wetted area of the reach minus pool area. For historical pool areas, we used the reference condition pool areas by slope class for the same calculations.

To determine where beaver ponds might exist, we examined two models of beaver pond potential. Pollock et al. (2004) created a stream power model for the Stillaguamish River basin based on channel slope and drainage area, and Dittbrenner et al. (2018) created an intrinsic potential model for the Snohomish River basin based on channel slope, channel width, and valley bottom width. While there was significant overlap in the predicted beaver potential from both models, the intrinsic potential model (Dittbrenner et al. 2018) generally predicted less potential beaver habitat than the stream power model (Pollock et al. 2004). For this study we use the Dittbrenner model for both historical and current conditions, but the model can also be run with the Pollock model if desired.

We estimated current beaver pond areas based on beaver dam densities observed in aerial imagery in the Stillaguamish basin (Pollock et al. 2004), applied to reaches that were predicted to have potential beaver occupation (Pollock et al. 2004, Dittbrenner et al. 2018). Pollock et al. (2004) found that current beaver pond area in the Stillaguamish River basin totaled 0.49 km^2 and estimated historical beaver pond area totaled 9.3 km^2. From their

Table 2-5. Mean percent pool by slope/land-cover stratum, with sample size in parentheses.

	Slope class		
Land use	**Low (<2%)**	**Moderate (2-4%)**	**Steep (>4%)**
Reference Condition	64	54	35
Forest/wilderness	56 (n=139)	31 (n=82)	27 (n=68)
Agriculture	42 (n=34)	36 (n=5)	38 (n=2)
Rural/Urban	56 (n=146)	35 (n=51)	36 (n=28)

data, we estimated a minimum current beaver pond density averaging 0.32 ponds/km. For comparison, we estimated current beaver pond density in the Chehalis basin at 0.55 ponds/km (Beechie et al. 2021a). Pollock et al. (2004) noted that a number of ponds observed in the field were not visible on aerial imagery, so the estimate of 0.32 ponds/km may be low. For the historical condition we estimated beaver pond areas based on a density of 6 ponds/km (Pollock et al. 2004). To translate current and historical beaver dam densities into pond area we multiplied the number of ponds by the approximate median pond size of 500 m^2 (Beechie et al. 2021a).

2.1.4 Large River Habitats (Wood and Bank Armor)

As with small streams, we did not have comprehensive wood data for current or historical conditions, so we could not directly model the influence of wood on habitat conditions. Therefore, we used a combination of aerial imagery analysis and extrapolation of other data sets to estimate the influence of wood on spawning and rearing habitats in each basin. For large-river spawning habitat in the Stillaguamish River basin, we digitized riffles at pool tail crests from recent aerial imagery for all large river reaches >30 m wide to represent current conditions. (We were unable to see channels 20-30 m wide in aerial imagery, so we used the small stream method to estimate spawning gravel areas in those channels; see section 2.1.3 for details). Areas of spawning riffles were then summed in each subbasin to estimate spawning capacity for each subpopulation. For natural potential conditions, we modeled a spawning area increase of 30% over current conditions (Beechie et al. 2021a), which was intended to reflect increased spawning gravel retention and holding pool formation as a function of higher wood abundance historically. For rearing habitats, wood does not change edge habitat types in large rivers. Rather, it changes the amount of wood cover, which affects densities of fish rearing in edge habitat types (described in the life-cycle model descriptions in Section 2.3).

To evaluate changes in large river rearing habitat in the Stillaguamish River basin, we digitized edge habitat types (bank, bar, backwater) based on methods described in Beechie et al. (2021b). Edge habitat types were defined as described in Table 2-3, which are adapted from studies in the Skagit River basin (Beamer and Henderson 1998, Beechie et al. 2005). Bank armor geo-spatial data were available, so we were able to classify armored banks with greater accuracy than from aerial imagery alone. For historical conditions we

assumed that all armored banks were natural banks, and all other bank and bar habitats remained the same. The historical backwater estimate was based on historical side channel lengths, assuming that there was a backwater pool at the downstream end of each side channel. The average size of digitized backwaters in the Stillaguamish basin was 0.048 ha and the average length of side channels measured in Snohomish County field studies was 0.439 km (Frank Leonetti, Snohomish County, unpublished data). Using these data, we estimated historical backwater habitat area per kilometer A_{bw} as:

A_{bw} = [(*SC length*)/0.439 km]*0.048 ha, or

A_b = (*SC length*)*0.109 ha/km

This value is only used in diagnostic or restoration scenarios that include floodplain reconnection.

We extrapolated percent spawnable areas from digitized riffles in the Stillaguamish basin to the Skykomish basin and other post-glacial or mountain valleys in the Snoqualmie basin because we were mainly limited to using existing data. However, we did not extrapolate data to the Snoqualmie River because it is in a unique geomorphic setting and valley type (glacial valley) (Collins and Montgomery 2011), whereas the Stillaguamish and Skykomish valleys are both classified as post-glacial. Glacial valleys are those that were scoured below present sea level during the last glaciation, and since glacier retreat, have been aggrading with alluvial sediments. As a result, the pre-development Snoqualmie River was an extremely low gradient meandering river with natural levees and extensive floodplain marshes (Collins and Montgomery 2011). In contrast, post-glacial valleys are those that were dammed by the ice sheet and accumulated deep outwash and lacustrine sediments during glaciation, and since glacier retreat have been incising into those sediments. Rivers in those valleys are island-braided with numerous side channels on the floodplain (Beechie et al. 2006b, Stefankiv et al. 2019). In the Snohomish, Snoqualmie, and Tolt Rivers we digitized spawning riffles based on redd survey data from King County and WDFW. Within the post-glacial valleys, we applied the average percent spawning gravel from confined reaches in the Stillaguamish (3.4%) to confined reaches in the Skykomish basin, and the average percent spawning gravel from unconfined reaches in the Stillaguamish (5.5%) to unconfined reaches in the Skykomish basin. We also applied Stillaguamish spawning gravel percentages to the lower 8.9 kilometers of the Skykomish River despite its location on the edge of the formerly glaciated Snohomish-Snoqualmie valley. Since the rest of Skykomish River lies in a post-glacial valley, the lower portion of it reflects a post-glacial sediment regime rather than a glacial one. The lower Raging River is in a similar setting, so we also classified the lower Raging River as post-glacial and extrapolated spawning gravel area percentages from the Stillaguamish.

2.1.5 Floodplain Habitats

We quantified change in three floodplain habitat types: marshes, ponds/lakes, and side channels (Figure 2-3). We obtained GIS data of historical floodplain marshes and ponds that were digitized at the University of Washington based on General Land Office (GLO)

surveys (Collins and Sheikh 2003). We then added polygons from the NHD+ waterbody layer (https://www.usgs.gov/core-science-systems/ngp/national-hydrography/nhdplus-high-resolution) to fill in gaps in the GLO data. We evaluated each polygon from the GLO surveys and NHD+ individually to note whether it was present only historically (e.g., drained marshes), only currently (e.g., constructed ponds), or both historically and currently (Beechie et al. 2021b). Vegetated marshes were assumed to be dry in summer and wet in winter, whereas ponds were assumed to be wet year-round (Figure 2-3) (Beechie et al. 2021b).

We estimated current side channel lengths and areas using a combination of field data (Frank Leonetti, Snohomish County, unpublished data) and data digitized from aerial imagery in the Salmon Habitat Status and Trends Monitoring Program (SHSTMP) (https://www.fisheries.noaa.gov/resource/map/salmon-habitat-status-and-trend-monitoring-program-data). In basins with comprehensive side channel field data, we used side-channel lengths from the field data directly. In post-glacial and mountain valleys (Collins and Montgomery 2011) with comprehensive field surveys, the ratio of field-surveyed side channel length to digitized side channel length was 2.47. In broad glacial valleys without comprehensive field surveys (primarily the Snoqualmie River), we used side channel lengths directly from the SHSTMP data with the assumption that most side channels would be visible in aerial imagery. For post-glacial and mountain valleys where we could not find comprehensive field surveys, we multiplied the total length of side channel digitized from aerial imagery by 2.47 to account for side channels that likely exist within the subbasin but were not visible from aerial imagery due to canopy cover.

We estimated historical side-channel and main-channel length using reference values from prior studies (Beechie et al. 2006b, Collins and Montgomery 2011), and evaluated each reach to estimate a historical main-channel and side-channel reach length multiplier based on potential channel pattern and natural confinement. The main-channel length ratio is

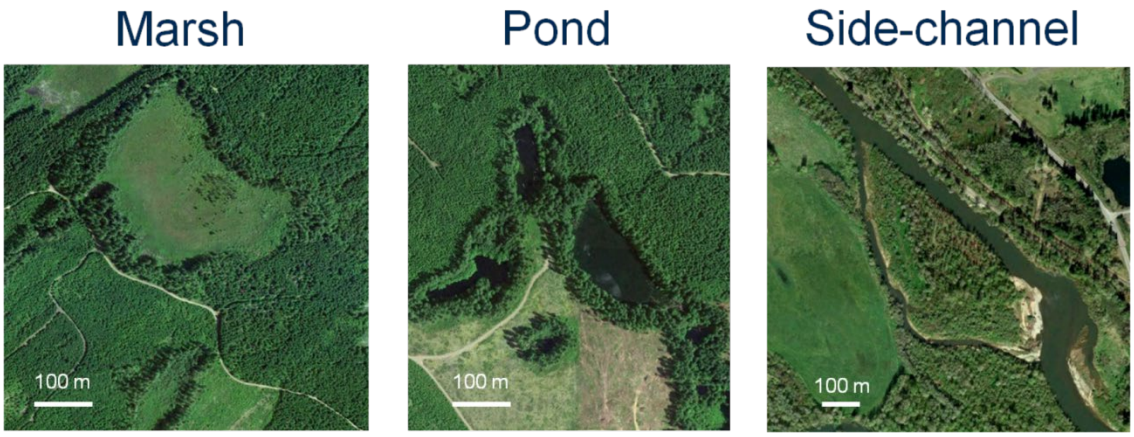

Figure 2-3. Illustration of floodplain habitat types from aerial imagery. Marshes are dry in summer and wet in winter, ponds are wet year-round, and side channels appear as pool-riffle channels branching off of the main channel. Images from the Chehalis River basin. (Figure from Beechie et al. 2021b).

historical sinuosity divided by current sinuosity, so a ratio of 1.5 means the main stem was 50% longer historically. The side-channel length ratio is the ratio of side-channel length divided by main-channel length, so a side-channel length ratio of 1.5 means that there were 1.5 km of side channel for each 1.0 km of main channel. Across both prior studies, reference site sinuosity for meandering channels ranged from 1.2 to 1.9 with a median of 1.6, and for island-braided channels it ranged from 1.05 to 1.5 with a median of 1.2. The median values of both studies were remarkably similar, and there was substantial overlap in the ranges of measured values. The median reference site side-channel length ratio was about 0.25 for meandering channels (range 0.1 to 1). For island braided-channels 20-40 m bankfull width, the reference site side-channel length ratio ranged from 0.4 to 3.5 with a median of about 1.3. For island braided-channels >40 m bankfull width, the reference site side-channel length ratio ranged from 0.7 to 4.7 with a median of about 2.5.

Where channels did not appear to have been straightened from their natural location, we set the main channel length multiplier at 1.0 to indicate that historical and current channel lengths were similar (Tables 2-6 and 2-7). Where channels appeared to have been

Table 2-6. Main-channel and side-channel length multiplier values for large river reaches in the Stillaguamish River basin. “Headwaters” indicates end of the large river segment and transition to small stream classification.

Reach Name	Reach Boundaries	Main-channel Multiplier	Side-channel Multiplier
Lower mainstem	Norman Rd. to confluence of NF and SF	1.1	2.5
NF Stillaguamish 1	Confluence to Deer Creek	1.0	1.0
NF Stillaguamish 2	Deer Creek to Boulder River	1.0	1.0
NF Stillaguamish 3	Boulder River to Squire Creek	1.0	1.2
NF Stillaguamish 4	Above Squire Creek	1.0	0.5
Pilchuck Creek	Mouth to headwaters	1.0	0.2
Deer Creek	Mouth to headwaters	1.0	0.3
Boulder River	Mouth to Boulder Falls	1.0	0.2
Squire Creek	Mouth to end of Squire Creek Rd.	1.0	0.2
SF Stillaguamish 1	Confluence to Canyon Creek	1.1	0.5
SF Stillaguamish 2	Robe Canyon	1.0	0
SF Stillaguamish 3	Robe Canyon to Twenty–two Creek	1.0	0.2
SF Stillaguamish 4	Twenty–two Creek to Mallardy Creek	1.0	0.3
SF Stillaguamish 5	Mallardy Creek to Buck Creek	1.0	0.4
Jim Creek	Mouth to headwaters	1.0	0.2
Canyon Creek	Mouth to headwaters	1.0	0.2

Table 2-7. Main-channel and side-channel length multiplier values for large river reaches in the Snohomish River basin. "Headwaters" indicates end of the large river segment and transition to small stream classification.

Reach Name	Reach Boundaries	Main-channel Multiplier	Side-channel Multiplier
MS Snohomish	Snohomish River from Hwy 9 to Confluence	1.0	0.7
Lower MS Skykomish	Confluence with Snoqualmie to Sultan	1.1	1.7
Upper MS Skykomish	Sultan to confluence of N. and S. Fork	1.05	2
Lower NF Skykomish	Confluence of N. and S. Fork to Silver Creek	1	2.5
Upper NF Skykomish	Silver Creek to Headwaters	1	0.8
Lower SF Skykomish	Confluence of N. and S. Fork to County Line	1	0.2
Middle SF Skykomish	County Line to Miller River	1	0.5
Upper SF Skykomish	Miller River to Foss River	1.2	1
Miller River	SF Skykomish to Headwaters	1	1.5
Beckler River	SF Skykomish to Headwaters	1	1
Foss River	SF Skykomish to Headwaters	1	0.8
Tye River	Foss River to Headwaters	1	0.8
Olney Creek	Wallace River to Headwaters	1	0.5
Wallace River	Skykomish River to Headwaters	1	0.2
Lower Snoqualmie	Skykomish River to Duvall	1	1
Middle Snoqualmie	Tuck Creek to Tolt River	1	0.3
Upper MS Snoq. 1	Langlois Creek to Raging River	1.05	0.3
Upper MS Snoq. 2	Raging River to Snoqualmie Falls	1	0.3
Lower Tolt River	Snoqualmie to Confluence of NF and SF Tolt	1	0.8
NF Tolt River	Confluence to Barrier	1	0.1
SF Tolt River	Confluence to Dam	1	0.4
Raging River	Snoqualmie River to Headwaters	1	0.5
Lower Pilchuck River	Snohomish River to Dubuque Creek	1	1
Middle Pilchuck River	Dubuque Creek to Worthy Creek	1	1.8
Upper Pilchuck River	Worthy Creek to Wilson Creek	1	1.2
Lower Sultan River	Skykomish River to end of Diversion	1	0.7

straightened, we used the reference values for the appropriate channel pattern to estimate historical channel length. Sinuosity at any location is partly a function of channel confinement for both channel types, so we used professional judgment and the mapped historical channel pattern (Collins and Sheikh 2003) to adjust the estimated historical sinuosity up or down based on confinement and historical maps.

Side channel lengths are also a function of channel confinement, and we used professional judgment to estimate historical side channel length ratios based on confinement and historical maps (Beechie et al. 2021b). For percent pool area in current side channels, we used the low-slope forested value of 56%, and for percent pool area in historical side channels we used the reference value of 64% for low-slope channels.

2.1.6 Riparian Shade (Canopy Opening Angle)

We calculated change in canopy opening angle for each reach based on lidar data for current condition and reference tree heights for the historical condition (Seixas et al. 2018, Beechie et al. 2021a). We calculated the canopy opening angle (θ) based on channel width (W) and average riparian tree height (z):

$$\theta = \left(90 - \left(\frac{z_L}{\frac{W}{2}}\right)\right) + \left(90 - \left(\frac{z_R}{\frac{W}{2}}\right)\right)$$

where z_L and z_R are tree height plus bank height on each side of the channel, and $W/2$ is the horizontal distance from the channel center to the first tree. The inverse tangent functions are subtracted from 90°, so a channel with complete canopy closure will have θ = 0° and a channel with no vegetation on either bank will have θ = 180°.

We were able to obtain lidar coverage for both study basins, except for a small portion of the upper Skykomish basin. For that part of the study area we obtained 2017 high-resolution Digital Aerial Photogrammetry canopy elevation data (Caleb Maki, Washington Department of Natural Resources, unpublished data), and calculated tree height by subtracting the 10-m NED elevation from the canopy elevation.

We generated a stream network from the bare earth coverage to assure that channel alignment best matched the location of the stream relative to riparian trees in the lidar data set. We then added a cross section every 10 m to calculate canopy opening angle based on the distance to each bank and the height of trees on each bank. We repeated the calculation for historical conditions at each cross section using the same channel width but substituting the reference tree height for the current tree height. Reference tree heights were 52 m for small streams and confined large rivers (mainly conifer forest) and 30.5 m for unconfined large rivers (mixed conifer and hardwoods of different ages) (Seixas et al. 2018, Beechie et al. 2021a).

2.1.7 Stream Temperature

We constructed local Spatial Statistical Network (SSN) models for the 7-day average daily maximum (7-DADM) and June 1-21 average daily maximum (Jun 1-21 ADM) temperature in each river basin. We first calculated the 7-DADM and Jun 1-21 ADM at each temperature sensor location, and then related those values to nine potential predictor variables (Table 2-8). When there was more than one year of temperature measurement at a location, we used the year with highest temperature. Sample sizes were n= 112 for the 7-DADM and n = 86 for the Jun 1-21 ADM in the Stillaguamish basin. In the Snohomish basin, sample sizes were n= 160 for the 7-DADM and n = 122 for the Jun 1-21 ADM. The final models are summarized in Table 2-9. We used these models to produce maps of current 7-DADM and Jun 1-21 ADM for each reach in each basin (Figures 2-4 and 2-5).

For historical temperatures, we used the change in canopy opening angle to estimate change in 7-DADM temperature due to changes in shade:

$$\Delta T_{7-DADM} = 0.035 \cdot \Delta\Theta$$

where $\Delta T_{7\text{-}DADM}$ is the change in 7-DADM temperature, and ΔΘ is change in canopy opening angle (Fogel et al. 2022). Stream temperatures were also reduced by floodplain reconnection to represent temperature decrease by hyporheic exchange (see Section 3.5.4).

Because changes in June 1-21 ADM as a function of Θ were smaller than changes in 7-DADM, we converted $\Delta T_{7\text{-}DADM}$ to $\Delta T_{Jun1\text{-}21ADM}$ via linear regression between observed Jun1-21 ADM and 7-DADM. The slope of this regression in the Snohomish basin was 0.69, so a 1 degree change in 7-DADM was considered equivalent to a 0.69 degree change in Jun1-21 temperature. In the Stillaguamish basin, the slope of the regression was 0.36, so a 1 degree change in 7-DADM was considered equivalent to a 0.36 degree change in Jun1-21 temperature.

Connected floodplains can have high rates of hyporheic exchange, potentially reducing mean stream temperature and creating small-scale thermal refuges (Poole et al. 2008, Arrigoni et al. 2008). In the HARP Model, reconnection of unconfined large rivers and small streams to historical floodplain features reduced the 7-DADM temperature by 0.29-1.43°C, depending on the channel width (Table 2-10) (Fogel et al. 2022). The model is based on prior work in the Willamette River basin (Seedang et al. 2008). We did not apply temperature changes to reaches with confinement ratios < 4 (floodplain width divided by bankfull width) or streams with gradients >3%. After calculating the change in 7-DADM, we converted the modeled change in 7-DADM to a change in Jun1-21ADM using the slopes from the basin-specific regression equations presented earlier for the Stillaguamish and Snohomish basins, respectively.

ΔJun1-21 ADM = 0.36 (Δ7DADM), and

ΔJun1-21 ADM = 0.69 (Δ7DADM)

Table 2-8. Potential predictor variables evaluated for the Spatial Statistical Network models for the Stillaguamish and Snohomish River basins.

Variable	Name	Description
Drainage area	Area_km2	Calculated from NED, in km^2
Mean upstream elevation	mn_elev	Mean elevation in drainage basin upstream of sensor (m)
Elevation of sensor	elev	Elevation at sensor location (m)
Mean August air temperature	air_tmp	Mean August air temperature at sensor location (°C), from PRISM
Mean annual precipitation	mn_precip	Mean annual precipitation in drainage basin upstream of sensor location (cm), from PRISM
Mean percent impervious	mn_imperv	Mean percent impervious area from C-CAP in drainage basin upstream of sensor
Canopy opening angle	can_ang	Canopy opening angle calculated in this study
Percent riparian forest	ripfor	Percent forest cover in 30-m buffer along the reach (forest data from C-CAP)
Percent alluvium	mn_alluv	Percent alluvium in the drainage basin upstream of the reach, from WA DNR
Floodplain width	fpw	Floodplain width calculated in this study

Table 2-9. Final Spatial Statistical Network models for 7-DADM temperature and Jun 1-21 ADM temperature in the Stillaguamish and Snohomish River basins. Pred R^2 is the portion of the total R^2 explained by the predictor variables and Spatial R^2 is the portion of the total R^2 explained by the spatial structure.

Model	Predictor variables	Pred R^2	Spatial R^2	Total R^2
Stillaguamish				
7-DADM	Elevation of sensor, percent riparian forest in the reach, percent alluvium	0.29	0.52	0.81
Jun 1-21 ADM	Mean annual precipitation, floodplain width	0.24	0.51	0.75
Snohomish				
7-DADM	Elevation of sensor, floodplain width	0.19	0.80	0.99
Jun 1-21 ADM	Elevation of sensor	0.11	0.79	0.90

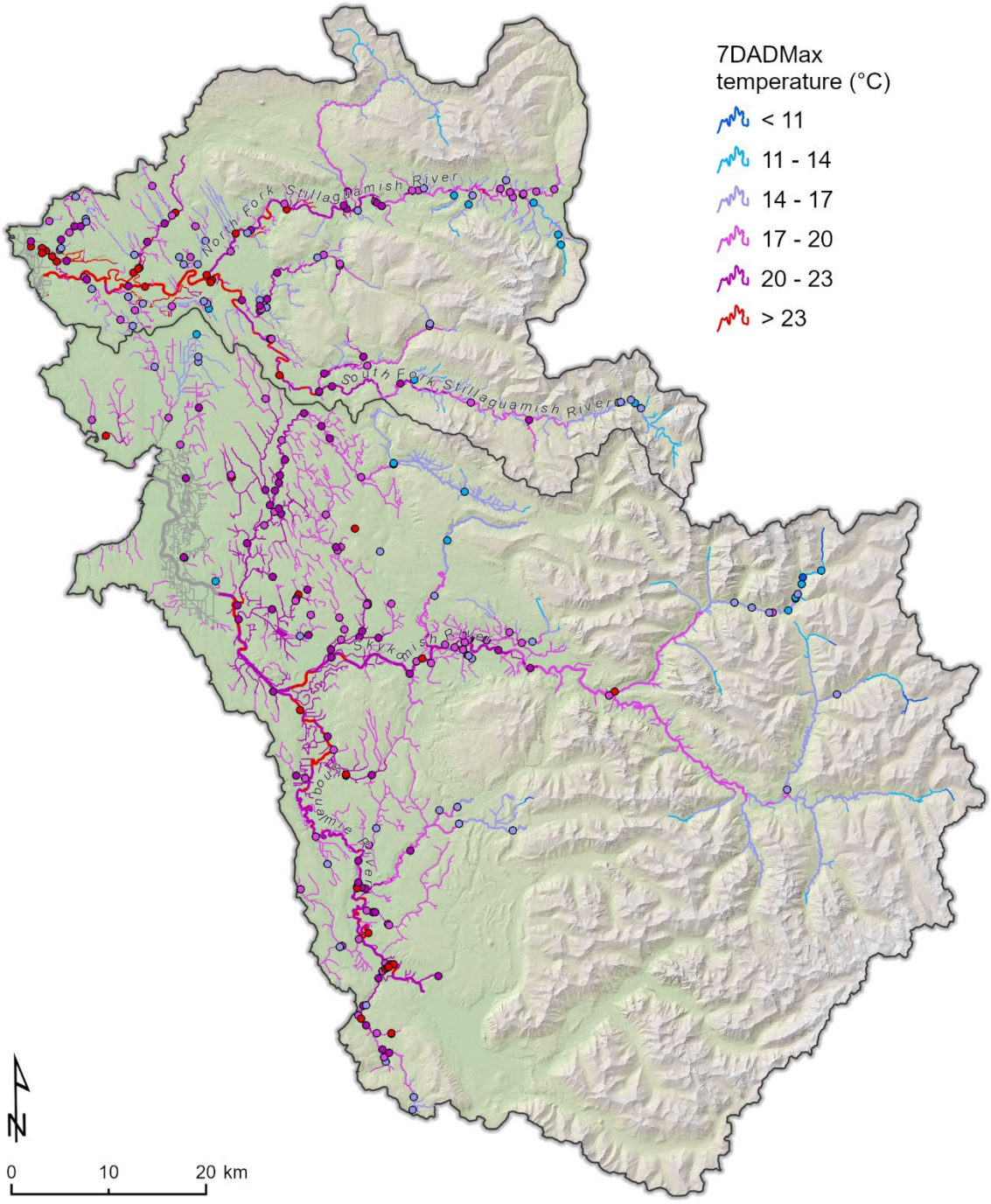

Figure 2-4. Map of predicted current 7-day average daily maximum temperature (stream lines) and measured 7-DADM at sensor sites (circles) in the Snohomish and Stillaguamish River basins.

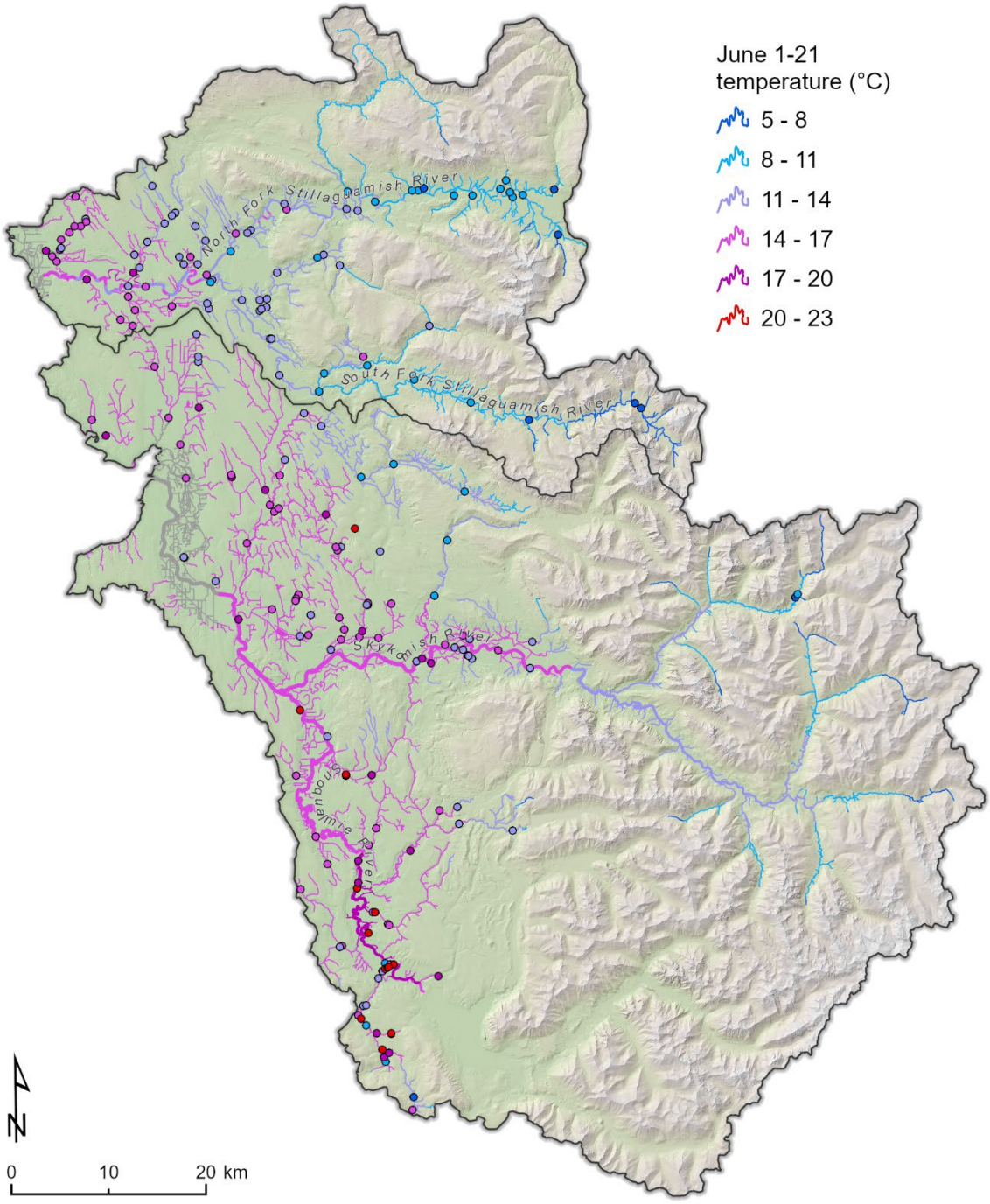

Figure 2-5. Map of predicted current June 1-21 average daily maximum temperature (stream lines) and measured Jun 1-21DADM at sensor sites (circles) in the Snohomish and Stillaguamish River basins.

Table 2-10. Modeled temperature change due to floodplain reconnection as a function of channel width.

Bankfull width	Width of connected floodplain	Temperature change (°C)
> 30m	305m	-1.43
20 - 30m	213m	-1.0
10 - 20m	152m	-0.72
< 10m	61m	-0.29

2.1.8 Fine Sediment

To estimate fine sediment in spawning gravels of the Stillaguamish and Snohomish River basins, we first compared two separate models developed for the Snohomish basin: one that used unpaved road density, drainage area upstream of the reach, and mean annual precipitation upstream of the reach as predictor variables, and another that used percent alluvium in the drainage basin upstream of the reach, drainage area upstream of the reach, and total forest cover in the drainage basin upstream of the reach (Bartz et al. 2006). Both models predict percent fine sediment less than 6.3 mm diameter. Neither model performed well for reach-scale fine sediment prediction, so we developed new models. Because fine sediment patterns differed among channel sizes and locations, we developed four separate models for (1) channels ≤30 m bankfull width, (2) channels 30-60 m in width, (3) the Snoqualmie River main stem, and (4) all remaining channels ≥60 m wide in the Stillaguamish and Snohomish River basins.

Channels ≤30 m bankfull width

We created separate models for channels ≤30 m bankfull width (n = 50) and 30-60 m bankfull width (n=25) from local data sets in streams <60 m bankfull width (Frank Leonetti, Snohomish County, unpublished data) (Beck and Reiser 2006, Purser et al. 2009, Stillaguamish Tribe Natural Resources Department 2011, Purser and Leif 2013). For channels ≤30 m wide, the fine sediment prediction equation is

$$fines_{6.3mm} = 60.05 - (0.81 \cdot forest) + (0.50 \cdot gldrift) + (0.95 \cdot alluv)$$

where $fines_{6.3mm}$ is percent fine sediment <6.3 mm, *forest* is percent forest cover in the basin upstream of the sample point, *gldrift* is percent glacial drift in the basin upstream of the sample point, and *alluv* is percent alluvium in the basin upstream of the sample point (n = 50, adj. $r^2 = 0.46$). Where the model predicts a value <0% fines we set the value to 0, and

where the model predicts a value greater than 100% fines we set the value to 100. This is the only model that reflects land use, and historical percent fines was estimated by setting *forest* to 100% for all modeled reaches.

Channels 30-60 m bankfull width

For channels 30-60 m wide, the equation is

$$fines_{6.3mm} = 13.75 + (0.69 \cdot A) - (0.84 \cdot gldrift) - (1.27 \cdot alluv)$$

where A is drainage area (n = 25, adj. r^2 = 0.78). Where the models predict a value <0% fines we set the value to 0, and where the model predicts a value greater than 100% fines we set the value to 100. This value was applied for both the current and historical condition because there was no discernable land use effect.

Snoqualmie River

In the Snoqualmie River basin, the longitudinal pattern of fine sediment values showed three distinct segments in which a tributary delivered gravels with relatively low fine sediment to the main stem, and then fine sediment values increased rapidly downstream until the next major tributary (Figure 2-6) (Booth et al. 1991). The best fit models were:

Tokul Creek to Raging River

$fines_{6.3mm} = 6403.79 - (70.88 \cdot updist_{km})$, (n=2, r^2=na)

Raging River to Tolt River

$fines_{6.3mm} = 483.25 - (5.41 \cdot updist_{km})$, (n=6, r^2=0.83)

Tolt River to Skykomish Confluence

$fines_{6.3mm} = 195.26 - (13.8 \cdot elev)$, (n=6, r^2=0.86)

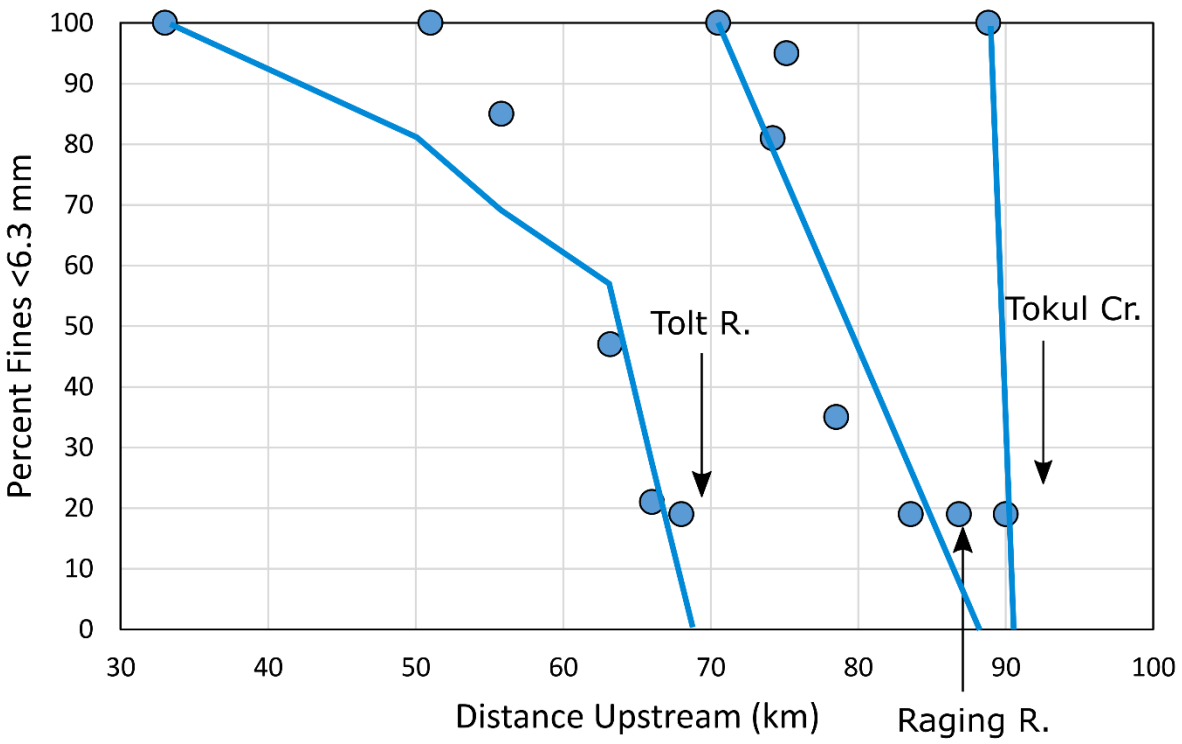

Figure 2-6. Longitudinal pattern of subsurface fine sediment in the Snoqualmie River. Data (blue points) from Figure 8 in Booth (1991). Lines are predicted fine sediment from the three equations.

where $fines_{6.3mm}$ is percent fine sediment <6.3 mm, *elev* is elevation, and $updist_{km}$ is upstream river distance. Where the model predicts a value <0% fines we set the value to 0, and where the model predicts a value greater than 100% fines we set the value to 100. These equations were applied for both the current and historical condition because there is no discernable land use effect.

Channels ≥60 m bankfull width excluding Snoqualmie River

For the remaining river segments ≥60 m bankfull width, we were only able to find surface grain size distributions from the Skykomish River at 10 sites, two at the lower end of the North and South Forks and eight on the mainstem Skykomish between the confluence of the North and South Forks and the confluence of the Skykomish and Snoqualmie Rivers (Figure 27 in (Nelson 1971)). Seven sites had 0% percent surface fines, and the remaining three sites had percent surface fines of 4%, 6%, and 10%. There was no apparent longitudinal pattern in percent fines or the median grain size, and median grain sizes were mostly in a relatively narrow range from about 32 mm to 64 mm. The average surface percent fines from all sites was 2%.

To translate the average surface percent fines into subsurface percent fines we compared surface and subsurface percent fines at 11 sites in the Snoqualmie River (Booth 1991). Surface percent fines were comparable to the Skykomish percent fines at only 4 sites (2%,

3%, 3%, and 5%), and the remaining sites were greater than 90% fines at the surface except for one site at 25% fines. The subsurface percent fines at the four comparable sites averaged 6 times that of the surface percent fines. Therefore, we multiplied the average surface percent fines in the Skykomish sites by 6 to estimate subsurface fines for all remaining reaches ≥60 m bankfull width except the Snoqualmie River. This average subsurface percent fines (12%), was applied for both the current and historical condition because there is no discernable land use effect. The fine sediment value of 12% equates to an incubation survival of 0.60 for Chinook and coho salmon and 0.52 for steelhead (see Section 3.8).

2.1.9 Impervious Surfaces and Paved Roads

In the HARP Model impervious surface area and paved roads are an external factor that alters prespawn productivity for coho salmon. Pre-spawn mortality has been estimated for most subbasins in Puget Sound as a function of road density, traffic intensity, and summer and fall precipitation (Feist et al. 2017). We converted those mortality values to productivities for each subbasin in the Stillaguamish and Snohomish River basins (Feist et al. 2017), and used those values as a productivity multiplier for the prespawn life stage. We applied these subbasin values to each coho spawning reach within a subbasin, but did not apply the mortality to large rivers where the concentration of pollutants from impervious surfaces is likely substantially diluted. Nor did we apply these mortalities to Chinook or steelhead because there are currently no data indicating that this same relationship applies to those species. For historical conditions, baseline prespawn survival is fixed at 0.95 for all species (but also modified by stream temperature for Chinook salmon and summer-run steelhead, see Sections 2.3.2 and 2.3.3).

2.1.10 Estuary Habitats

To estimate current habitat availability in the estuaries, we used digitized estuary habitat features from NOAA's Salmon Habitat Status and Trends Monitoring Program (SHSTMP) (https://www.fisheries.noaa.gov/resource/map/salmon-habitat-status-and-trend-monitoring-program-data) and the Puget Sound large River Delta Tidal Restriction and Wetland Mapping project by Cramer Fish Sciences (https://salishsearestoration.org/wiki/Puget_Sound_Large_River_Delta_Tidal_Restriction_and_Wetland_Mapping). SHSTMP data is comprised of non-restored and restored estuarine habitat features that were digitized using aerial and satellite imagery from 2010-2011 and 2017-2020, respectively. Estuary boundaries were adopted from the SHSTMP data set, which includes estuarine emergent marsh, estuarine forest transition, and forested riverine tidal wetlands. Distributaries and tidal channels were mapped as separate feature types (Table 2-3). Distributaries were digitized from aerial imagery, and confidence in feature area is high because the channels are clearly visible. Usable habitat area in distributaries is along the channel margins, so we estimated useable habitat area with a 2-m inside buffer along distributaries (Chamberlin et al. 2022). Visible tidal channel areas were also digitized from aerial imagery, but some tidal channels may not be visible due to vegetation cover. Only distributary and tidal channel habitat features were used in delta capacity calculations. Features were excluded from the current habitat area calculation if access was

classified as restricted. We only included features that were within the SHSTMP delta boundaries, except that we extended distributaries seaward of the delta boundaries to allow calculation of connectivity of delta front habitats. Adjacent features of the same type were merged into one feature to facilitate the analysis.

Historical distributaries and estuarine wetlands had been previously digitized from General Land Office (GLO) survey maps and notes (Collins and Sheikh 2003). Current distributary locations in the Snohomish basin are similar to their historical locations, so the current feature areas are similar to the historical distributary area. In the Stillaguamish basin, the current main channel (Hat Slough) and distributary (Old Mainstem) have switched from their historical locations, which alters both the habitat areas and connectivity pathways.

Although the historical data set included some tidal channels, the tidal channel drainage density (channel length divided by tidal wetland area) was much lower in the historical data set than in the current data set. This difference is likely related to the field survey methods that produced the historical data set rather than a fundamental change in tidal channel geomorphology. However, the surveyed historical tidal wetland areas appeared to be an accurate representation of actual historical wetland area. Therefore, we used a set of basin-specific allometry equations (Hood 2015) to estimate historical tidal channel area from estuarine emergent marsh, estuarine forest transition, and forested riverine tidal areas:

Snohomish

$$\text{Tidal channel area (ha)} = 10^{-2.398} * (\text{Tidal wetland area (ha)})^{1.52}$$

Stillaguamish

$$\text{Tidal channel area (ha)} = 10^{-2.871} * (\text{Tidal wetland area (ha)})^{1.52}$$

The allometry equations were developed using a data set of blind tidal channels draining relatively low-lying estuarine emergent marsh (EEM) areas. A different allometric scaling relationship might exist between tidal channel area and the area of estuarine forest transition (EFT) or forested riverine tidal (FRT) wetland areas. However, few such wetlands still exist, so we applied the same equations to all estuary marsh types.

Substantial time and resources have already been devoted to freshwater and estuarine habitat restoration in both study basins. At least 39 hectares of tidal channel have been restored in the Snohomish Delta between 1994 and 2020, and at least 14 hectares of tidal channel have been restored in the Stillaguamish delta between 2013 and 2019. (Note that this is not total marsh area, but tidal channel area within marshes.) Because the HARP model relies on recently updated habitat data to describe "current" conditions, the model does not directly quantify any benefits that might have been gained by restoration actions that have previously been implemented and that are already integrated into the current habitat condition datasets. Conversely, any recent restoration projects that have not yet been integrated into the habitat data sets are not described within the current condition

scenario. Benefits resulting from these very recent projects would be included in HARP's modeled restoration potentials.

2.2 Calculating Capacities and Productivities

Each habitat condition in the HARP model can be altered by land use, restoration, and climate change, and changes in habitat conditions are quantitatively linked to changes in life-stage capacity (c) or productivity (p) values. Hence, the current and historical habitat conditions can be translated into a variety of diagnostic or restoration scenarios by adjusting life-stage capacities or productivities for each habitat attribute, species, and subbasin to represent effects of restoration, land use, or climate change. This model step (the habitat analysis) creates life-cycle model input data containing all of the life-stage c and p values for each scenario, species, and subbasin. The inputs to the habitat analysis are the habitat condition files created from the spatial model.

2.2.1 Subbasin Capacities and Productivities

Subbasin capacity values under current habitat conditions are based on areas of each habitat type multiplied by the species- and habitat-specific densities of spawners, eggs, or juveniles that each habitat can support. Capacity of each habitat unit (c_h) is the product of habitat area (A) and potential fish density (d, we use the 95th percentile of observed densities from field studies), scaled by habitat quality (β) (Jorgensen et al. 2021):

$$c_h = A \cdot d \cdot \beta$$

These values are then aggregated to the reach level for each reach (r) and life stage (l) by summing the individual units j, and multiplying by density d and the habitat quality multiplier (β) (Jorgensen et al. 2021):

$$c_{l,r,h} = \sum_j A_{l,r,h,j} \cdot d_{l,h} \cdot \beta_{l,r}$$

where

- $c_{l,r,h}$ is the capacity of life stage l, reach r, and habitat type h
- $\Sigma A_{l,r,h,j}$ is the sum of area A for life stage l, reach r, habitat type h, and habitat unit j
- $d_{l,h}$ is the density of fish in life stage l, and habitat type h (densities of fish in each habitat unit type are in Section 2.3)
- $\beta_{l,r}$ is the habitat quality multiplier for life stage l and reach r

Finally, we aggregate to the subbasin level to create the life-stage capacities (c_l) for each subpopulation in the life-cycle model (Jorgensen et al. 2021):

$$c_l = \sum_r \sum_h c_{l,r,h}$$

Life-stage capacities can be altered by changes in habitat area or changes in density. For example, changes in wood abundance can alter habitat area and therefore capacity, whereas changes in temperature can alter fish density and therefore capacity. Details of the calculations are more fully explained in Jorgensen et al. (2021) and Beechie et al. (2021a).

Productivity (p) for each subpopulation (subbasin) is also a function of habitat type and quality, and is based on a current-condition productivity value that represents density-independent survival in current habitats with low wood abundance and no temperature limitation (Jorgensen et al. 2021). The HARP model uses productivity multipliers to change productivities as a function of changes in habitat quality (e.g., a change in fine sediment or a change in summer stream temperature). The productivity for any life stage is calculated as the average of the habitat-specific productivity values, weighted by the capacity of each habitat type (Jorgensen et al. 2021):

$$p_l = \sum_r p_{l,h} \cdot \beta_{l,r} \cdot w_{l,r,h}$$

where p_l is the weighted average productivity for life stage l, $p_{l,h}$ is the productivity of habitat type h and life stage l, $\beta_{l,r}$ is the habitat quality multiplier for reach r and life stage l, and $w_{l,r,h}$ is the weight for habitat type h, reach r, and life stage l. The weight ($w_{l,r,h}$) is simply $c_{l,r,h}/\ c_l$, where $c_{l,r,h}$ is the capacity of a reach, and c_l is the total capacity for the life stage.

For each habitat scenario and species, the habitat analysis produces a table of life-stage capacities and productivities for each subbasin and the estuary. Each subbasin is modeled as a separate subpopulation, although juveniles and adults mix in lower-river, estuary, and marine habitats. These parameter tables are then run through the life-cycle models to estimate run size and spawner abundance for each subpopulation.

2.2.2 Estuary Capacity and Productivity

In the HARP Model the estuary life stage is modeled as density independent for coho and steelhead, so there are no capacity estimates for those species. The estuary life stage is a density-dependent movement stage for Chinook salmon.

Chinook Estuary Rearing Capacity

We estimated Chinook subyearling rearing capacity in estuaries using rearing densities of Chinook fry for each habitat type, residence time, and total length of the rearing period, where densities are scaled by a connectivity parameter that determines the relative number of juveniles that migrate to a given part of the estuary (Beamer et al. 2005, Chamberlin et al. 2022). Maximum capacity per unit area is a function of daily maximum fish density (# fish/ha), mean residence time (days), and length of the rearing period (days). We estimated maximum juvenile Chinook fry and parr rearing capacity for each estuary habitat unit in the Snohomish estuary using

$$c = (d * t)/r$$

where c is maximum capacity per unit area, d is maximum daily density (fish/ha), t is the length of the rearing period (# of days), and r is the mean residence time (# of days) (Chamberlin et al. 2022). From this calculation, the maximum density of fry in distributary edge habitats was 23,548 fry/ha and the maximum density in tidal channels was 47,096 fry/ha (Chamberlin et al. 2022). We then scaled fish densities across the estuary by connectivity, which decreases as a function of bifurcation order and distance from the upstream end of the delta. We used the following equation developed for the Snohomish Delta (Chamberlin et al. 2022) to convert delta connectivity values to salmon capacity:

$$ln(c) = 1.4544 \times ln(Con) + 12.482$$

This equation overestimates densities of fish near the upper end of the delta, so we capped densities based on habitat type (23,548 fry/ha in distributary edge habitats and 47,096 fry/ha in tidal channels) (Chamberlin et al. 2022).

Chinook Estuary Rearing Productivity

For the density-independent estuary productivity parameter for Chinook salmon, we estimated the value as a function of the SAR value, estuary capacity, and the proportions of fry and parr outmigrants (Appendix B). We had four widely ranging estimates of delta capacity, which produced estimates of estuary p ranging from 0.11 to 0.49. This is consistent with data from the Sacramento-San Joaquin delta which found that survival of Chinook fry (<70m fork length) through the delta ranged from 0.10 to 0.51 among years for fry released below Red Bluff Diversion Dam and 0.03 to 0.33 among years for fry released in various delta locations (Brandes and McLain 2000). Median values were 0.29 (n=7) and 0. 19 (n = 5), respectively. For this model we chose to use a value of p = 0.35 for the Chinook fry and parr migrant estuary rearing life-stage.

Steelhead Estuary Rearing Productivity

Because the steelhead estuary life stage is modeled as density independent (Section 2.3), we only estimated estuary rearing productivity for the estuary life stage. There were three unknown smolt rate and survival parameters that we calibrated simultaneously for summer- and winter-run populations (Appendix C). The unknown parameters were the percent of age-1 juveniles that smolt, the percent of age-2 juveniles that smolt, and combined estuary and Puget Sound productivity. The three parameters were calibrated simultaneously so that smolt-to-adult-return (SAR) rate and proportions of age-1, age-2, and age-3 smolts in the adult return matched the target rates and proportions based on observed SAR (1.6%, Appendix D) and proportions of age groups in adult returns.

Coho Salmon Estuary Rearing Productivity

For coho salmon, estuary rearing was also density independent, and estuary rearing productivity was the only unknown parameter. Therefore, we back-calculated the estuary/nearshore productivity value by diving the target SAR (4.1%, Appendix D) by the ocean productivities. This yields a density-independent estuary productivity of 0.0837 which, when multiplied by the ocean productivities, reproduces the target SAR.

2.3 Life-cycle Models

The life-cycle model is run with each habitat scenario for each species to diagnose which habitat restoration options will likely have the greatest benefit for Chinook salmon, coho salmon, and steelhead populations. The life-cycle model inputs are the life-stage capacities and productivities for each species and subbasin, which are unique to each scenario (Section 2.2). Subbasins and species spawning and rearing ranges are in Appendix A. The model may be run deterministically or stochastically. In either case, the model is initialized by seeding an empty array with spawners for 10 model years. Then the model is allowed to run for 50 years (for Chinook or coho) or 150 years (for steelhead) to burn in. Burn-in periods were selected to produce stable deterministic models. After the burn-in period, the model is run over a 100-year time series. When the model is run deterministically, the equilibrium spawner abundance (N_{eq}) is the modeled number of spawners for the 100th model year. When the model is run stochastically, we report median spawner abundance over the 100 model years. The deterministic model also yields life-stage capacities (c_n) and productivities (p_n) for each species (Moussalli and Hilborn 1986), and the stochastic model yields separate p_n and c_n values for each life stage in each model year.

For all of the salmon life-cycle models, the freshwater life-stages are modeled as a series of linked density-dependent and density-independent stages (Moussalli and Hilborn 1986, Jorgensen et al. 2021). Density-dependent stages are modeled using a Beverton-Holt function with the subpopulation c and p values calculated as described previously. The Beverton-Holt function is:

$$N_{stage+1} = \frac{p \cdot N_{stage}}{1 + \left(\frac{p}{c}\right) \cdot N_{stage}} \quad ,$$

where N_{stage} is abundance of eggs or fish at the beginning of the stage, c is capacity, p is productivity, and $N_{stage+1}$ is abundance of fish at the end of the stage. Density-independent functions have no capacity limit:

$$N_{stage+1} = p \cdot N_{stage} \quad .$$

Estuary and marine productivities are estimated separately. Marine productivities are taken from literature, and estuary productivities are either back-calculated from empirical SAR values (average of the most recent 10 years, Appendix D) divided by the total marine productivity, or, for subyearling Chinook salmon, back-calculated from life history-specific marine survival data (Appendix B). When multiplied together they produce an estuary/ocean productivity value in the range of observed SAR values.

2.3.1 Coho Salmon

The coho salmon life-cycle model has six freshwater life stages that are influenced by freshwater habitat conditions (upstream migration, spawning, egg incubation, fry

colonization, summer rearing, and winter rearing) (Figure 2-7, Table 2-11). Each life stage influences the abundance of salmon at the end of that time period (spawners, eggs, emergent fry, end-of-spring fry, end-of-summer parr, and end-of-winter smolts). Smolts then leave the basin, and experience emigration, estuary, and marine mortality. The parameter estimates for current conditions are summarized in Table 2-12 (capacity) and Table 2-13 (productivity and fecundity). These parameter estimates define the baseline (current condition) scenario for the life-cycle model.

For coho salmon upstream migration and holding, we model prespawn mortality as a function of road density, traffic intensity, and summer and fall precipitation (Feist et al. 2017). We then model the spawning life stage with a Beverton-Holt function, using estimated redd capacity and fecundity to calculate egg production (c) (Table 2-12). We use a density-independent productivity (F) of 2500 eggs per female (Salo and Bayliff 1958), and redd capacity is a function of spawning gravel area divided by redd area (6 m^2) (Gallagher and Gallagher 2005):

$$c_{eggs} = \frac{(Spawning\ gravel\ area)}{Redd\ area} \times fecundity\ .$$

When the number of returning spawners is well-below capacity, the number of eggs is the number of adults × 0.5 × fecundity. Spawning capacity is influenced by migration barriers and wood abundance in the habitat scenarios.

The incubation stage is modeled using density-independent incubation productivity as a function of percent fine sediment and bed scour due to peak flows (Jensen et al. 2009, Zimmerman et al. 2015). We first estimate productivity as a function of percent fine sediment <6.3 mm using:

$$p_{fs} = \frac{1}{1 + e^{-(0.0932 - 0.0022 \cdot sed)}}$$

where p_{fs} is productivity and sed is percent fine sediment in spawning gravel (Bjornn 1969). The maximum incubation productivity with this equation is 0.75 (see Section 3.8.1 for more detail). Incubation survival is then modified by a peak-flow scalar, which alters egg mortality as a function of flood recurrence interval (Zimmerman et al. 2015, Nicol et al. 2022).

Scour-related survival as a function of peak flow is:

$$log_e p_{pf} = a \cdot RI^b$$

where p_{pf} is the annual egg-to-migrant survival, RI is the recurrence interval, and a and b are fitted coefficients (a = -1.869, b = 0.108). We then converted the peak-flow-related p_{pf} values to a multiplier (p_{scalar}) using the equation:

$$p_{scalar} = 1 + \frac{p_{pf_i} - p_{pf_{med}}}{p_{pf_{med}}}$$

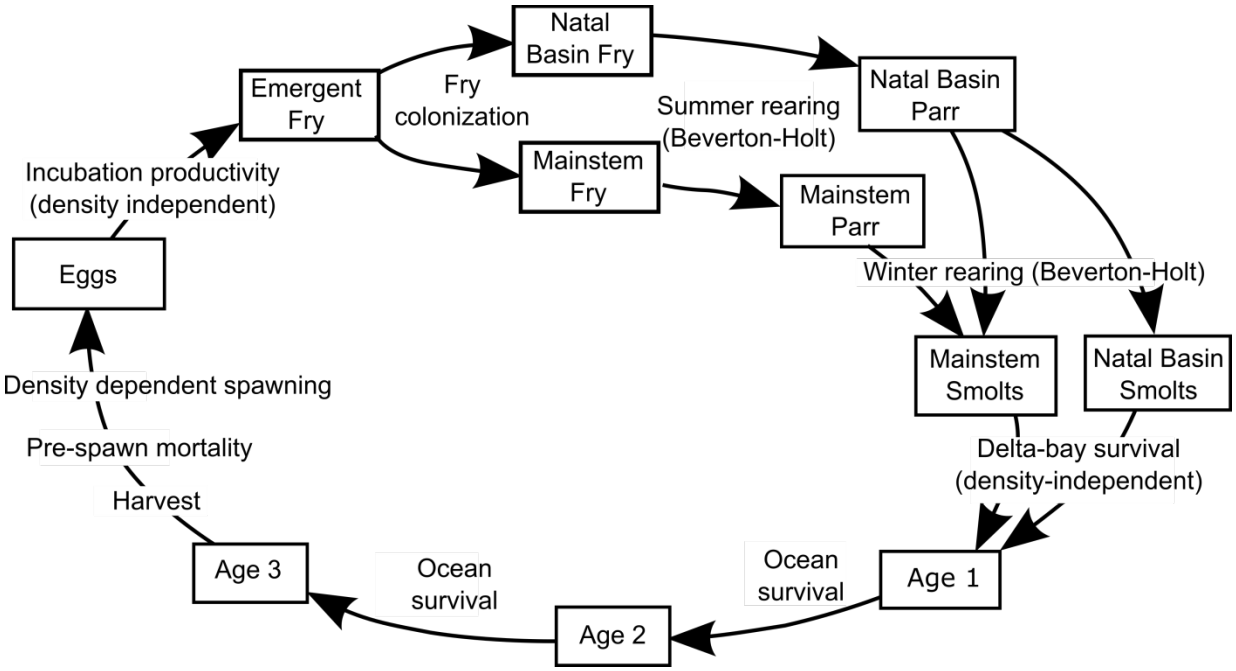

Figure 2-7. Schematic diagram of the life-cycle model for coho salmon.

Table 2-11. Definitions of fish stage-location names in Figure 2-7.

Term	Definition
Spawners/eggs	Spawners are adult coho that have returned to spawn and survived upstream migration; number of eggs is fecundity × number of females (females = spawners × 0.5)
Emergent fry	Fry emerging from the gravel (prior to fry colonization stage)
Natal basin fry	Post-colonization fry staying in their natal subbasin (prior to summer rearing)
Mainstem fry	Post-colonization fry that moved to the mainstem (prior to summer rearing)
Natal basin parr	Juveniles in natal subbasin at end of summer rearing
Mainstem parr	Juveniles in mainstem at end of summer rearing
Natal basin smolts	Juveniles leaving natal subbasin at end of winter rearing
Mainstem smolts	Juveniles leaving mainstem at end of winter rearing
Adults	Age-3 adults returning to spawn

Table 2-12. Density and fecundity data used to estimate life-stage capacities in the coho salmon life-cycle model. Gray shading indicates freshwater life stages. Small stream data from coastal Oregon streams (Nickelson 1998) and large river data from the Skagit River (Beamer and Henderson 1998).

Life Stage (Equation Form)	Data Used to Estimate Life-stage Capacities (current condition)
Upstream migration and holding (density independent)	NA (we found no data to estimate holding capacity)
Spawning (Beverton-Holt)	*Fecundity* = 2500 eggs/female (Salo and Bayliff 1958) *Number of redds:* Digitized or calculated riffle area divided by redd area (6 m^2)
Incubation (density independent)	NA (assumes that density dependence is in the spawning stage, and once eggs are in the gravel there is only density-independent productivity)
Fry colonization (density independent)	NA (assumes that fry rearing and movement are density independent)
Summer rearing (Beverton-Holt)	*Density (fish/m^2):* Bank (natural) = 1.96 Bank (modified) = 0.96 Bar (gravel or sand) = 0.0 Backwater = 1.86 Pool (sm. stream) = 1.7 Riffle (sm. stream) = 0.3 Beaver pond = 1.2 Lake (>5 ha) = 0 Side-channel pool = 1.7 Side-channel riffle = 0.3 Pond/Slough – small = 1.8 Pond/Slough – large = 0.9
Winter rearing (Beverton-Holt)	*Density (fish/m^2):* Bank (natural) = 0.32 Bank (modified) = 0.0 Bar = 0.0 Backwater = 0.64 Pool (sm. stream) = 0.4 Riffle (sm. stream) = 0.01 Beaver pond = 1.2 Marsh = 0.32 Lake (>5 ha) = 0.0025 Side-channel pool = 0.4 Side-channel riffle = 0.01 Pond/Slough – small = 1.8 Pond/Slough – large = 0.9
Estuary	NA (modeled as density independent)
Ocean	NA (modeled as density independent)

Table 2-13. Data used to estimate life-stage productivities in the coho salmon life-cycle model. Gray shading indicates freshwater life stages.

Life Stage (Equation Form)	Productivity or fecundity (current condition)
Upstream migration and holding (density independent)	Varies with percent impervious area and road density (Feist et al. 2017).
Spawning (Beverton-Holt)	Fecundity =2500 eggs/female (Salo and Bayliff 1958).
Incubation (density independent)	Incubation productivity is a function of percent fine sediment <6.3 mm and peak flow.
Fry colonization (Beverton-Holt)	Current condition p = 0.78. Fixed in all scenarios (Reeves et al. 1989).
Summer rearing (Beverton-Holt)	Current condition (low wood abundance, T < 18°C) p = 0.84 (Reeves et al. 1989)
Winter rearing (Beverton-Holt)	Current condition in small stream with (low wood abundance, T < 18°C) p = 0.35, ponds and sloughs p = 0.78, lakes p = 0.4 (Ogston et al. 2015)
Estuary productivity (includes outmigrant productivity)	Productivity p = 0.084. Back-calculated from SAR of 0.041 and annual ocean productivities (i.e., 0.084 * 0.7 * 0.7 = 0.041). Fixed in all scenarios.
Ocean age 1 productivity	Productivity, p = 0.7 (Ricker 1976). Fixed.
Ocean age 2 productivity	Productivity, p = 0.7 (Ricker 1976). Fixed. All adults return to spawn.
Harvest	Optional (currently modeled without harvest).

where p_{pf_i} is the scour-related survival at a given flow as calculated above, and $p_{pf_{med}}$ is the scour-related survival at the median peak flow, or a flow where RI = 2. We multiplied p_{fs} by p_{scalar} to get the final incubation survival (Nicol et al. 2022).

The fry colonization stage was modeled as density-independent, using density-independent spring rearing productivity as the input (Reeves et al. 1989, Nickelson 1998). We also modeled movement of fry downstream from tributaries to the mainstem subbasins, with a fixed percentage of fry (5%) leaving their natal subbasins and moving downstream to the mainstem and adjacent floodplain (Jorgensen et al. 2021). Each tributary subbasin is connected to a mainstem subbasin, so any fry leaving a natal tributary encounter a mainstem subbasin as the first spatial unit downstream, and fry remain in the mainstem subbasin they first encounter through summer rearing. Mainstem subbasins contain both a stretch of large river and the adjacent floodplain features. In the current condition model, coho juveniles occupy all accessible small streams and river-adjacent rearing habitats (side-channels, ponds, lakes, and marshes) within the subbasins they occupy. In floodplain restoration scenarios, coho juveniles also have access to all disconnected pond, marsh, and

lake rearing within the subbasin polygon. Blocked tributaries are not reconnected in floodplain restoration scenarios, but are reconnected in the barrier removal scenarios. Productivity for this stage was set at 0.78 (Reeves et al. 1989).

We modeled the summer rearing stage (fry-to-parr) as a Beverton-Holt function, using summer rearing capacity and density-independent summer rearing productivity as inputs. Summer rearing capacity (*c*) for each subbasin is a function of the cumulative areas of each habitat type in large rivers, small streams, and floodplains, multiplied by type- and season-specific densities to estimate rearing capacity. Fish densities for summer rearing in small streams were from prior studies in western Washington and Oregon (Nickelson 1998), whereas densities in large river habitats were the 95th percentiles of data from the Skagit River (Beamer and Henderson 1998, Beechie et al. 2021b) (Table 2-12). Productivity for this stage is initially set at 0.84 (Reeves et al. 1989) (Table 2-13), but it can be modified by wood abundance and stream temperature.

After summer rearing, a percentage of coho parr move downstream to the nearest mainstem subbasin, and then distribute to all downstream mainstem subbasins for winter rearing. We modeled 11% of parr leaving subbasins under current conditions, 7% when we used historical wood abundance, and 3% when we used historical beaver ponds or floodplain habitat (Beechie et al. 2021b). Our rationale is that fewer parr leave a subbasin as winter rearing habitat quality increases. In the floodplain diagnostic scenario, we modeled an 11% parr outmigration rate from subbasins where there had been no modeled floodplain habitat loss.

The winter rearing stage (parr-to-smolt) is modeled as a Beverton-Holt function, using winter rearing capacity and density-independent winter rearing productivity as inputs. During winter rearing, coho juveniles that have moved downstream to mainstem subbasins can occupy all accessible side channels, ponds, marshes, and lakes within the subbasin boundary, so those habitats are included in the capacity and productivity estimates for each mainstem subbasin. Winter rearing density values for each habitat type were taken from Beechie et al. (2021a). Productivity for this stage was initially set at 0.35 for small streams and large rivers with low wood abundance (75th percentile from Ogston et al. 2015) and 0.78 for ponds (75th percentile from Ogston et al. 2015). Productivity in small streams and large rivers can be further modified by wood abundance.

We modeled coho salmon productivity in the estuary and ocean with fixed productivity rates, followed by prespawn mortality and optional fixed rates of harvest (Table 2-13). We modeled estuary productivity with a productivity of 0.0837, which was back-calculated from a SAR of 0.041 (see Appendix D) divided by two years of ocean productivity (0.7 per year) (Ricker 1976). Based on the recommendation of local biologists, we assumed that all returning spawners were age 3, with harvest rate set to zero in these model runs and prespawn mortality applied prior to spawning.

2.3.2 Summer- and Fall-run Chinook Salmon

The summer- and fall-run Chinook salmon model has eight freshwater life-stages that are influenced by freshwater habitat conditions (upstream migration, spawning, egg incubation, fry colonization, fry-migrant outmigration, subyearling rearing, yearling-type summer rearing, and yearling-type winter rearing) (Figure 2-8, Table 2-14). Each life stage influences the abundance of salmon at the end of that time period (spawners, eggs, emergent fry, fry migrants, subyearling migrants, and yearling migrants). In the models, fry colonize natal subbasin rearing habitats first, and fry exceeding the natal subbasin rearing capacity move downstream through the mainstem to the estuary as fry migrants. Fry migrants are assumed to be in freshwater for one week in their natal basin, followed by a density independent outmigration stage, and parr-sized subyearling migrants are in freshwater for twelve weeks (Jorgensen et al. 2021). Fry outmigration productivity is calibrated so that the modeled ratio of fry outmigrants to parr outmigrants matches the ratio observed at the smolt traps (Tulalip Tribes, WDFW, unpublished data) (Appendix C). Some subyearling migrants become yearlings, with the percentage that stay to become yearlings calibrated to produce the approximate percentage of yearlings observed in adult returns. Yearling migrants are in freshwater through summer and winter, with density-dependent summer and winter rearing survival calculated with Beverton-Holt curves.

Estuary productivity is modeled as a density-dependent movement stage for fry and parr migrants but as a density-independent stage for yearling migrants. Subyearling Chinook enter the estuary as either fry or parr migrants. Estuary occupancy by fry and parr migrants is calculated using a Beverton-Holt curve, and the remainder of the migrants are moved to the nearshore (Figure 2-9). This yields four groups of outmigrants: estuary-rearing fry, estuary-rearing parr, nearshore-rearing fry, and nearshore-rearing parr.

After leaving the estuary, parr-sized and yearling outmigrants experience density-independent survival in the nearshore, Puget Sound, and open ocean. The likelihood of survival to adulthood at a given age is the product of an initial nearshore/sound survival rate and one or more ocean survival rates, depending on how many years the fish spends in saltwater. Subyearling and yearling outmigrants have different nearshore/sound survival rates, which are calibrated to the population age structure and SAR (Appendix C).

The parameter estimates for current conditions are summarized in Table 2-15 (capacity) and Table 2-16 (productivity). Because the two runs (summer and fall) have similar life stages and phenology, they are modeled together and therefore share input parameters.

For upstream migration and holding, we modeled the life stage as density independent with productivities estimated as a function of subbasin-averaged stream temperature (Bowerman et al. 2018):

$$p_{prespawn} = 1 - \frac{e^{(-9.053 + .387T)}}{1 + e^{(-9.053 + .387T)}}$$

Where T is the 7-day average of daily maximum stream temperatures.

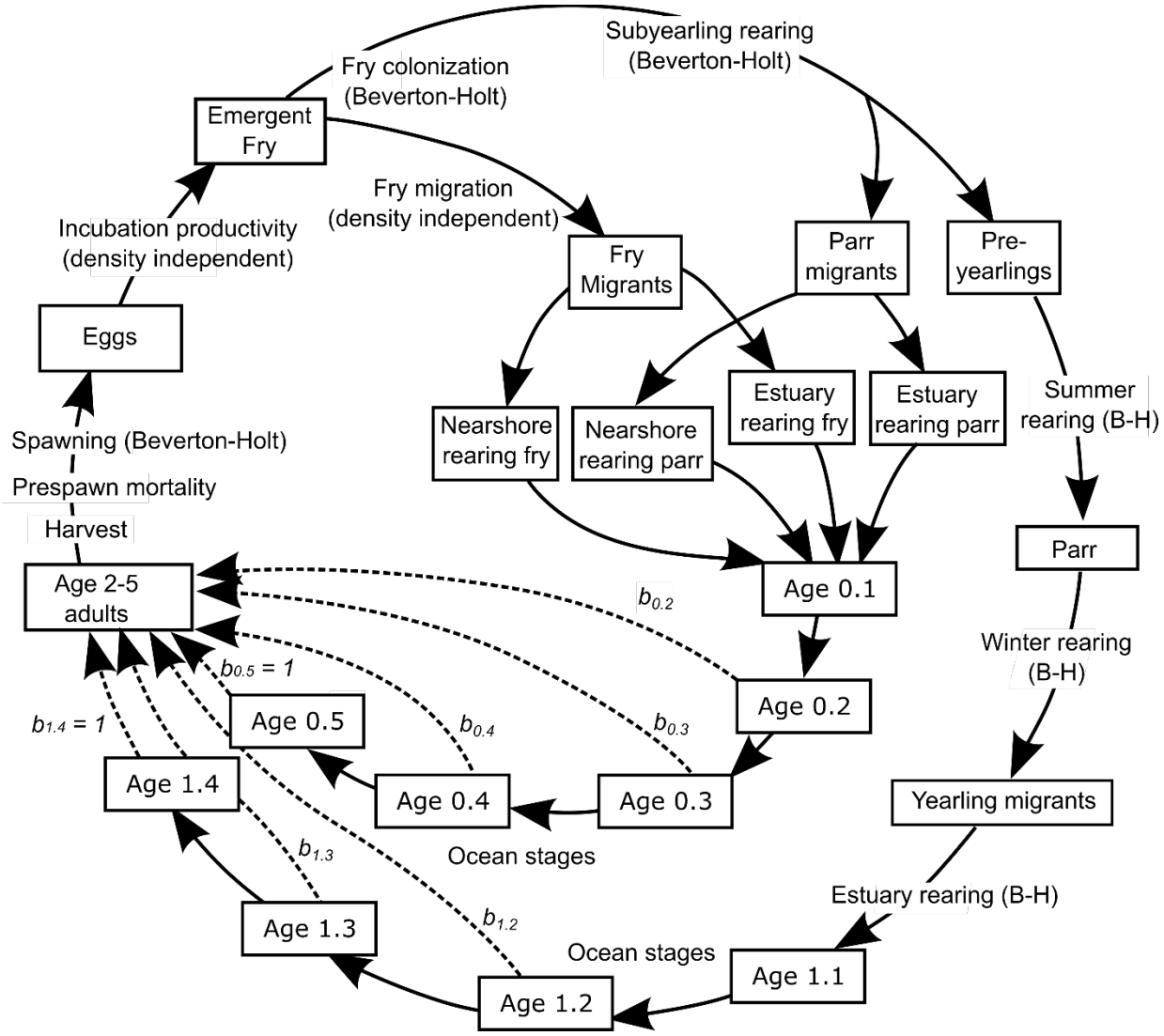

Figure 2-8. Schematic diagram of the life-cycle model for summer- and fall-run Chinook salmon. B-H indicates Beverton-Holt density-dependent calculation for the life stage.

For the spawning life stage (Beverton-Holt form), we use a density-independent fecundity (*F*) of 5400 eggs per female (Greene and Beechie 2004) (Table 2-16). Spawning capacity is expressed as egg capacity (*c*), which is the estimated maximum number of redds multiplied by the fecundity (Table 2-15), and redd capacity is a function of spawning gravel area (digitized from aerial photography or calculated from geomorphic attributes) divided by redd area (14.1 m^2) (Beechie et al. 2006a). When the number of returning spawners is below capacity, the number of eggs is number of spawners × 0.5 × fecundity.

The incubation stage was modeled as for coho salmon, calculating density-independent incubation productivity as a function of fine sediment (p_{fs}). The maximum incubation productivity with this equation is 0.75 for Chinook salmon (see Section 3.8.1 for more detail). The fine-sediment derived productivity was then multiplied by the peak flow scalar (p_{scalar}) to produce the final productivity value.

Table 2-14. Definitions of life stage names in Figure 2-8.

Term	Definition
Spawners/eggs	Spawners are adult Chinook that have returned to spawn and survived upstream migration; number of eggs is fecundity × number of females (females = spawners × 0.5)
Emergent fry	Fry emerging from the gravel (prior to fry colonization stage)
Fry	Post-colonization fry staying in their natal subbasin
Fry migrants	Fry entering estuary after 1 week of rearing
Parr migrants	Subyearlings entering estuary after 12 weeks of rearing
Pre-yearlings	Subyearlings that remain to become yearlings
End-of-summer parr	Juveniles at the end of summer rearing
Nearshore-rearing fry	Fry that pass directly through the estuary into the nearshore without residing for a substantial amount of time in the estuary
Estuary-rearing fry	Fry that rear for several weeks in the estuary after rearing for 1 week in freshwater
Nearshore-rearing parr	12-week old fish that pass directly through the estuary into the nearshore without residing for a substantial amount of time in the estuary
Estuary-rearing parr	Fish that rear for several weeks in the estuary after rearing for 12 weeks in freshwater
Yearling migrants	Juveniles entering estuary at the end of winter rearing
Adults	Age 2-6 adults in ocean prior to returning to spawn

Table 2-15. Density and fecundity data used to estimate life-stage capacities in the summer- and fall-run Chinook salmon life-cycle model. Gray shading indicates freshwater life stages.

Life Stage (Equation Form)	Data Used to Estimate Life-stage Capacities (current condition)
Upstream migration and holding (density independent)	NA (we found no data to estimate holding capacity)
Spawning (Beverton-Holt)	*Fecundity* = 5400 eggs/female (Greene and Beechie 2004) *Number of redds* = Digitized or calculated spawning gravel area divided by redd area (14.1 m^2) (Beechie et al. 2006a)
Incubation (density independent)	NA (assumes that density dependence is in the spawning stage, and during incubation there is only density-independent productivity)
Fry colonization - natal basin and mainstem (Beverton-Holt)	*Density (fish/m^2):* Bank (natural) = 1.27 (Beamer and Henderson 1998) Bank (modified) = 0.14 (King Co., unpublished data) Bar (gravel) = 0.64 (Beamer and Henderson 1998) Bar (sand) = 0.32 Bar (boulder) = 0 Backwater = 1.91 (Beamer and Henderson 1998) Mid-channel = 0.0038 (Jorgensen et al. 2021) Pool (sm. stream and side channel) = 0.05 (J. Thompson, unpublished data) Riffle (sm. stream and side channel) = 0.02 (J. Thompson, unpublished data) Pond/slough (sm. stream, floodplain) = 0.05 (assumed same as ponds above) Marsh = 0 Lake (>5 ha) = 0
Subyearling rearing - (Beverton-Holt)	Same as fry colonization, but multiplied by (t/r)
Summer rearing- Yearling type (Beverton-Holt)	*Density (fish/m^2):* Bank (natural) = 0.47 (E. Lowery, unpublished data) Bank (modified) = 0.02 (E. Lowery, unpublished data) Bar (gravel, sand, boulder) = 0.11 (E. Lowery, unpublished data) Backwater = 0.20 (E. Lowery, unpublished data) Md-channel = 0.0038 (Jorgensen et al. 2021) Pool = 0.20 (E. Lowery, unpublished data) Riffle = 0.05 (E. Lowery, unpublished data) Pond/slough = 0.17 (E. Lowery, unpublished data) Marsh = 0 (no data) Lake (>5 ha) = 0 (no data available)
Winter rearing -Yearling type (Beverton-Holt)	*Density (fish/m^2):* Bank (natural) = 0.03 (King Co., unpublished data) Bank (modified) = 0.08 (King Co., unpublished data) Bar (gravel, sand, boulder) = 0.04 (King Co., unpublished data) Backwater = 0.03 (King Co., unpublished data) Mid-channel = 0.0038 (Jorgensen et al. 2021) Pool = 0.003 (E. Lowery, unpublished data) Riffle = 0 (E. Lowery, unpublished data) Pond/slough = 0.102 (E. Lowery, unpublished data) Marsh = 0 (no data) Lake (>5 ha) = 0 (no data)

Table 2-16. Chinook salmon data used to estimate life-stage productivities in the summer- and fall-run Chinook life-cycle models. Gray shading indicates freshwater life stages.

Life Stage (Equation Form)	Productivity or fecundity (current condition)	
Upstream migration and holding (density independent)	Productivity fixed at 0.95	
Spawning (Beverton-Holt)	Fecundity = 5400 eggs/female	
Incubation (density independent)	Incubation productivity is a function of modeled percent fine sediment <6.3 mm and peak flow.	
Fry colonization and outmigration natal basin/mainstem (density independent)	Colonization, current condition p = 0.894 (1 week) *Stillaguamish:* Outmigration, fixed p = 0.063 *Snohomish:* Outmigration, fixed p = 0.127	
Subyearling rearing - natal basin (Beverton-Holt)	Stream and river, p = 0.26 (11 weeks) Floodplain habitats, p = 0.50	
Subyearling rearing - main stem (Beverton-Holt)	Stream and river, p = 0.26 Floodplain habitats, p = 0.50	
Subyearling outmigration rate	*Stillaguamish*: 99.9%, *Snohomish*: 98.9%	
Yearling summer rearing (Beverton-Holt)	Current condition (low wood abundance, T < 18°C) p = 0.84 (assumed to be the same as coho salmon), mid-channel p = 0.85	
Yearling winter rearing (Beverton-Holt)	Current condition in small stream (low wood abundance, T < 18°C) p = 0.35, ponds and sloughs p = 0.78 (assumed to be the same as coho salmon)	
Estuary and Puget Sound productivity	*Stillaguamish*: Fry and parr migrants (estuary): p = 0.35 Delta-rearing fry and parr migrants (Puget Sound): p = 0.025 Yearling migrants (combined): p = 0.043 *Snohomish*: Fry and parr migrants (estuary): p = 0.35 Delta-rearing fry and parr migrants (Puget Sound): p = 0.036 Yearling migrants (combined): p = 0.043	
Ocean productivity	Age 1: p = 0.6 Age 2: p = 0.7 Age 3: p = 0.8 Age 4: p = 0.9 Age 5: p = 0.9	
Maturation rate	*Stillaguamish:* bsy_2 = 0.050 bsy_3 = 0.34 bsy_4 = 0.92 bsy_5 = 1.0 byr_2 = 0.08 byr_3 = 0.48 byr_4 = 1	*Snohomish*: bsy_2 = 0.021 bsy_3 = 0.17 bsy_4 = 0.85 bsy_5 = 1.0 byr_2 = 0.08 byr_3 = 0.48 byr_4 = 1
Harvest (optional)	Modeled without harvest	

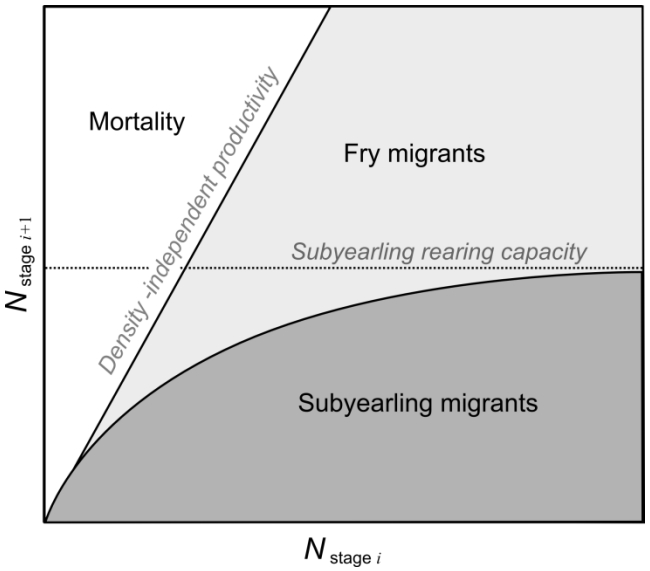

Figure 2-9. Illustration of the Beverton-Holt density-dependent movement calculations in the summer- and fall-run Chinook model for fry colonization and estuary rearing. For colonization, fry between the Beverton-Holt curve and the density independent productivity line (light gray) leave the river in the first week as fry migrants; fry below the Beverton-Holt curve (dark gray) stay in freshwater to become subyearling or yearling migrants. For estuary rearing, fry between the Beverton-Holt curve and the density independent productivity line move to the nearshore as fry, and fry below the Beverton-Holt curve stay in the estuary and grow to parr size before moving to the nearshore.

Fry colonization (week one of Chinook rearing) in natal subbasins was modeled with density-dependent movement using the Beverton-Holt function (Figure 2-9) (Jorgensen et al. 2021). Fry below the Beverton-Holt curve remain in their natal stream, and fry above the curve move downstream to the estuary, creating two age groups: fry migrants and subyearlings. Of the subyearlings, a percentage of them leave as subyearling migrants after 11 more weeks of rearing, and the remainder stay for summer and winter rearing (Beverton-Holt functions), and then leave the basin as yearling migrants.

Fry rearing survival is density independent and subyearling and yearling rearing survival are density dependent (Anderson and Topping 2018). Subyearling-migrants are redistributed in equal proportions across the natal basin and all mainstem reaches downstream of each subbasin after the first week (Jorgensen et al. 2021). Subyearlings experience density-dependent rearing in their new locations, giving subyearlings the average rearing experience of all reaches they pass through.

For Chinook salmon, we estimate subyearling rearing capacity as a function of daily maximum fish density, mean residence time, and the temporal extent of the rearing period to account for multiple groups of fish moving through the same habitats (Jorgensen et al. 2021):

$$c = d \cdot A \cdot \frac{t}{r}$$

where, c is capacity (# of fish), d is maximum daily density (fish/ha), A is habitat area (ha), t is the extent of the rearing period (weeks), and r is the mean residence time (weeks). In the Stillaguamish and Snohomish basins, we used a total rearing period (t) of 12 weeks and mean residence time in the natal subbasin (r) of 12 weeks, so c is $d \cdot A \cdot 1$. For yearling type juveniles, summer and winter rearing capacities were simply

$$c = d \cdot A$$

because there is only one cohort residing through summer and winter (i.e., t = r for each season).

Rearing densities were from prior studies (Jorgensen et al. 2021) as well as from local data, and all density parameters are shown in Table 2-15. Productivity for the fry colonization stage (first week) under current conditions is 0.894 (Table 2-16). The cumulative 12-week productivity for subyearling rearing under current conditions is 0.26 for streams and rivers and 0.50 for floodplain habitats, including the fry colonization stage (Table 2-16) (Jorgensen et al. 2021). We found no yearling survival data specific to summer or winter rearing in natal streams, so we applied the coho salmon summer and winter rearing productivities to Chinook yearling summer and winter rearing.

We modeled estuary rearing as density dependent, with capacity estimated as described in Section 2.2.2. For the HARP model we chose to use a mid- to upper-range value of p = 0.35 for the density-dependent Chinook fry migrant estuary rearing life stage (Appendix B). Based on Skagit River data showing that only ~0.2% of nearshore rearing fry survive to become spawning adults (Beamer et al. 2005), we assume 100% mortality for nearshore rearing fry for simplicity. The remaining three groups have similar SAR values as they all leave the estuary at parr size (i.e., estuary rearing fry achieve parr size before they leave the estuary) (Table 2-16). We used an SAR of 1.1% in the Snohomish basin and 1.2% in the Stillaguamish basin (Appendix D), where SAR is survival to the end of the first ocean year.

Each age class of fish in the ocean also has a propensity to spawn (b), which we initially adopted from the Chehalis basin (Jorgensen et al. 2021). We then modified the maturation rates for each population so that the model reproduced the saltwater age structure of recent spawning populations in the Stillaguamish and Snohomish River basins (Table 2-17, Appendix E).

$$\frac{n_{x.i}}{n_{x.i-1}} = \frac{s_i b_{x,i} \cdot (1 - b_{x.i-1})}{b_{x.i-1}} \quad \text{, and} \quad b_{x.final} = 1$$

where $n_{x.i}$ is the number of returning spawners of freshwater age x and saltwater age i, s_i is the ocean survival rate for individuals of saltwater age i, $b_{x.i}$ is the maturation constant for individuals of freshwater age x and saltwater age i, and $b_{x.final}$ is the maturation constant for individuals remaining in the ocean up to the greatest possible saltwater age allowed for the model for each freshwater age. The variable $b_{x.final}$ was always set to 1, and the final year

Table 2-17. Percentages of freshwater and saltwater age groups in adult natural spawning returns for summer- and fall-run Chinook in the Stillaguamish, Snoqualmie, and Skykomish River basins. These data were used to calibrate Chinook maturation rates in the HARP model. Percentages shown for the Skykomish do not total 100% due to rounding, but age structure coefficients used in the model account for 100% of returners. Stillaguamish data from Kate Konoski, Stillaguamish Tribe, unpublished data, and Snohomish data are from Diego Holmgren, Tulalip Tribes, unpublished data.

	Age (fw.sw)						
	0.2	**0.3**	**0.4**	**0.5**	**1.2**	**1.3**	**1.4**
Stillaguamish	8%	36%	52%	4%			
Snohomish (Snoqualmie)	3%	18%	56%	8%	1%	7%	7%
Snohomish (Skykomish)	3%	14%	54%	9%	3%	9%	7%

was determined by the age structure data. When the model is run without stochastic variation in stream flow or temperature, it will produce an age structure that closely matches Table 2-17. However, the stochastic model may not produce the same age structure each year because annual variation in freshwater survival will alter the number of fish in each cohort, leading to differences in age structure from year to year.

In the Stillaguamish basin, we used age groups from coded wire tag and scale samples in adult natural spawning (hatchery and natural origin) returns for summer- and fall-run Chinook (Appendix E). The vast majority of returning adults in the Stillaguamish River basin were fall-run and age-0 outmigrants. There were insufficient data to determine summer-run age structure, or to model summer-run and winter-run populations separately. In the Snohomish River basin, we estimated Chinook age structure based on data from 2006-2020 (Diego Holmgren, Tulalip tribes, personal communication). Chinook salmon in the Snohomish River basin have a significant percentage of age-1 outmigrants. Age-1 outmigrants tend to return as 4 and 5 year-old adults, whereas age-0 outmigrants tend to return as 3 and 4 year-old adults. In the Stillaguamish basin, we used the age-1 outmigrant saltwater age structure from the Snohomish basin to estimate saltwater residency of the small portion of returning yearling-type individuals.

2.3.3 Summer- and Winter-run Steelhead

The steelhead life-cycle model has nine life stages that are influenced by freshwater habitat conditions: upstream migration, spawning, egg incubation, age-0+ summer rearing, age-1 winter rearing, age-1+ summer rearing, age-2 winter rearing, age-2+ summer rearing, and age-3 winter rearing (Figure 2-10). Definitions of fish stage-location names in boxes of Figure 2-10 are in Table 2-18. Habitat conditions for each life stage influence the abundance of steelhead at the end of that time period. Steelhead may smolt at age 1, 2 or 3, which we calibrate in the model using local age structure data. Because some age-1 parr move down to the mainstem at the end of the first winter (not shown in diagram), age-1+

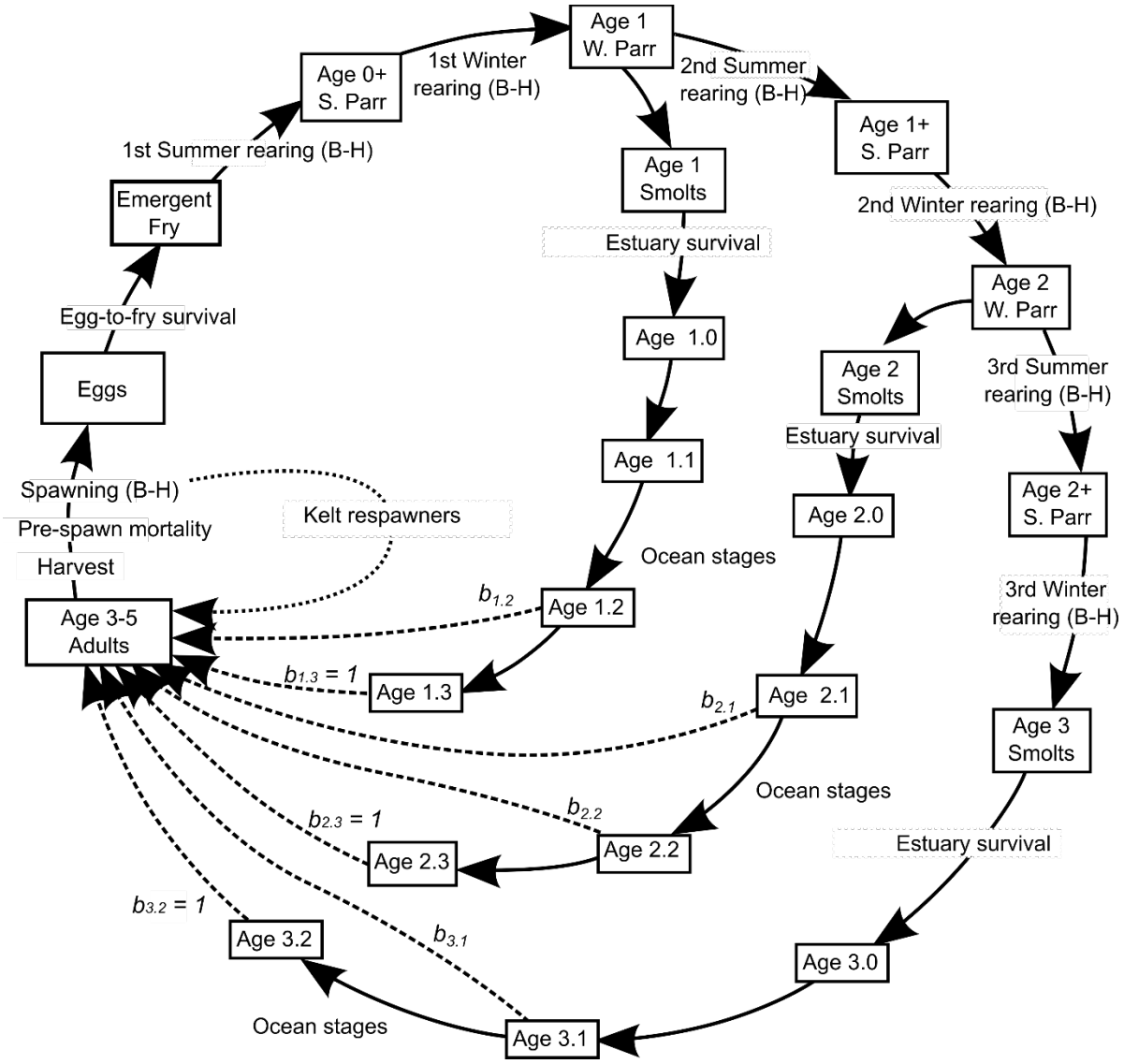

Figure 2-10. Schematic diagram of the life-cycle model for steelhead. Natal basin and mainstem splits not shown for simplicity.

and-2+ parr are split into natal and mainstem groups. The parameter estimates for current conditions are summarized in Table 2-19 (capacity) and Table 2-20 (productivity). These parameter estimates define the baseline scenario (current habitat conditions) for the life-cycle model. In the next section we describe how we modify these parameter estimates given a change to historical habitat conditions for any of the habitat factors that we model in our diagnostic scenarios.

For upstream migration and holding under current conditions, we model the stage as density-independent using an estimated productivity of 0.95 scaled by the passage rating and weighted by egg capacity, with no additional mortality due to temperature or

development for winter-run steelhead. For summer-run steelhead, we modeled the life stage as density independent with productivities estimated as a function of subbasin-averaged stream temperature (Bowerman et al. 2018):

$$p_{prespawn} = 1 - \frac{e^{(-9.053 + .387T)}}{1 + e^{(-9.053 + .387T)}}$$

Where T is the 7-day average of daily maximum stream temperatures.

Table 2-18. Definitions of fish stage-location names in Figure 2-9. Migration from natal basin to mainstem not shown in Figure, but modeled natal basin and mainstem groups are included here for completeness.

Term	Definition
Spawners/eggs	Spawners are adults that have returned to spawn and survived upstream migration; number of eggs is fecundity x number of females (females = spawners x 0.5)
Fry	Fry emerging from redds (all stay in their natal subbasin)
Age-0+ summer parr	Juveniles at end of first summer rearing (all in natal subbasin)
Age-1 winter parr	Juveniles at end of first winter rearing that do not go the estuary as smolts (all in natal subbasin)
Age-1 smolts	Age-1 juveniles entering estuary at end of first year winter rearing (all from natal subbasin)
Age-1+ natal basin summer parr	Age-1+ juveniles in natal subbasin at end of summer rearing
Age-1+ mainstem summer parr	Age-1+ juveniles in mainstem at end of summer rearing
Age-2 natal basin winter parr	Age-2 juveniles in natal subbasin at end of winter rearing
Age-2 mainstem winter parr	Age-2 juveniles in mainstem at end of winter rearing
Age 2 natal basin smolts	Age-2 juveniles entering estuary from natal subbasin at end of second year winter rearing (all from natal subbasin)
Age 2 mainstem smolts	Age-2 juveniles entering estuary from mainstem at end of second year winter rearing (all from natal subbasin)
Age 2+ natal basin summer parr	Age-2+ juveniles in natal subbasin at end of summer rearing
Age 2+ mainstem summer parr	Age-2+ juveniles in mainstem at end of summer rearing
Age 3 natal basin smolts	Age-3 juveniles entering estuary from natal subbasin at end of third year winter rearing (all from natal subbasin)
Age 3 mainstem smolts	Age-3 juveniles entering estuary from mainstem at end of third year winter rearing (all from natal subbasin)
Age 3-7 adults	Adults returning to spawn (all age classes)

Table 2-19. Data used to estimate life-stage capacities in the steelhead life-cycle model. Gray highlight indicates freshwater life stages.

Life Stage (Equation Form)	Data Used to Estimate Life-stage Capacities (current condition)
Upstream migration and holding (density independent)	NA (we found no data to estimate holding capacity)
Spawning (Beverton-Holt)	Fecundity = 5400 eggs/female for maiden spawners; 8000 for respawners *Number of redds:* Spawning gravel area divided by redd area (5.4 m^2)
Incubation (density independent)	NA (assumes that density dependence is in the spawning stage, and once eggs are in the gravel there is only density-independent productivity)
First year summer rearing -- age 0+ (Beverton-Holt)	*Density (fish/m^2):* Bank (natural) = 1.27 Bank (modified) = 0.64 Bar (boulder) = 1.59 Bar (gravel) = 1.59 Bar (sand) = 0 Backwater = 1.27 Mid-channel = 0.064 Pool (sm. stream) = 0.70 Riffle (sm. stream) = 0.53 Pond (<5 ha) = 0 Lake (>5 ha) = 0 Marsh = 0 Side-channel pool = 0.70 Side-channel riffle = 0.53 Floodplain pond (<5 ha) = 0 Slough = 0
First year winter rearing – age 1 (Beverton-Holt)	*Density (fish/m^2):* Bank (natural) = 0.31 Bank (modified) = 0.31 Bar (boulder) = 0.31 Bar (gravel) = 0.31 Bar (sand) = 0 Backwater = 0 Mid-channel = 0.016 Pool (sm. stream) = 0.16 Riffle (sm. stream) = 0.11 Pond (<5 ha) = 0.03 Lake (>5 ha) = 0 Marsh = 0 Side-channel pool = 0.16 Side-channel riffle = 0.11 Floodplain pond (<5 ha) = 0.03 Slough = 0

Table 2-19 (cont.). Data used to estimate life-stage capacities in the steelhead life-cycle model. Gray highlight indicates freshwater life stages.

Life Stage (Equation Form)	Data Used to Estimate Life-stage Capacities (current condition)
Second and third year summer rearing -- age 1+ and 2+ (Beverton-Holt)	*Density (fish/m²)* Bank (natural) = 0.39 Bank (modified) = 0.20 Bar (boulder) = 0.49 Bar (gravel) = 0.49 Bar (sand) = 0 Backwater = 0.39 Mid-channel = 0.11 Pool (sm. stream) = 0.18 Riffle (sm. stream) = 0.07 Pond (<5 ha) = 0.07 Lake (>5 ha) = 0 Marsh = 0 Side-channel pool = 0.18 Side-channel riffle = 0.07 Floodplain pond (<5 ha) = 0.07 Slough = 0
Second and third year winter rearing – age 2 and 3 (Beverton-Holt)	*Density (fish/m²)* Bank (natural) = 0.096 Bank (modified) = 0.096 Bar (boulder) = 0.096 Bar (gravel) = 0.096 Bar (sand) = 0 Backwater = 0 Mid-channel = 0.027 Pool (sm. stream) = 0.09 Riffle (sm. stream) = 0.04 Pond (<5 ha) = 0.01 Lake (>5 ha) = 0 Marsh = 0 Side-channel pool = 0.09 Side-channel riffle = 0.04 Floodplain pond (<5 ha) = 0.01 Slough = 0
Estuary rearing	NA (currently modeled as density independent)

Table 2-20. Data used to estimate life-stage productivities in the steelhead life-cycle model. Gray shading indicates freshwater life stages.

Life Stage (Equation Form)	Productivity or Fecundity (current condition)			
Upstream migration and holding	Current and historical, $p = 0.95$.			
Spawning	Fecundity = 5400 eggs/female for maiden spawners; 8000 eggs/female for respawners (Jorgensen et al. 2021).			
Incubation (density independent)	$p = \frac{1}{1 + e^{-(1.989 - 0.185 \cdot sed)}}$			
First year summer rearing	Current condition in small stream and large river (low wood abundance, T < 18°C) $p = 0.60$ (Grantham et al. 2012), pond and floodplain habitats $p = 0.74$ (Martens and Connolly 2014).			
First year winter rearing	Current condition in small stream and large river (low wood abundance, T < 18°C) $p = 0.49$ (McHugh et al. 2017); side-channel, pond, and floodplain habitat $p = 0.52$ (Martens and Connolly 2014).			
Second and third year summer rearing	Current condition in small stream and large river (low wood abundance, T < 18°C) $p = 0.72$ (0.85^2, based on (Harvey et al. 2005)), pond and floodplain habitats $p = 0.74$ (Martens and Connolly 2014).			
Second and third year winter rearing	Current condition: small stream and large river with low wood abundance, and pond and floodplain habitat $p = 0.58$ (McHugh et al. 2017).			
Smolt rate	Stillaguamish:		Snohomish:	
	Winter Run:	Summer Run:	Winter Run:	Summer Run:
	Age1 = 0.028	Age1 = 0.005	Age1 = 0.028	Age1 = 0.005
	Age2 = 0.718	Age2 = 0.629	Age2 = 0.718	Age2 = 0.629
	Age3 = 1	Age3 = 1	Age3 = 1	Age3 = 1
Estuary productivity	Winter-run $p = 0.022$, summer-run $p = 0.024$. Back-calculated from SAR of 0.016 and annual ocean productivities. Fixed in all scenarios.			
Ocean productivity	$p = 0.8$ per year.			
Maturation rate	*Stillaguamish*:		*Snohomish:*	
	Winter Run:	Summer Run:	Winter Run:	Summer Run:
	$b_{1.1} = 0.35$	$b_{1.2} = 0.45$	$b_{1.1} = 0.35$	$b_{1.2} = 0.45$
	$b_{1.2} = 1$	$b_{1.3} = 1$	$b_{1.2} = 1$	$b_{1.3} = 1$
	$b_{2.1} = 0.45$	$b_{2.1} = 0.03$	$b_{2.1} = 0.45$	$b_{2.1} = 0.03$
	$b_{2.2} = 0.97$	$b_{2.2} = 0.95$	$b_{2.2} = 0.97$	$b_{2.2} = 0.95$
	$b_{2.3} = 1$	$b_{2.3} = 1$	$b_{2.3} = 1$	$b_{2.3} = 1$
	$b_{3.1} = 0.32$	$b_{3.1} = 0.04$	$b_{3.1} = 0.32$	$b_{3.1} = 0.04$
	$b_{3.2} = 1$	$b_{3.2} = 1$	$b_{3.2} = 1$	$b_{3.2} = 1$
Respawn rate	0.049 (from age structure data)			
Harvest (optional)	No harvest in these model runs.			

Egg capacity (c) is the redd capacity multiplied by fecundity (Table 2-19). Redd capacity is spawning gravel area (digitized from aerial photography for large rivers or calculated from geomorphic attributes for small streams) divided by redd area (5.4 m^2) (Orcutt et al. 1968). Fecundity (F) is 5,400 eggs per female for first-time spawners (Stober et al. 1983) (unpublished Queets River data) and 8,000 eggs per female for repeat spawners (R2 Resource Consultants, Inc. 2008) (Table 2-20). When the number of returning spawners is well below capacity, the number of eggs is the number of adults × 0.5 × fecundity.

The incubation stage is modeled similarly to coho salmon, calculating density-independent incubation productivity as a function of fine sediment (p_{fs}). The maximum incubation productivity with this equation is 0.52 for steelhead (see Section 3.8.1 for more detail). The fine-sediment derived productivity was then multiplied by the peak flow scalar (p_{scalar}) to produce the final productivity value (Nicol et al. 2022).

The age-0+, age-1+, and age-2+ summer and winter rearing stages are modeled as Beverton-Holt functions, using summer and winter rearing capacity and density-independent summer and winter rearing productivity (Beechie et al. 2021b, Jorgensen et al. 2021). Based on fish age data in the Snohomish River basin from 2013-2020 (Pete Verhey, WDFW, unpublished data), we calibrated the percentage of age-1 juveniles leaving the Stillaguamish and Snohomish River basins as smolts after their first winter to produce 10.4% of first-time returning adults as age-1 smolts, 78.0% of returning adults as age-2 smolts, and 11.3% of returning adults as age-3 smolts (Table 2-21). The remaining juveniles leave the basin at age-4 and comprise just 0.3% of the returning adults, so we did not include age 4 smolts in the model. Smolting constants were calibrated alongside estuary survival constants using the R package 'nloptr' (Johnson 2022)(Appendix C).

Some steelhead parr move downstream from their natal basin to the mainstem at the end of the first summer, and another percentage at the end of their first winter. For the end-of-summer migration, we estimated that 10% of juveniles leave subbasins <150 km^2, 2% of juveniles leave subbasins 150-450 km^2, and no fish leave subbasins >450 km^2 (Jorgensen et al. 2021, Beechie et al. 2021a). For the end-of-winter migration, we estimated that 18% of juveniles leave subbasins <50 km^2, 10% of juveniles leave subbasins 50-450 km^2, and no fish leave subbasins >450 km^2.

We modeled estuary and Puget Sound productivity with values of 0.022 for winter-run steelhead and 0.024 for summer-run steelhead, which were back-calculated to achieve a total weighted average SAR of ~1.6% (N. Kendall, personal communication). Once in the ocean, all fish receive the same fixed annual productivity rates (0.8), followed by harvest (optional) (Table 2-20). Each age class of fish in the ocean also has a maturation rate (b), so some proportion of each age class leaves the ocean population each year. We calibrated the maturation rates for winter steelhead so that the overall model age structure matched the observed age structure from the Snohomish River basin. There were no recent data for the Stillaguamish River basin, so we used the Snohomish age structure in both basins (Tables 2-21 and 2-22). A percentage of females for each age class also survive spawning and return to spawn again, and the observed respawn rate in these basins is between 4 and 5%. We assumed a 4.9% respawn rate based on Snohomish River data.

Table 2-21. Age at first spawning for winter-run steelhead in the Stillaguamish and Snohomish River basins.

	Age (fw.sw)							
Basin	**1.1**	**1.2**	**2.1**	**2.2**	**2.3**	**3.1**	**3.2**	**4.1**
Stillaguamish	4%	6%	39%	38%	1%	4%	7%	0%
Snohomish	4%	6%	39%	38%	1%	4%	7%	0%

Table 2-22. Age at first spawning for summer-run steelhead in the Stillaguamish and Snohomish River basins.

	Age (fw.sw)							
Basin	**1.2**	**1.3**	**2.1**	**2.2**	**2.3**	**3.1**	**3.2**	**4.1**
Stillaguamish	1%	1%	2%	74%	3%	1%	18%	0%
Snohomish	1%	1%	2%	74%	3%	1%	18%	0%

3. Modeled Effects of Habitat Change on Life-Stage Capacity and Productivity

The HARP Model simulates effects of habitat change from historical to current conditions, as well as effects of future restoration actions or climate change. In each case, the model relies on functional relationships that relate a change in a habitat condition to a change in a life-stage capacity or productivity (or both). The following descriptions of model functions are excerpted or modified from Appendix I in Beechie et al. (2021b), summarized from HARP model publications (Jorgensen et al. 2021, Fogel et al. 2022), or modified for application in the Stillaguamish and Snohomish River basins.

In this project we model only changes from historical to current conditions, and use those model results to construct diagnostic habitat scenarios. The purpose of the diagnostic scenarios is to help understand the relative restoration potential of each restoration action for each species. We developed a current condition scenario and eight diagnostic habitat scenarios (Table 3-1) to evaluate influences of the potential restoration actions on coho salmon, Chinook salmon, and summer- and winter-run steelhead (Beechie et al. 2021a).

Table 3-1. Description of the current condition scenario and the eight diagnostic habitat scenarios evaluated with the life-cycle models.

Scenario	Description
Current	Current conditions for all habitat variables
No migration barriers	Current conditions for all habitats but migration barriers are removed
Historical fine sediment	Current conditions with historical fine sediment and incubation productivity
Historical wood abundance	Current conditions with historical wood abundance in small streams and large rivers (current temperatures)
Historical shade	Current conditions with historical shade and temperature in small streams and large rivers
Historical large river length and bank conditions	Current conditions with historical main-channel length and no large river bank armoring
Historical beaver ponds	Current conditions with historical beaver pond areas in suitable small streams
Historical floodplain habitat	Current conditions with historical side channel length, marsh area, and pond area in floodplains and with reduced temperatures in shallow, unconfined streams. Manmade habitat features (e.g., intentionally created ponds) are retained.
Historical estuary habitat	Current conditions with historical distributary edge habitat and tidal channel area

3.1 Overview of Diagnostic Scenarios

The current conditions scenario sets all habitats to current conditions, which produces life-cycle model input data containing all of the current life-stage capacities and productivities for each species. In the eight diagnostic scenarios, one habitat factor at a time is set to historical conditions while keeping all others at current conditions. These diagnostic scenarios are used to evaluate which habitat losses most constrain recovery of salmon and steelhead populations for each subpopulation.

In the following sections we describe how we modeled the effects of each habitat change on habitat capacity and productivity to produce the diagnostic scenarios. Each habitat change affects one or more life stage parameters for one or more species in the HARP Model. Tables 3-2 and 3-3 summarize which life stage parameters are modified by each habitat factor for each species.

Table 3-2. Checklist of life stage capacities (c) and productivities (p) affected by each habitat factor for coho salmon and steelhead (c_{egg} = egg capacity, p_{incub} = incubation productivity, c_{sr} = summer rearing capacity, p_{sr} = summer rearing productivity, c_{wr} =is winter rearing capacity, p_{wr} = winter rearing productivity).

Habitat factor	Spawning Capacity	Egg Incubation	Summer Rearing[1]		Winter Rearing[1]	
	c_{egg}	p_{incub}	c_{sr}	p_{sr}	c_{wr}	p_{wr}
Barriers	X[2]		X[3]	X[3]	X[3]	X[3]
Fine sediment		X				
Wood loading	X		X	X	X	X
Shade			X	X		
Bank condition			X	X	X	X
Beaver pond area	X		X	X	X	X
Floodplain	X		X	X	X	X

1. One year of rearing for coho salmon; three years of rearing for steelhead.
2. Barriers additionally affect upstream migration productivity, p_{migr}.
3. Effect expressed only when barrier is 100% blocking.

Table 3-3. Checklist of life stage capacities (c) and productivities (p) affected by each habitat factor for summer- and fall-run Chinook (column headings as in Table 3-2 except c_{sub} = subyearling rearing capacity and p_{sub} = subyearling rearing productivity).

Habitat factor	Spawn. Capacity	Egg Incub	Subyearling Rearing		Yearling Summer Rearing		Yearling Winter Rearing	
	c_{egg}	p_{incub}	c_{sub}	p_{sub}	c_{sr}	p_{sr}	c_{wr}	p_{wr}
Barriers	X[1]		X[2]	X[2]	X[2]	X[2]	X[2]	X[2]
Fine sediment		X						
Wood loading	X		X	X	X	X	X	X
Shade				X	X	X		
Bank condition			X	X	X	X	X	X
Beaver pond area	X		X	X	X	X	X	X
Floodplain	X		X	X	X	X	X	X

1. Barriers additionally affect upstream migration productivity, p_{migr}.
2. Effect expressed only when barrier is 100% blocking.

3.2 Migration Barrier Effects

In the HARP model migration barriers directly influence spawning capacities, rearing capacities, and prespawn productivity, and they indirectly affect prespawn, incubation and rearing productivity (Beechie et al. 2021b). Prespawn productivities are affected by migration barriers both directly and indirectly (via weighting). Migration barriers influence upstream migration of all adult salmon and steelhead, but not upstream migration of juveniles as most migration is in the downstream direction.

3.2.1 Spawning and Rearing Capacity

We calculated reduced spawning and rearing capacity in all anadromous salmon reaches upstream of a barrier based on the passage ratings at each barrier (Beechie et al. 2021b, Jorgensen et al. 2021). Where there were multiple barriers in sequence on a stream, the passability ratings were multiplicative, so that the proportion of returning spawners was successively reduced with each barrier. For example, spawning capacity above a single barrier with a passage rating of 0.33 is ~1/3 of its full capacity, whereas spawning capacity above three barriers with ratings of 0.33 is ~1/27 (0.036) of its full capacity.

These reduced capacities also influenced subbasin-averaged productivities through weighting of reach-level productivities for incubation and prespawn life stages. Barriers do not influence juvenile movements in the model, as most juvenile movements are in the downstream direction (Beechie et al. 2021b). Upstream movement of juveniles within

subbasins is implicitly modeled, as juveniles have access to all available habitat in a subbasin except upstream of fully blocking migration barriers. This also applies to floodplain segments, in which fish have access from the mainstem to all available marsh, pond, side channel, and tributary habitat within the floodplain boundary. We do not model upstream movement of juveniles between subbasins (e.g., upstream between mainstem reaches). For the historical condition all man-made barriers were removed from the model, and all reach-level cumulative passage ratings were set to 1.

Rearing capacity is not affected by a barrier unless the passage rating is 0. When the passage rating is >0, we assume that some spawners can make it to that reach, and the juveniles they produce have access to the full rearing capacity. When the passage rating is 0, we assume that no spawners access that reach and no juveniles will be produced to use that habitat. Therefore, we do not include the rearing capacity of reaches above barriers with a passage rating of 0 in the total rearing capacity for a subbasin. The elimination of rearing capacities in fully inaccessible reaches also influences subbasin-averaged rearing productivities because rearing productivities in inaccessible reaches arre not included in the weighted average.

3.2.2 Prespawn and Incubation Productivity

We weight both prespawn and incubation productivity by egg capacity. That is, when we calculate the subbasin-level average prespawn productivity we weight the reach-level productivities by egg capacity, which is reduced above each barrier using the passage rating as described in Section 3.2.1. Similarly, incubation productivity for a subbasin is calculated as the weighted average of reach-level incubation productivities, where the weight is egg capacity.

3.3 Wood Abundance Effects

3.3.1 Spawning Capacity

We first estimated the change in pool spacing in small streams with changing wood abundance (Section 2.1.3), and then estimated the change in spawning gravel area from low wood abundance (current) to high wood abundance (historical) using the following equation:

*Spawning Area = # pools * wetted width * (wetted width * 0.5).*

Current spawning areas in large rivers were manually digitized from aerial imagery, and increased by 30% for historical spawning areas (Section 2.1.4). All small-stream and large-river spawning areas were then summed to the subbasin level. Total spawning area was divided by redd area for each species to estimate species-specific redd capacities under both current and historical conditions (Section 2.3), and historical and current redd capacities were multiplied by species-specific fecundities to calculate egg capacity for each species and subbasin.

3.3.2 Summer Rearing Capacity

In the HARP model, wood loading modifies rearing capacity in all large river, small stream, and side channel habitats. For summer rearing in small streams and side channels (all species), we modeled the effect of wood abundance on rearing capacity through changes in pool area as a function of land cover, using land cover type as a surrogate for wood loading. As described earlier, we stratified habitat surveys conducted by WDFW by slope class and land cover, and extrapolated those values to the remaining reaches in each category to calculate current pool area (Beechie et al. 1994, 2001). We set all pool areas to the reference condition to calculate historical pool areas. Changes in rearing capacity were then estimated as the change in pool and riffle areas multiplied by their respective rearing densities for each species.

In large rivers, we modified summer rearing capacity for all species using an estimated increase in wood cover in edge habitats, which increases juvenile rearing densities. We relied on data from the Skagit River basin to document differences in juvenile fish densities with and without wood cover in edge habitats (bank and bar edge) (Beamer and Henderson 1998) to estimate habitat-type specific density and productivity multipliers. Bar multipliers ranged from 1.011 to 1.2 across species and life stages, and bank edge multipliers ranged from 1.052 to 1.21 (Table 3-4). We then used estimates of percent wood cover under historical conditions from Beechie et al. (2021b) to calculate a weighted average wood multiplier for each species and subbasin, where the weights were proportions of bank edge and bar edge length. The multipliers are then used to modify large river rearing capacities for historical conditions (Section 2.2). For the restoration scenarios, we scale the capacity multiplier between 1 and the historical value depending on restoration intensity, so that a multiplier of 1 = no restoration, and the full multiplier = 100% restoration.

Table 3-4. Habitat- and season-specific wood multipliers for each species.

	Wood multiplier		
Unit type/season	**Coho**	**Chinook subyearling/yearling**	**Steelhead (all ages)**
Bank edge - summer	1.2	1.16/1.16	1.052
Bar edge - summer	1.02	1.03/1.03	1.011
Bank edge - winter	1.21	NA/1.21	1.069
Bar edge - winter	1.09	NA/1.09	1.108

3.3.3 Winter Rearing Capacity

For winter rearing capacity in small streams and side channels (all species), we estimated that winter pool areas were 30% of summer pool areas (Beechie et al. 2021b). We made that adjustment based on habitat surveys in the same reaches at summer and winter base flows, which showed that much more of the habitat is classified as high velocity riffles in winter than in summer (Beechie 1990). The remaining 70% of summer pool area was reclassified as riffle. Changes in rearing capacity were then estimated as the change in pool and riffle areas multiplied by their respective rearing densities for each species.

For large river winter rearing habitat capacity, the basin-specific wood multipliers were calculated as above for summer rearing habitat and were used to increase rearing capacity under historical conditions and in restoration scenarios.

3.3.4 Rearing Productivity

For coho summer rearing productivity in small streams and side channels, we used the same wood multipliers as for large river capacities (Beechie et al. 2021b), yielding a high wood productivity of 0.9 (Table 3-5). For winter rearing, we assigned a density-independent productivity of 0.35 at low wood abundance (Ogston et al. 2015), and 0.58 at high wood abundance (Quinn and Peterson 1996) (Table 3-5). For Chinook subyearling productivities in small streams, we assumed a productivity increase similar to that for coho salmon winter rearing (multiplier of 1.67), changing juvenile Chinook subyearling rearing productivity from 0.26 to 0.43 in small streams (Beechie et al. 2021b). For Chinook yearlings in small streams we assumed productivity increases similar to those for coho salmon summer and winter rearing. For steelhead rearing in small streams, for all seasons and years we used the highest large river wood multiplier for each season for small streams (1.052 for summer and 1.108 for winter) (Table 3-4). All final productivity values for low and high wood abundance conditions in small streams and side channels are shown in Table 3-5.

In large rivers, we scaled summer and winter productivity increases due to increased wood abundance using the weighted average wood multipliers calculated for rearing capacities described above. As with capacity, the multipliers are used to modify large river productivities for historical conditions, and to modify rearing productivities in restoration scenarios (Section 2.2). For the restoration scenarios, we scale the productivity multiplier between 1 and the historical value depending on restoration intensity, so that a multiplier of 1 = no restoration, and the full multiplier = 100% restoration.

3.4 Beaver Dam Effects

Beaver ponds have strong influences on overwintering capacity and productivity of coho salmon in particular (Pollock et al. 2004, Ogston et al. 2015), but have less influence on rearing capacities and productivities for other species and life stages.

Table 3-5. Summary of species-, habitat-, and season-specific productivity values for low wood abundance and high wood abundance scenarios in small streams and side channels.

	Productivity	
Species and Season	**Low wood**	**High wood**
Coho salmon		
Small stream and side channel pool and riffle - summer	0.84	0.9
Small stream and side channel pool and riffle - winter	0.35	0.58
Chinook subyearling		
Small stream and side channel pool and riffle - spring	0.26	0.43
Chinook yearling		
Small stream and side channel pool and riffle - summer	0.84	0.9
Small stream and side channel pool and riffle - winter	0.35	0.58
Steelhead		
Small stream and side channel pool and riffle - summer 1	0.6	0.63
Small stream and side channel pool and riffle - winter 1	0.49	0.54
Small stream and side channel pool and riffle - summer 2,3	0.72	0.76
Small stream and side channel pool and riffle - winter 2,3	0.58	0.64

3.4.1 Spawning Capacity

To account for inundation of spawning gravel by beaver ponds in small streams, we used a typical pond length of 25 m, which inundates 15% of the suitable stream length in the historical condition with 6 ponds/km (Beechie et al. 2021a). Therefore, we reduced spawning habitat capacity in suitable beaver streams by 15% for the historical condition in small streams to account for inundation by ponds. In the current condition with 0.32 ponds/km, we reduced spawning habitat capacity in suitable beaver streams by 0.8%.

3.4.2 Rearing Capacity and Productivity

We assumed that rearing densities of coho salmon in beaver ponds are similar under current and historical conditions, but that the area of beaver ponds was substantially greater historically (Pollock et al. 2004). For beaver ponds in small streams, we set density at 1.2 fish/m^2 in both summer and winter (Jorgensen et al. 2021). Baseline summer rearing productivity in beaver ponds was set at 0.84 (Reeves et al. 1989), and is considered the same for historical and current conditions. Winter rearing productivity in beaver ponds is 0.78 (Ogston et al. 2015). To account for inundation of rearing pools and riffles by ponds,

we reduced pool and riffle rearing areas by 0.8% (current condition) or 15% (historical condition) as described above.

In the summer- and fall-run Chinook models, we assumed that subyearling rearing densities are the same in pools and ponds (0.05) (Beechie et al. 2021b). We used a density of 0.17 fish/m^2 in ponds for yearling Chinook summer rearing and 0.102 for winter rearing (E. Lowery, unpublished data). In contrast, juvenile steelhead densities in beaver ponds are lower than in pools. First-year summer and winter densities are 0 and 0.03 fish/m^2 in ponds (0.7 and 0.16 in pools), and second-year summer and winter densities are 0.07 and 0.01 fish/m^2 in ponds (0.18 and 0.09 in pools) (Johnson et al. 1993).

For all species and life stages, we set baseline beaver pond productivity equal to the baseline productivity for other floodplain habitats (Table 2-13, Table 2-16, Table 2-19).

3.5 Floodplain Connectivity Effects

Reductions in the area of floodplain habitats that were historically available (side-channels, marshes, and ponds) have decreased spawning, summer rearing, and winter rearing habitat capacities and productivities for all species of salmon (Jorgensen et al. 2021, Beechie et al. 2021a). Therefore, restoring floodplain connectivity should increase each of those parameters.

3.5.1 Spawning Capacity

Current side channel lengths were mapped from aerial imagery or taken directly from field surveys (Section 2.1.5), and spawning capacity for current conditions was estimated as described for small streams with low wood abundance (Section 3.3.1) (Beechie et al. 2021b). Our historical scenario includes increases in side-channel length based on side channel length multipliers described in Section 2.1.5, as well as the increase in spawning gravel area as a function of increased wood abundance in each side channel (using the same method as for small streams, Section 3.3.1).

3.5.2 Rearing Capacity

For current summer and winter rearing habitat capacity, we treat side channels as small streams with a wetted width of 6.82 m (the mean field-measured side channel width) and percent pool area for low-slope forested channels (54%). We then use the average of pool and riffle densities to estimate rearing capacity in summer and winter. For historical conditions we use the added side channel length described in Section 2.1.5, and treat each channel as a small, low gradient stream with the reference pool area (64%).

Marshes are typically dry in the summer, so there is no summer rearing fish density for that habitat type. In winter, marshes are assigned species-specific rearing densities (listed in Section 2.3 for each species). Floodplain lakes, ponds, and beaver ponds are assigned species-specific rearing densities, as described in Section 2.3.

3.5.3 Rearing Productivity

Rearing productivities in side channels are the same as for small streams with high wood abundance (historical condition) or low wood abundance (current condition), as described in Sections 2.3 and 3.3. Rearing productivities in current and historical marshes and ponds are described in Section 2.3.

3.6 Temperature Effects

In the HARP Model, temperature is partly controlled by shade and floodplain connectivity (Section 2.1.7), and temperature alters summer rearing capacity and productivity for coho, steelhead, and late sub-yearling migrant Chinook (Jorgensen et al. 2021, Fogel et al. 2022). We model effects of the 7-day average daily maximum summer stream temperature (7-DADM) for coho salmon, yearling Chinook salmon, and steelhead juveniles because those fish are in freshwater during the period of high temperatures. Most summer- and fall-run Chinook migrate to the bay as sub-yearlings prior to high temperatures in summer, and therefore we only model a June temperature effect on late migrating Chinook juveniles. Because juvenile coho, Chinook, and steelhead have different thermal tolerances, we model the temperature effect with a different functional relationship for each species.

3.6.1 Coho Summer Rearing Capacity and Productivity

We estimated a temperature-driven productivity multiplier for coho salmon based on 7-day average daily maximum (7-DADM) stream temperature, which decreases summer rearing productivity from its base value according to the function (Jorgensen et al. 2021, Fogel et al. 2022):

$$Temp\_multiplier_{coho} = \begin{cases} 1 & if\ T < 17°C \\ -0.09\,T + 2.53 & if\ 17°C \leq T < 28°C \\ 0 & if\ T \geq 28°C \end{cases}$$

That is, at temperatures <17°C, the multiplier is 1, so there is no change in summer rearing productivity (Figure 3-1). From 17°C to 28°C, the multiplier decreases linearly from 1 to 0, and above 28°C the multiplier is 0. We used the same multiplier for capacity that we use for productivity. We estimated historical summer rearing productivity using the same function, but the historical reach-level temperatures were based on historical shade conditions (Sections 2.1.6 and 2.1.7).

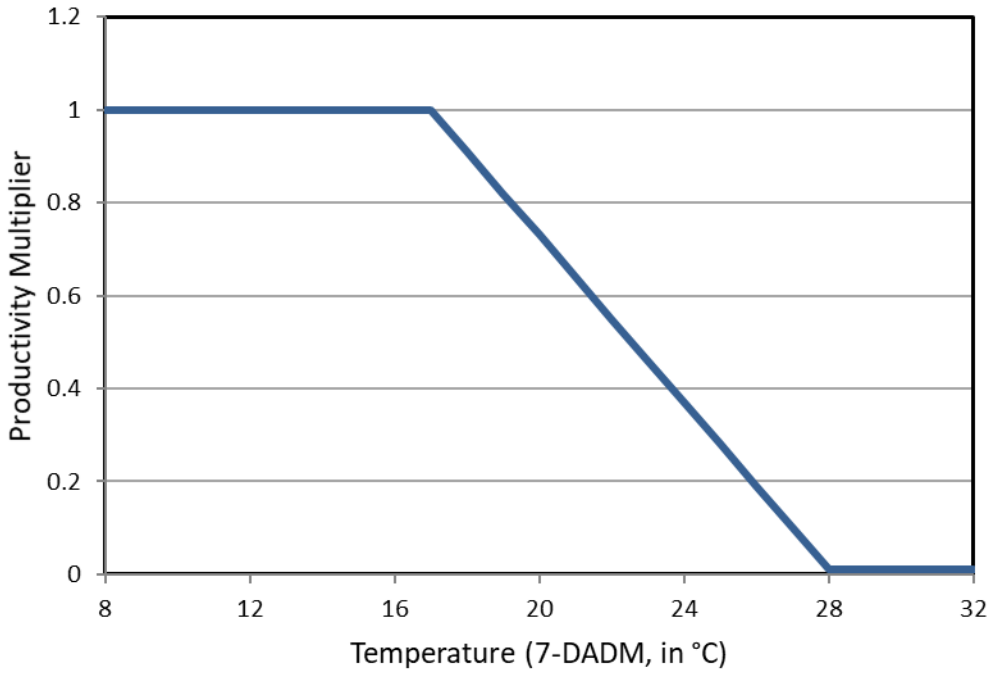

Figure 3-1. Functional relationship between the summer rearing productivity multiplier and the 7-day average daily maximum stream temperature for coho salmon.

3.6.2 Steelhead Summer Rearing Capacity and Productivity

For steelhead, we use an experimentally derived relationship between juvenile steelhead survival and stream temperature to create the temperature multiplier (Bear et al. 2007). The regression equation is:

$$Temp\_multiplier_{steelhead} = \frac{97.88}{1 - e^{-((T-24.3522)/-0.5033)}}$$

where T is the 7-DADM for current conditions (Figure 3-2). This same multiplier is applied to summer rearing capacity (Jorgensen et al. 2021, Fogel et al. 2022). We estimated historical summer rearing productivity using the same function, but the historical reach-level temperatures were based on historical shade conditions (Sections 2.1.6 and 2.1.7).

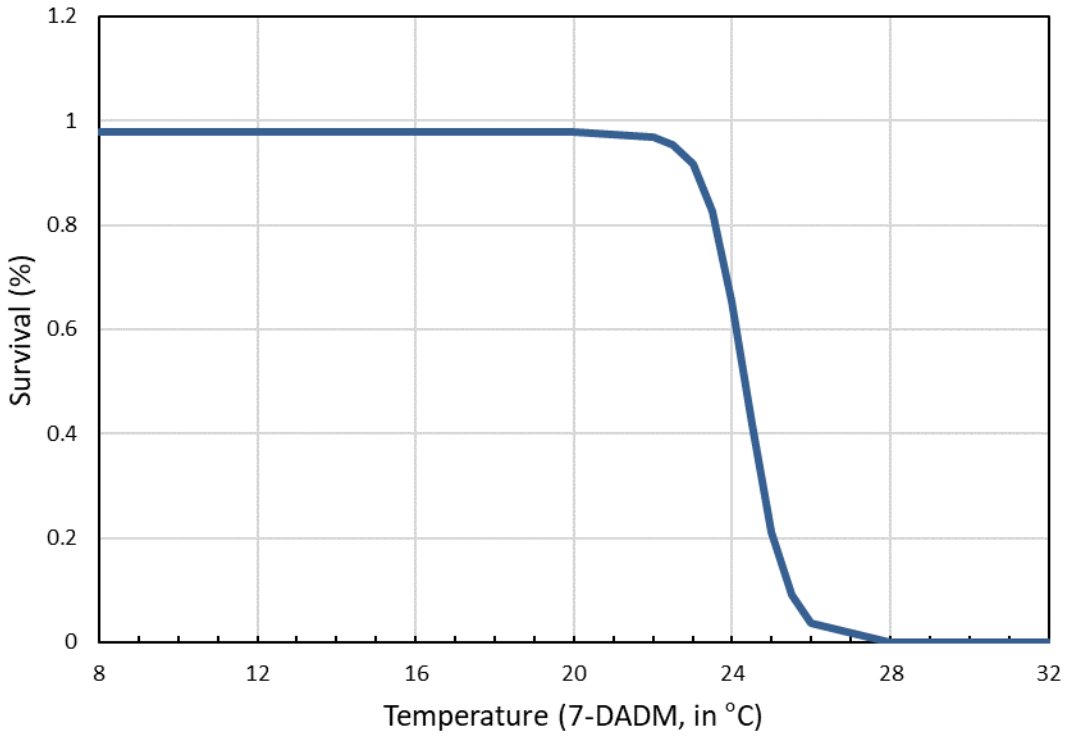

Figure 3-2. Functional relationship between the summer rearing productivity multiplier and the 7-day average daily maximum stream temperature for steelhead.

3.6.3 Chinook Rearing Capacity and Productivity

For summer- and fall-run Chinook, we used the June 1-21 average daily maximum temperature to estimate the temperature effect on productivity of juvenile Chinook parr emigrating in June (Figure 3-3) (Jorgensen et al. 2021). The functional relationship between the June 1-21 average daily maximum temperature and summer- and fall-run Chinook outmigrant productivity multiplier is:

$$Temp\_multiplier_{chinook} = \begin{cases} 1 & if\ T < 18°C \\ -\frac{1}{6}T + 4 & if\ 18°C \leq T < 24°C \\ 0 & if\ T \geq 24°C \end{cases}$$

Where T_J is the June 1-21 ADM. This equation is applied to the 34% of juveniles that are migrating from June 1-21, based on Stillaguamish smolt trap data.

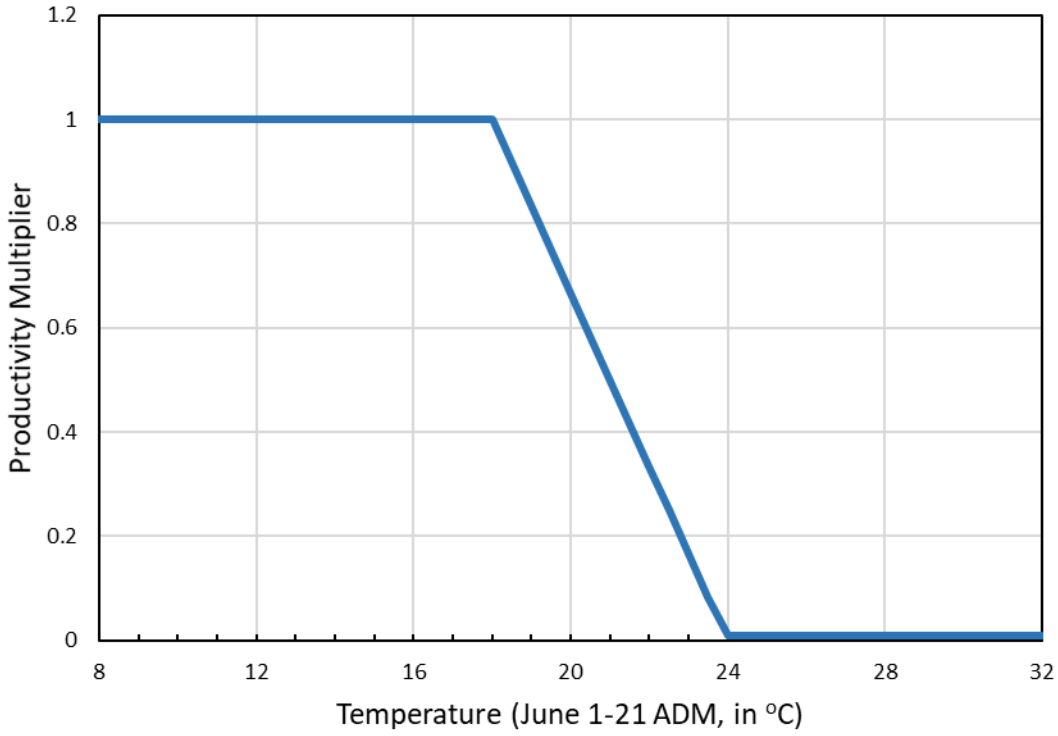

Figure 3-3. Functional relationship between the outmigration productivity multiplier for Chinook salmon and the June 1-21 average daily maximum (ADM) stream temperature.

We used the same equation for yearling-type Chinook rearing through summer, except we use the 7-DADM temperature as for coho and steelhead (T_{7D}):

$$Temp\_multiplier_{chinook} = \begin{cases} 1 & if\ T < 18°C \\ -\frac{1}{6}T + 4 & if\ 18°C \leq T < 24°C \\ 0 & if\ T \geq 24°C \end{cases}$$

In both cases, we used the same multiplier for capacities that we used for productivities. We calculated historical summer rearing productivities and capacities using the same functions, but the historical reach-level temperatures were based on historical shade conditions (Section 2.1.6).

3.7 Channel Straightening and Bank Armor Effects

Large river channel straightening reduces both spawning and rearing habitat areas, and therefore spawning and rearing capacities of all species. In the HARP Model, re-meandering of large rivers is included in large river restoration scenarios. Straightening or re-

meandering of small streams is not currently included in the HARP Model because we do not have a hydrography dataset representing historical tributary locations. Bank armoring affects the density of rearing salmonids, and therefore the rearing capacity of large rivers for all species. Bank armor removal is modeled alongside large river re-meandering.

Channel straightening reduces main channel length in rivers, leading to reduced spawning and rearing capacities for all species. We estimated the difference in habitat areas between current and historical conditions using reach-specific channel length multipliers in large rivers (Section 2.1.5), which increase habitat unit areas by the specified multiplier in each reach. For example, a channel length multiplier of 1.15 means that the channel was 15% longer historically, and we therefore increased habitat areas of all unit types in that reach by 15% (we assume that unit widths do not change). Rearing densities for all species remain the same in the current and historical channel length scenarios, so rearing capacity also increases by 15%. Channel length multipliers ranged from 1.0 (no change) to 1.3 (30% longer historically).

Bank armor does not affect rearing habitat areas, but it changes rearing densities and therefore rearing capacities for each species (Beamer and Henderson 1998). Density changes for armored and unarmored banks are shown in Section 2.3 for each species.

3.8 Fine Sediment Effects

Fine sediment affects density-independent incubation productivity in redds as a function of percent fine sediment in spawning gravels (Jensen et al. 2009). We modeled reach-level percent fine sediment <6.3mm in spawning gravels as a function of forest cover, glacial deposits, alluvium, drainage area and distance from major river confluences (see Section 2.1.8). Only the model for streams <30m in width was influenced by land use, and we modeled historical fine sediment for streams <30m in width using 100% forest cover. We did not model any fine sediment reduction that could result from any other potential future actions (e.g., forest road modifications, reduced bank erosion). We then modeled density-independent incubation productivity as a function of percent fine sediment in each reach as described below.

3.8.1 Fine Sediment Effect on Incubation Productivity

Once we estimated percent fines for each reach, we modeled incubation productivity for those reaches based on data for Chinook and steelhead eggs (Bjornn 1969). We plotted the raw data for each species, and then created a linear regression for Chinook salmon, and a segmented regression for steelhead (Figure 3-4 and Figure 3-5). The functional relationship for Chinook salmon is

$$Sed\_multiplier_{Chinook} = \begin{cases} -0.014 \times sed + 0.75 & if\ sed \leq 54\% \\ 0 & if\ sed > 54\% \end{cases}$$

where *sed* is percent fine sediment <6.3 mm (Figure 3-4). The functional relationship for steelhead is

$$Sed\_multiplier_{steelhead} = \begin{cases} 0.52 & if\ sed\ \leq 20\% \\ 0.52 - 0.025 \times (sed - 20) & if\ 20\% < sed < 40\% \\ 0.02 & if\ sed\ \geq 40\% \end{cases}$$

where *sed* is percent fine sediment <6.3 mm (Figure 3-5). There were no data available for coho salmon with fine sediment classified as <6.3 mm. Because coho survival is typically higher than Chinook survival at the same level of fines (Jensen et al. 2009), we used the Chinook function for coho because Chinook survival is slightly higher than for steelhead. Current and historical reach-level sediment-based productivity values were further modified by peak flow multipliers (see Section 3.10).

3.9 Impervious Surface and Road Effects

Effects of impervious surfaces and roads on prespawn mortality have been documented for coho salmon (Feist et al. 2011, 2017, Tian et al. 2020), but effects have not been documented for other species to date. In the HARP model we include this effect only for coho salmon.

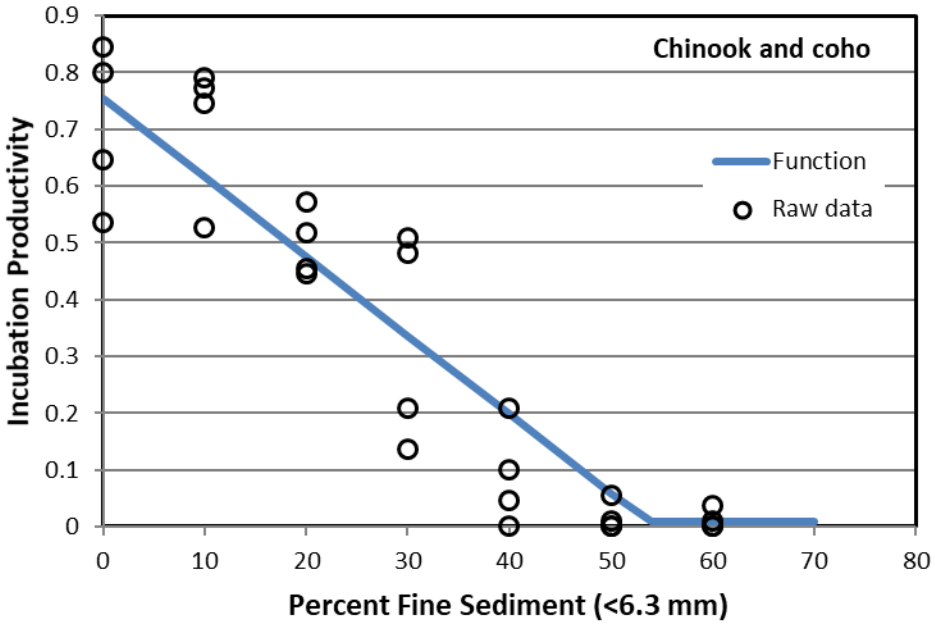

Figure 3-4. Functional relationship used to calculate incubation productivity from percent fine sediment <6.3 mm for Chinook and coho based on data from Bjornn (1969).

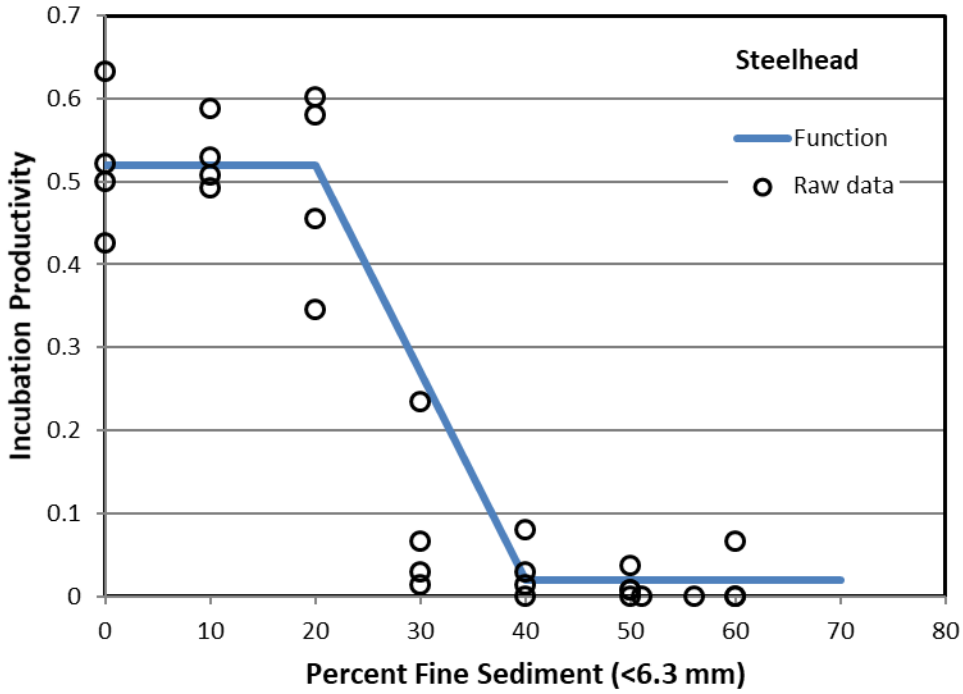

Figure 3-5. Functional relationship used to calculate incubation productivity from percent fine sediment <6.3 mm for steelhead based on data from Bjornn (1969).

3.9.1 Coho Prespawn Productivity

Prespawn mortality in coho salmon is correlated with a number of development metrics (e.g., road density, percent impervious area) (Feist et al. 2011, 2017). In the HARP Model for Puget Sound salmon populations, the modeled prespawn mortalities were adopted from Feist et al. (2017). Feist et al. (2017) estimated prespawn mortality as a function of summer and fall precipitation along with indicators of urbanization including road density and traffic intensity. They predicted a prespawn mortality value for each geospatial unit (smaller than a subbasin), which we converted to a productivity multiplier ($\beta_{prespawn}$):

$$\beta_{prespawn} = 1 - Prespawn\ mortality$$

This value was applied to each small stream reach within a geospatial unit, but not to large rivers because Feist et al. (2017) did not include data from, nor model prespawn mortality for large rivers. Prespawn productivity for each reach was then calculated as the base coho prespawn productivity (0.95) multiplied by $\beta_{prespawn}$, and the subbasin productivity was the weighted average of the reach level prespawn productivities (Section 2.2), where the weight is egg capacity.

We do not have a restoration scenario for this cause of mortality because it does not currently appear feasible to reduce the main pollutant, which is a highly toxic quinone transformation product of N-(1,3-dimethylbutyl)-N'-phenyl-p-phenylenediamine (6PPD), a tire rubber antioxidant (Tian et al. 2020). Filtration swales have been shown to effectively reduce pollutants and increase salmon survival (McIntyre et al. 2015, Spromberg et al. 2016), but it is not evident that there is sufficient restoration opportunity to widely implement that action. It is also possible that altering the tire rubber antioxidant formula may eventually eliminate the pollutant, but it is not clear how soon this can occur. However, the eventual change could eliminate the pollutant in the future, decreasing prespawn mortality for coho salmon.

3.10 Peak Flow Effects

The HARP Model can incorporate stochastic functions to influence productivity parameters from year to year, such as an annually varying effect of peak flow on incubation productivity (Nicol et al. 2022). Such effects create annually varying smolt abundances, which are reflected in adult returns.

3.10.1 Incubation Productivity

Effects of peak flows on egg to migrant fry survival have been documented in Chinook salmon in the Skagit River basin (Zimmerman et al. 2015), and are presumed to reflect scour of eggs in the gravel due to the overlap in timing of floods and the incubation period. A similar effect is presumed to occur in other river basins and for other species with incubation periods that overlap with the period of peak flows (Nicol et al. 2022).

In the HARP Model, incubation survival is modified by a peak-flow scalar, which alters egg mortality as a function of flood recurrence interval. The original scour-related survival function is:

$$log_e p_{pf} = a \cdot RI^b$$

where p_{pf} is the annual egg-to-migrant survival, RI is the recurrence interval, and a and b are fitted coefficients (a = -1.869, b = 0.108). We then converted the peak-flow-related p_{pf} values to a multiplier (p_{scalar}) using the equation:

$$p_{scalar} = 1 + \frac{p_{pf_i} - p_{pf_{med}}}{p_{pf_{med}}}$$

Where p_{pf_i} is the scour-related survival at a given flow as calculated above, and $p_{pf_{med}}$ is the scour-related survival at the median peak flow, or a flow where RI = 2. We multiplied p_{fs} (the fine sediment related productivity) by p_{scalar} to get the final incubation survival (Nicol et al. 2022). A weighted average incubation productivity was then calculated for each subbasin, where the weight is egg capacity.

4. Results

4.1 Habitat Change

The habitat change analysis shows significant reductions in habitat quantity and quality compared to natural potential. We briefly summarize habitat changes for each of the habitat factors assessed for the diagnostic scenarios.

4.1.1 Migration Barriers

Man-made structures that are full or partial migration barriers affect up to 20% of anadromous salmonid habitat length in the Stillaguamish basin, and up to 22% in the Snohomish River basin. Because species ranges vary substantially, the length of habitat above man-made barriers differs among species (Table 4-1). However, it is important to note that not all barriers are 100% blocking, so the effects on spawning capacity and population size will be less than the percentage listed here (see section 4.2 for life-cycle model results). Cumulative passability ratings by reach for each river basin are shown in Figure 4-1.

Table 4-1. Summary of habitat lengths above man-made migration barriers in the Stillaguamish and Snohomish River basins. Not all barriers are 100% blocking, so the effects on populations are less than the percentages shown here.

River Basin	Species	Percent Habitat Above Barriers
Stillaguamish	Coho	20%
	Summer- and fall-run Chinook	1%
	Summer-run Steelhead	3%
	Winter-run Steelhead	10%
Snohomish	Coho	22%
	Summer- and fall-run Chinook	9%
	Summer-run Steelhead	7%
	Winter-run Steelhead	13%

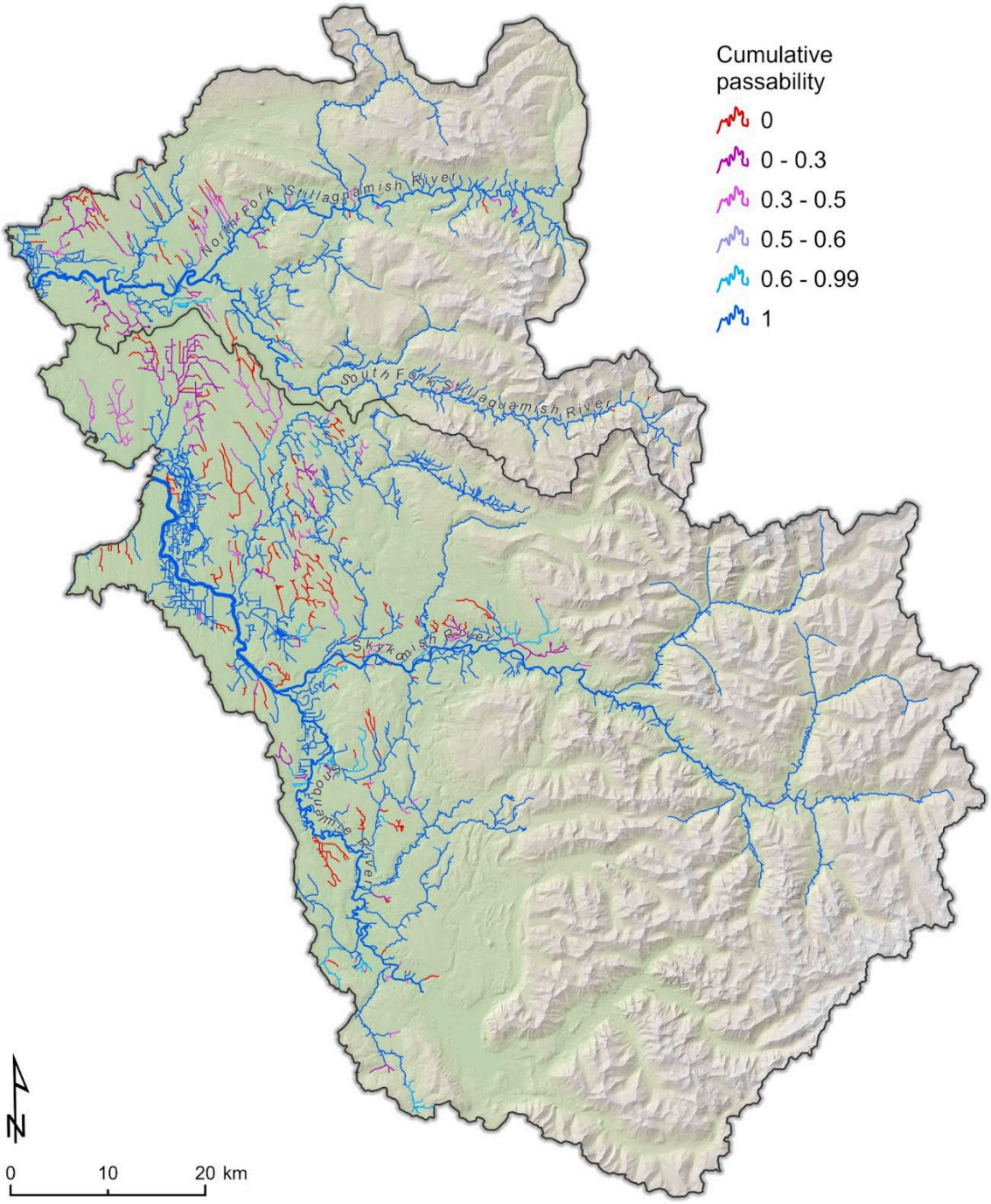

Figure 4-1. Cumulative passability ratings above man-made migration barriers in the Stillaguamish and Snohomish River basins.

4.1.2 Wood Abundance

Current wood abundance in the Stillaguamish and Snohomish River basins is assumed to be low relative to natural conditions. Low wood abundance results in reduced spawning gravel area in small streams and large rivers, reduced pool areas in small streams, and reduced wood cover in small streams and large rivers. These all reduce spawning and rearing capacity for all species (example for coho salmon in Figure 4-2).

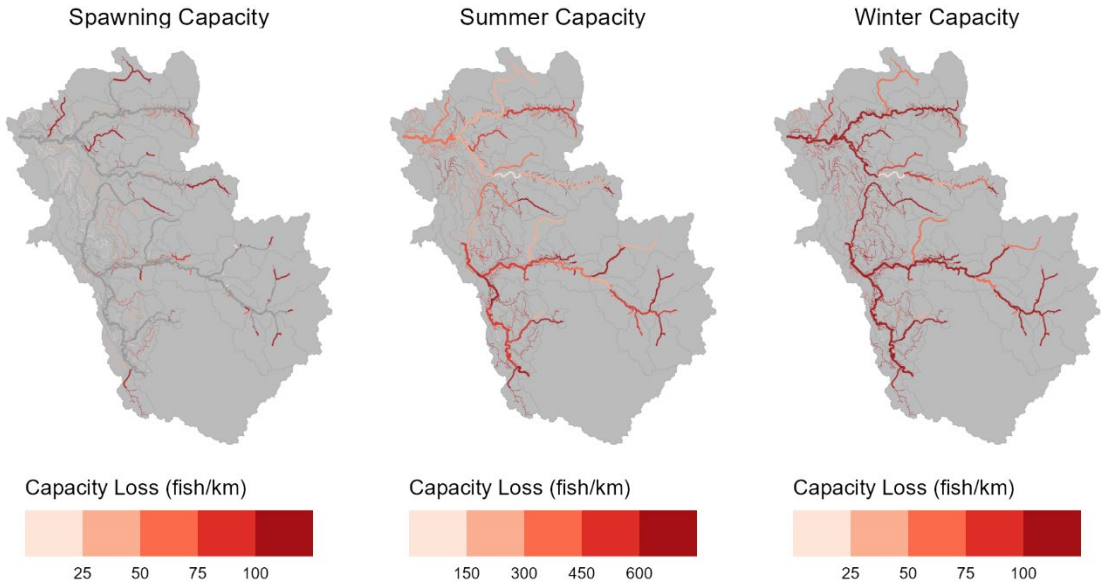

Figure 4-2. Modeled reduction in habitat capacity for coho salmon spawning, summer rearing, and winter rearing as a function of wood loss relative to historical conditions in the Stillaguamish and Snohomish River basins. Spawning capacity is in units of spawners/kilometer of spawning habitat and rearing capacity is in units of juveniles per kilometer of rearing habitat.

4.1.3 Beaver Dams

The two beaver intrinsic potential models predicted somewhat different distributions of potential beaver habitat in small streams, but there was a high degree of overlap in most of the stream network (Figure 4-3). Both models show that most of the potential beaver habitat is in the western portion of each basin where low-elevation glacial deposits have low relief and most small streams are low gradient (Figure 4-3). In contrast, the eastern portion of each basin is in the steeper Cascade Mountains where there is very little potential beaver habitat, except in the post-glacial valleys of the North Fork Stillaguamish, South Fork Stillaguamish, and Skykomish Rivers. For this project we used the Dittbrenner model to estimate current and historical beaver pond areas, although using the Pollock model is also an option in the model.

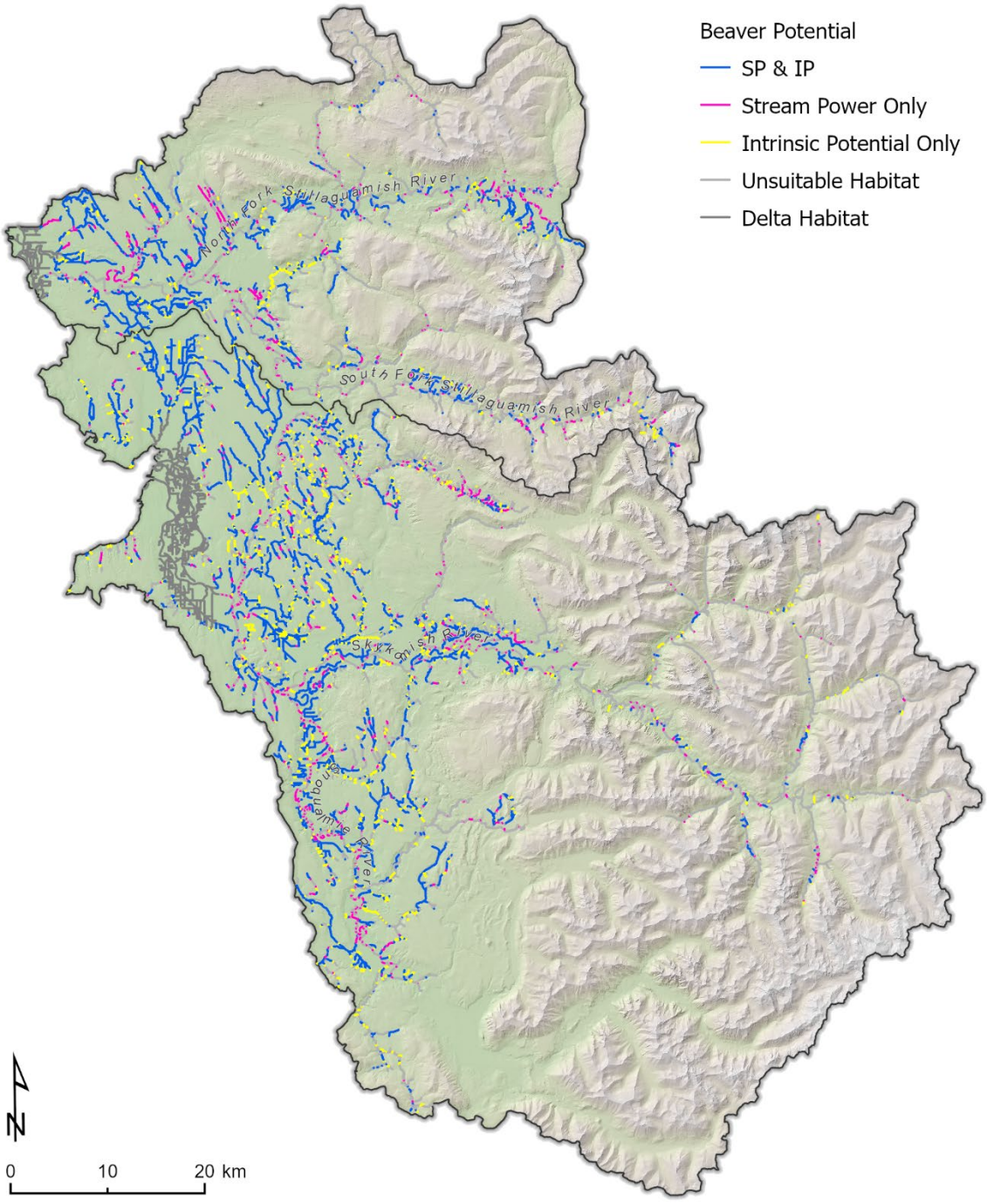

Figure 4-3. Map of beaver intrinsic potential habitat in the Stillaguamish and Snohomish River basins using a stream power model (Pollock et al. 2004) and an intrinsic potential model (Dittbrenner et al. 2019). Reaches predicted to be beaver habitat by both models are shown in blue, reaches predicted only by the stream power model shown in pink, and reaches predicted only by the intrinsic potential model are shown in yellow.

Historical beaver dam densities in small streams were likely 10-20 times higher than current densities, indicating large potential changes in availability of slow water habitats. However, because beaver intrinsic potential varies by subbasin, estimated historical beaver habitat area differs among subbasins. The models predict generally similar distributions of beaver habitat area by subbasin, except that the stream power model predicts slightly more beaver pond area in smaller tributaries in glacial sediments and the IP model predicts more beaver pond area in the large river floodplains.

4.1.4 Floodplain Habitat

The largest losses of floodplain habitats in both subbasins were marshes and side channel habitats. Historically, the Snohomish basin had much more marsh habitat than the Stillaguamish basin (~4500 ha and ~800 ha, respectively) (Figure 4-4). Floodplain marshes have been reduced in area by roughly 80% in both basins. By contrast, pond and lake areas were smaller historically, and the reductions in area have been less.

The majority of historical floodplain habitats in both basins were in lower mainstem floodplains. Floodplain marshes and ponds were concentrated in the lower main stem area in the Stillaguamish River basin, and in the Snoqualmie and lower Snohomish River floodplains in the Snohomish River basin (Figure 4-5). The Snohomish and Snoqualmie Rivers historically had very large areas of freshwater marsh and pond due to its meandering channel pattern and natural levees that promoted development of floodplain wetlands.

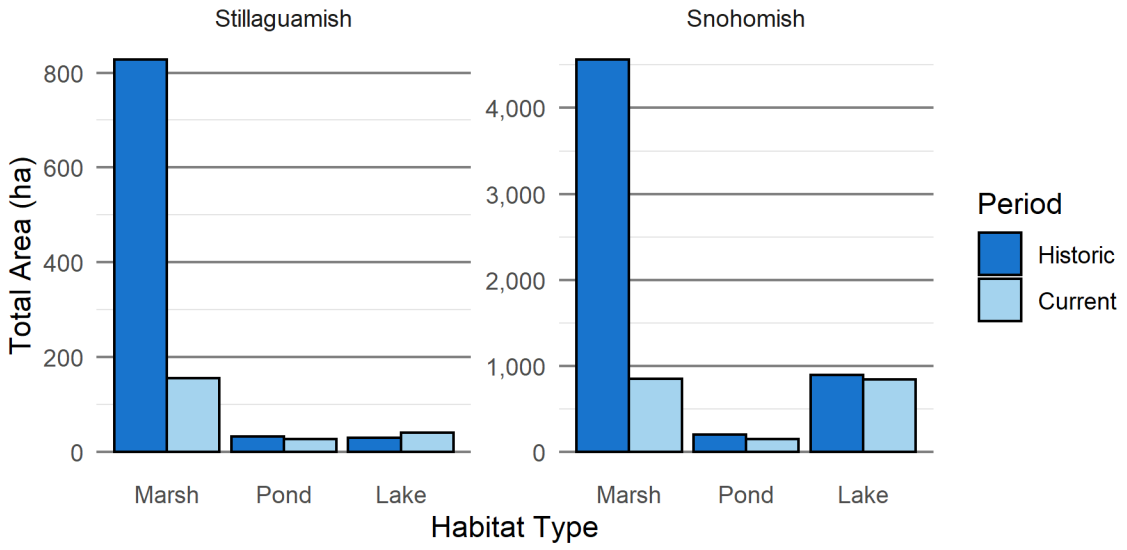

Figure 4-4. Comparison of current and historical floodplain rearing habitats (marshes, ponds, and lakes) in the Stillaguamish (A) and Snohomish (B) River basins. Decreases in marshes are due to a great extent to valley draining from agriculture and urban development.

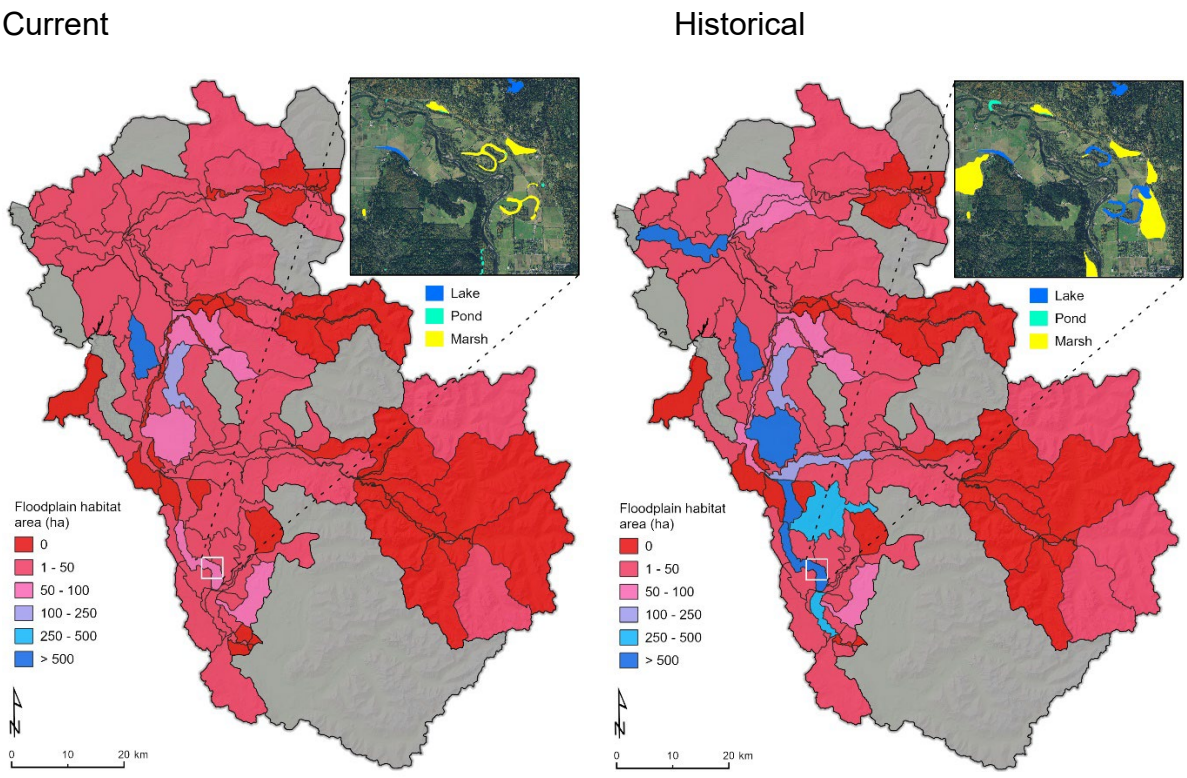

Figure 4-5. Subbasin-level floodplain rearing habitat areas (marshes, ponds, and lakes) in the Stillaguamish and Snohomish River basins for current conditions (left panel) and historical conditions (right panel). Subbasins in gray are deltas or are outside the ranges of salmon and steelhead for this model.

We estimated that 59% of side channel length has been lost in the Stillaguamish basin and 63% in the Snohomish basin (Table 4-2 and Table 4-3). Historical side channels were concentrated in the lower main stem Stillaguamish subbasin, and in the Skykomish River in the Snohomish River basin, and the greatest restoration potentials for side channels are in those reaches. In the Stillaguamish basin, the vast majority of potentially restorable side channel length (67 km) was in the lower mainstem. Other reaches with lesser, but still significant, restorable length are the lower North Fork (12 km) and lower South Fork Stillaguamish subbasins (8 km). In the Snohomish basin, the majority of potentially restorable side channel length is the mainstem and North Fork Skykomish (83 km) and in the Pilchuck River (77 km).

Table 4-2. Estimated historical and current side channel lengths by subbasin in the Stillaguamish River basin. ("Headwaters" indicates upper end of anadromous access.)

Reach Name	Reach Boundaries	Historical Side Channel Length (km)	Current Side Channel Length (km)	Change
Lower Mainstem	Norman Rd. to confluence of NF and SF	61.51	4.21	-93%
NF Stillaguamish 1	Confluence to Deer Creek	23.96	12.31	-49%
NF Stillaguamish 2	Deer Creek to Boulder River	14.43	10.23	-29%
NF Stillaguamish 3	Boulder River to Squire Creek	14.46	10.68	-26%
NF Stillaguamish 4	Above Squire Creek	3.86	0.00	-100%
Pilchuck Creek	Lower Pilchuck Creek	3.89	2.33	-40%
Deer Creek	Mouth to Higgins Creek	11.09	7.45	-33%
Boulder River	Mouth to Boulder Falls	1.03	1.18	14%
Squire Creek	Mouth to end of Squire Creek Rd.	1.62	0.00	-100%
SF Stillaguamish 1	Confluence to Canyon Creek	13.20	4.17	-68%
SF Stillaguamish 2	Robe Canyon	0.00	0.00	NA
SF Stillaguamish 3	Robe Canyon to Twenty–two Creek	2.24	0.94	-58%
SF Stillaguamish 4	Twenty–two Creek to Mallardy Creek	3.17	2.79	-12%
SF Stillaguamish 5	Mallardy Creek to Buck Creek	6.42	6.52	3%
Jim Creek	Mouth to Headwaters	4.53	4.07	-10%
Canyon Creek	Mouth to Headwaters	4.90	3.61	-26%
Total		**170.31**	**70.49**	**-59%**

Table 4-3. Estimated historical and current side channel lengths by subbasin in the Snohomish River basin. ("Headwaters" indicates upper end of anadromous access.)

Reach Name	Reach Boundaries	Historical Side Channel Length (km)	Current Side Channel Length (km)	Change
MS Snohomish	Snohomish River from Hwy 9 to Confluence	8.94	4.97	-44%
Lower MS Skykomish	Confluence with Snoqualmie to Sultan	48.65	27.93	-43%
Upper MS Skykomish	Sultan to confluence of N. and S. Fork	46.24	18.87	-59%
Lower NF Skykomish	Confluence of N. and S. Fork to Silver Creek	42.00	20.99	-50%
Upper NF Skykomish	Silver Creek to Headwaters	18.27	4.79	-59%
Lower SF Skykomish	Confluence of N. and S. Fork to County Line	2.14	1.47	-31%
SF Skykomish	County Line to Miller River	7.42	5.09	-31%
Upper SF Skykomish	Miller River to Foss River	9.22	2.41	-74%
Miller River	SF Skykomish to Headwaters	18.56	10.34	-44%
Beckler River	SF Skykomish to Headwaters	27.31	7.83	-71%
Foss River	SF Skykomish to Headwaters	11.17	7.89	-29%
Tye River	Foss River to Headwaters	10.98	3.28	-70%
Olney Creek	Wallace River to Headwaters	0.60	0.45	-25%
Wallace River	Skykomish River to Headwaters	3.07	1.68	-47%
Snoqualmie Mouth	Skykomish River to Duvall	16.84	0.31	-98%
Mid-MS Snoqualmie	Duvall to Tolt River	6.83	0.09	-99%
Upper MS Snoqualmie 1	Tolt River to Raging River	5.24	0.33	-94%
Upper MS Snoqualmie 2	Raging River to Snoqualmie Falls	1.95	0.00	-100%
Lower Tolt River	Snoqualmie to Confluence of NF and SF Tolt	10.90	8.83	-19%
NF Tolt River	Confluence to Headwaters	0.76	0.00	-100%
SF Tolt River	Confluence to Dam	5.30	5.04	-5%
Raging River	Snoqualmie River to Headwaters	4.56	0.76	-83%
Lower Pilchuck River	Snohomish River to Dubuque Creek	13.56	0.21	-98%
Middle Pilchuck River	Dubuque Creek to Worthy Creek	56.37	7.80	-86%
Upper Pilchuck River	Worthy Creek to Headwaters	17.38	2.01	-88%
Lower Sultan River	Skykomish River to end of Diversion	18.47	9.67	-48%
Total		**412.73**	**153.04**	**-63%**

4.1.5 Shade and Temperature

The number of reaches in the highest canopy opening angle class is 2 to 3 times higher than it was historically in both basins, increasing from 10% of reaches to 28% in the Stillaguamish River basin and from 13% to 34% in the Snohomish River basin (Figure 4-6). The number of reaches in the lowest canopy opening angle class (<10°) decreased from 47% of reaches historically to 33% currently in the Stillaguamish River basin and from 49% historically to 34% currently in the Snohomish River basin. The largest changes in canopy opening angle are along small streams in the glacial lowlands (western portion) of each basin (Figure 4-7, Figure 4-8), especially along small streams and ditches in intensive agricultural areas. However, ditched areas were likely marshlands historically, and it's not clear how much channel length would have existed there.

Modeled current 7-day average daily maximum (7-DADM) stream temperatures are relatively high in both river basins (Figure 4-9), often exceeding optimal rearing temperatures. The highest temperatures are in the lower mainstem reaches of both basins, as well as in lowland streams and ditches that have little or no shade. Modeled historical temperatures were generally lower in both basins (Figure 4-10). In the Stillaguamish River basin, 23% of reaches have increased more than 2°C, and in the Snohomish River basin, 28% of reaches have increased more than 2°C (Figure 4-11). However, many of those reaches are lowland ditches that were historically marshlands.

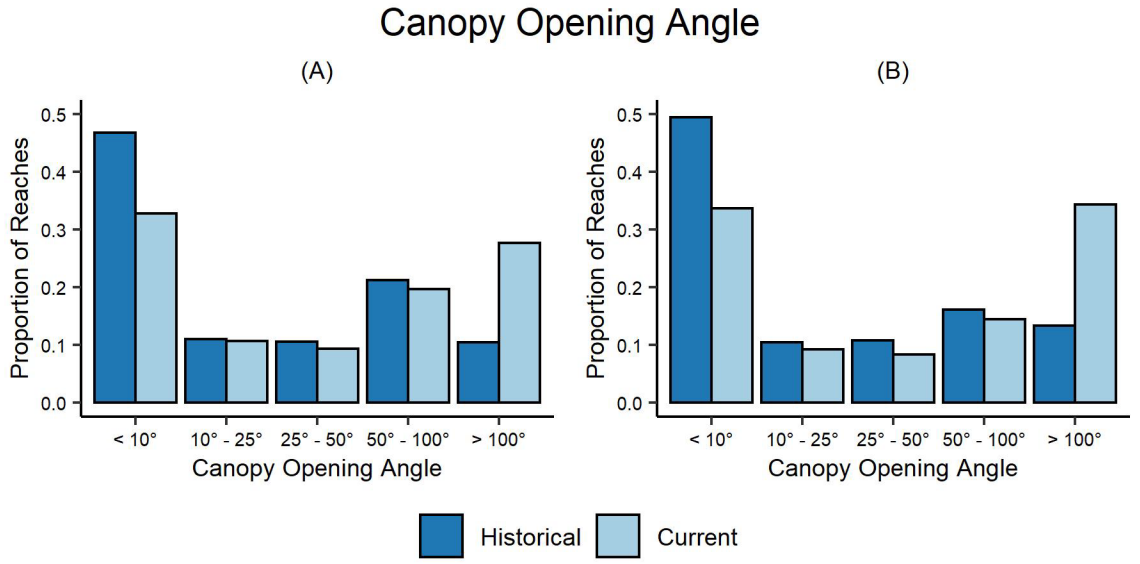

Figure 4-6. Frequency distributions (proportion of total reaches) of historical and current canopy opening angles in the Stillaguamish (A) and Snohomish (B) River basins. Note the significant decrease in narrow canopy opening angles (<10°) and increase in wide canopy opening angles (>100°).

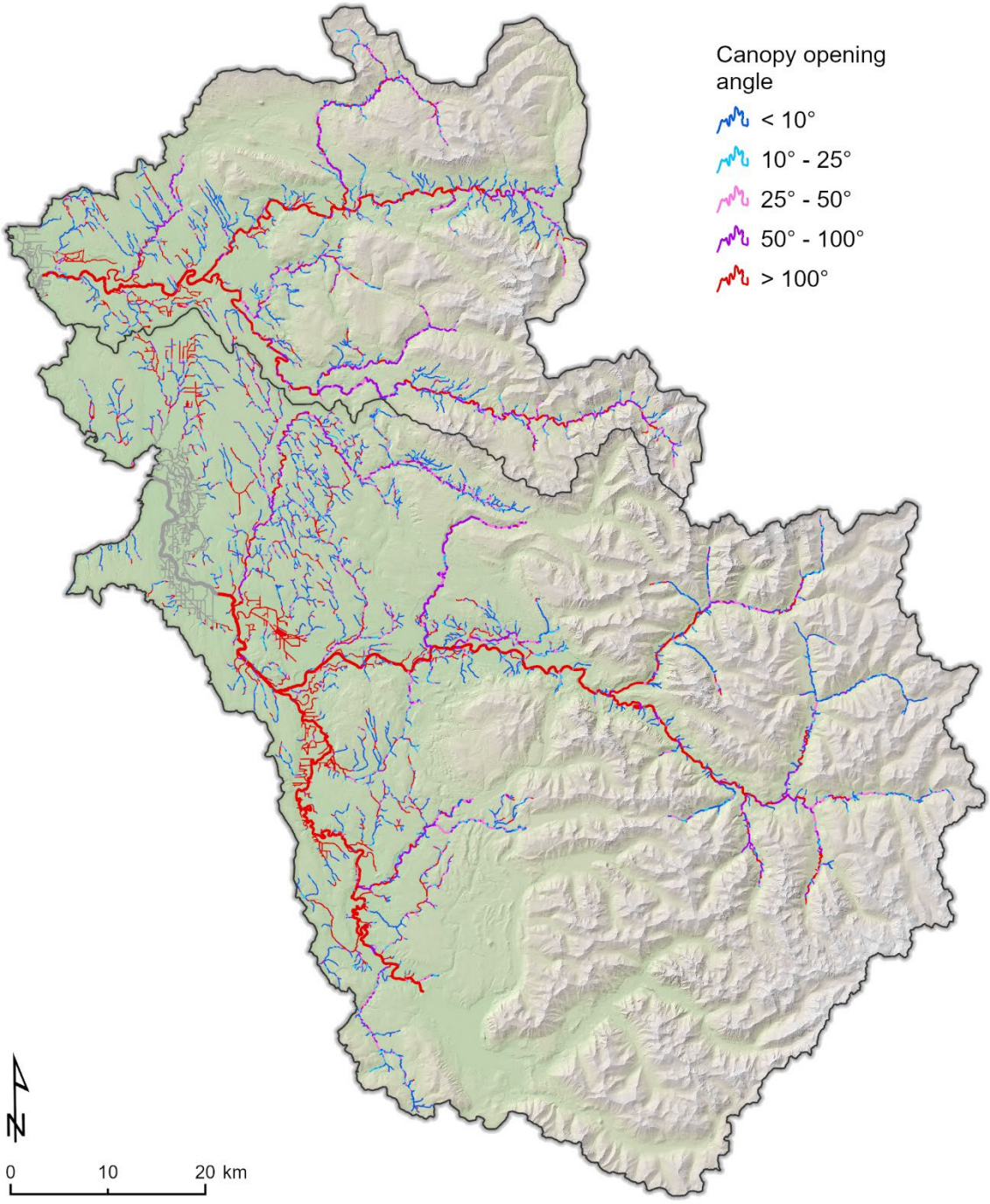

Figure 4-7. Current canopy opening angles (°) in the Stillaguamish and Snohomish River basins.

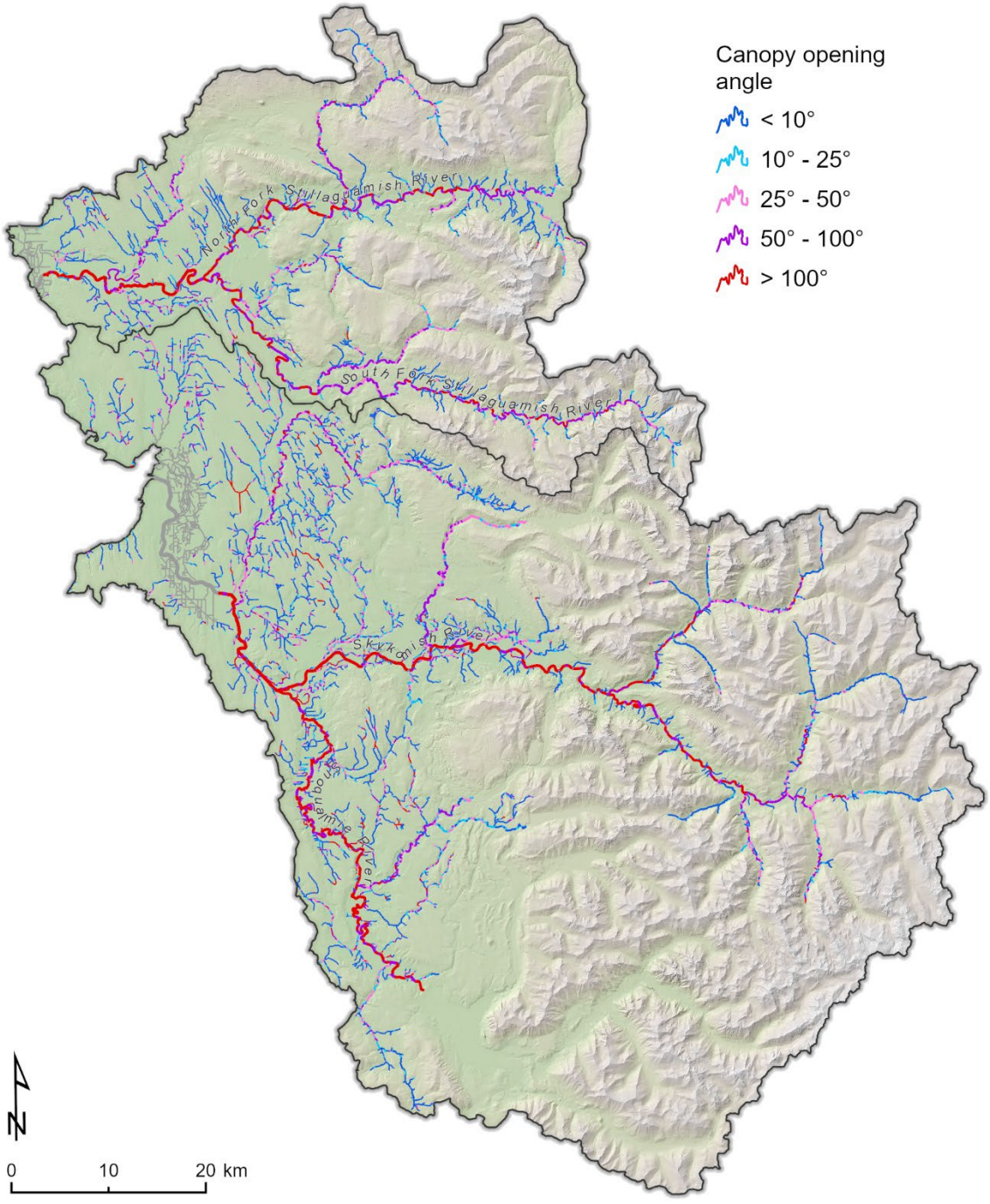

Figure 4-8. Historical canopy opening angles (°) in the Stillaguamish and Snohomish River basins.

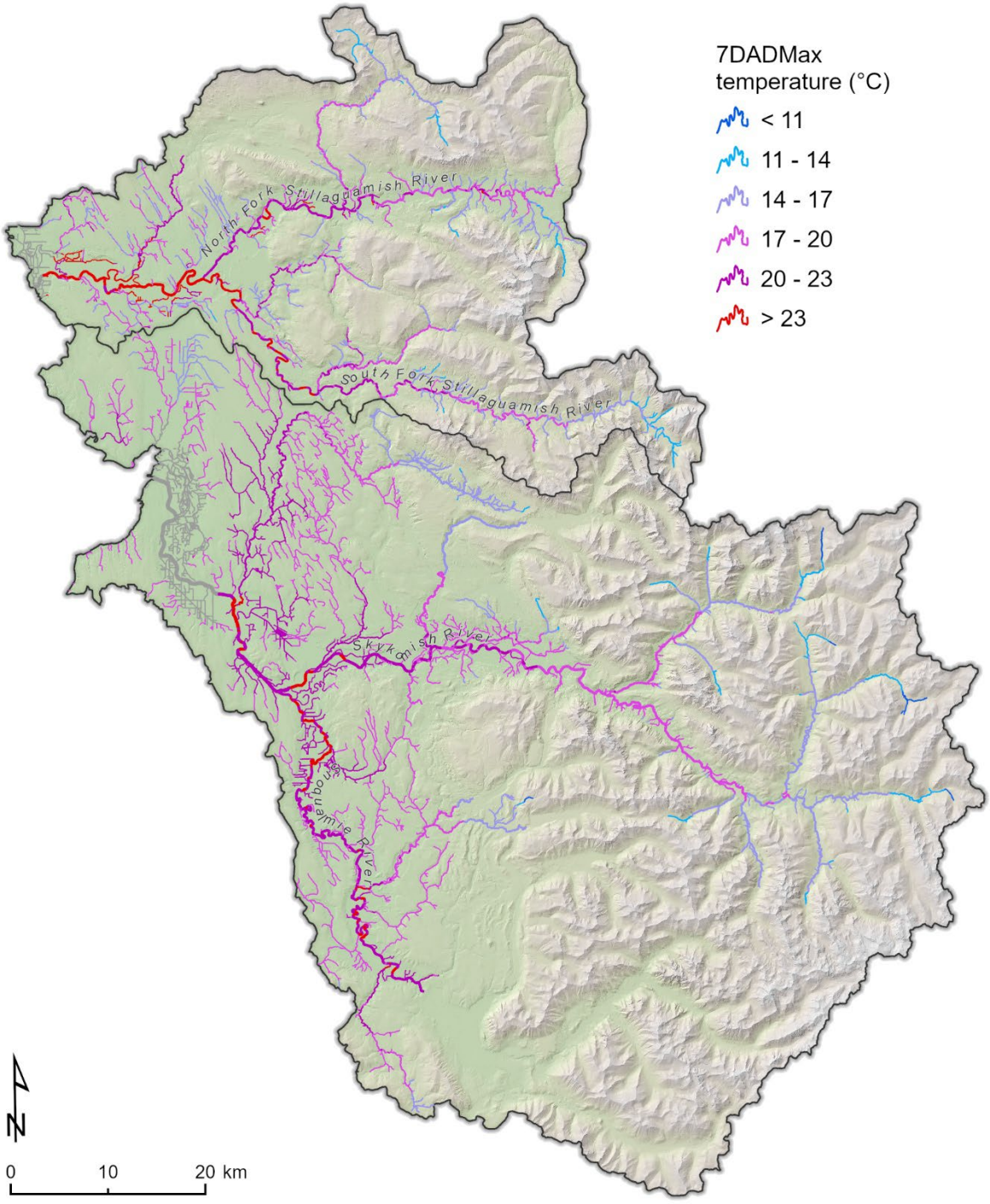

Figure 4-9. Modeled current 7-DADM stream temperature (°C) in the Stillaguamish and Snohomish River basins.

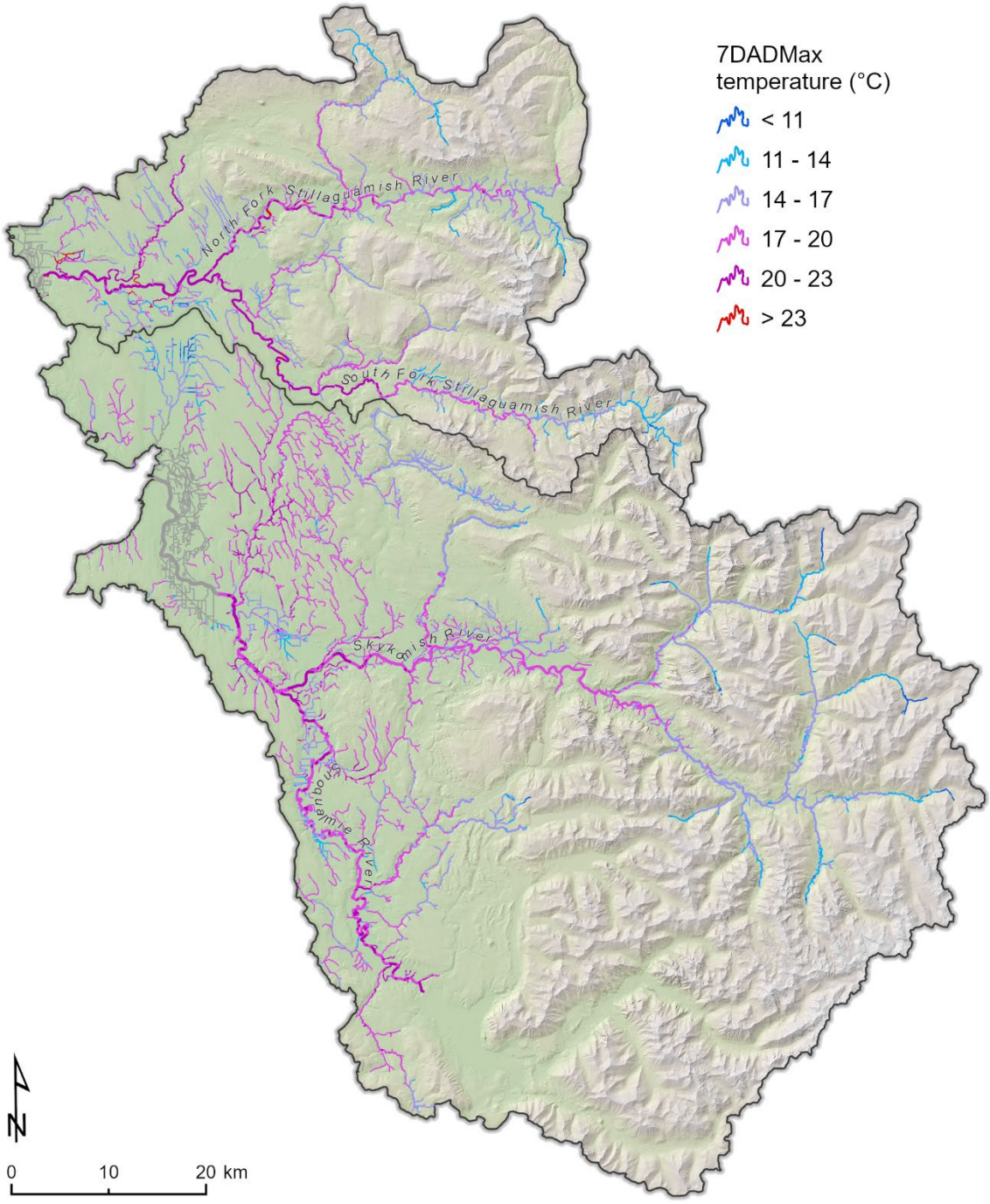

Figure 4-10. Modeled historical 7-DADM stream temperature (°C) in the Stillaguamish and Snohomish River basins based on modeled temperature reduction from current condition using a shade-temperature model (Seixas et al. 2017).

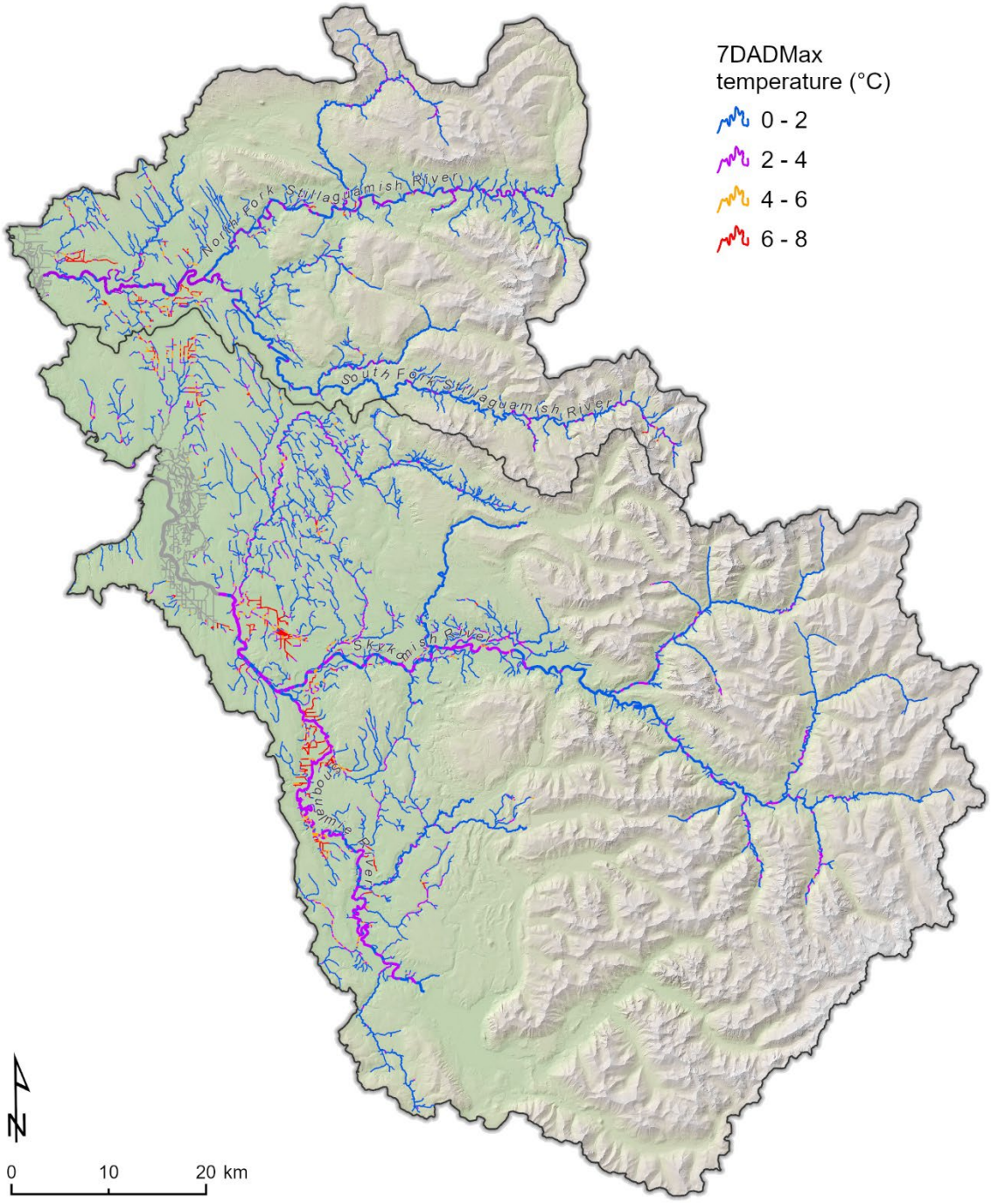

Figure 4-11. Change in 7-DADM from historical to current conditions in the Stillaguamish and Snohomish River basins.

4.1.6 Channel Straightening and Bank Armor

Based on GLO maps of the study areas (Collins and Shiekh 2003), there is little indication of channel straightening of large rivers in the Stillaguamish and Snohomish River basins, although some meander bends have been cut off or shortened by infrastructure such as railroad grades or roads. Otherwise, the large rivers are generally in their historical locations, but often leveed and armored in place to prevent channel migration. The Stillaguamish basin has 59 km of armored bank out of 628 km total edge habitat length (9%) (Figure 4-12). The Snohomish River basin has 122 km of armored bank out of 950 km total edge habitat length (13%). Much of the riprap in the Snohomish basin is in the Snoqualmie River, largely impacting spawning reaches below the Raging and Tolt Rivers, as well as rearing habitat in the lower Snoqualmie River (Figure 4-12).

4.1.7 Fine Sediment

The fine sediment models estimate that some reaches in both basins have high levels of fine sediment <6.3 mm in diameter (Figure 4-13). Modeled reach-level fine sediment values range from 0% to 100% in both basins, but most areas have <20% fine sediment according to the models. One major exception is that the lower several kilometers of the Snoqualmie River have percent fines > 80%.

4.1.8 Impervious Surfaces and Roads

Impervious surface areas and road densities are highest in the lower Snohomish basin near Everett, moderate near smaller towns such as Arlington, Monroe, or Carnation, and low in forested areas of the basin. Predicted pre-spawn mortality of coho salmon adults is highest in small streams near Arlington (Portage Creek) and Marysville (Quilceda Creek), moderate in other lowland streams in the western portion of both basins, and low in the valleys of the Cascade Mountains where land use is predominantly forestry (Figure 4-14).

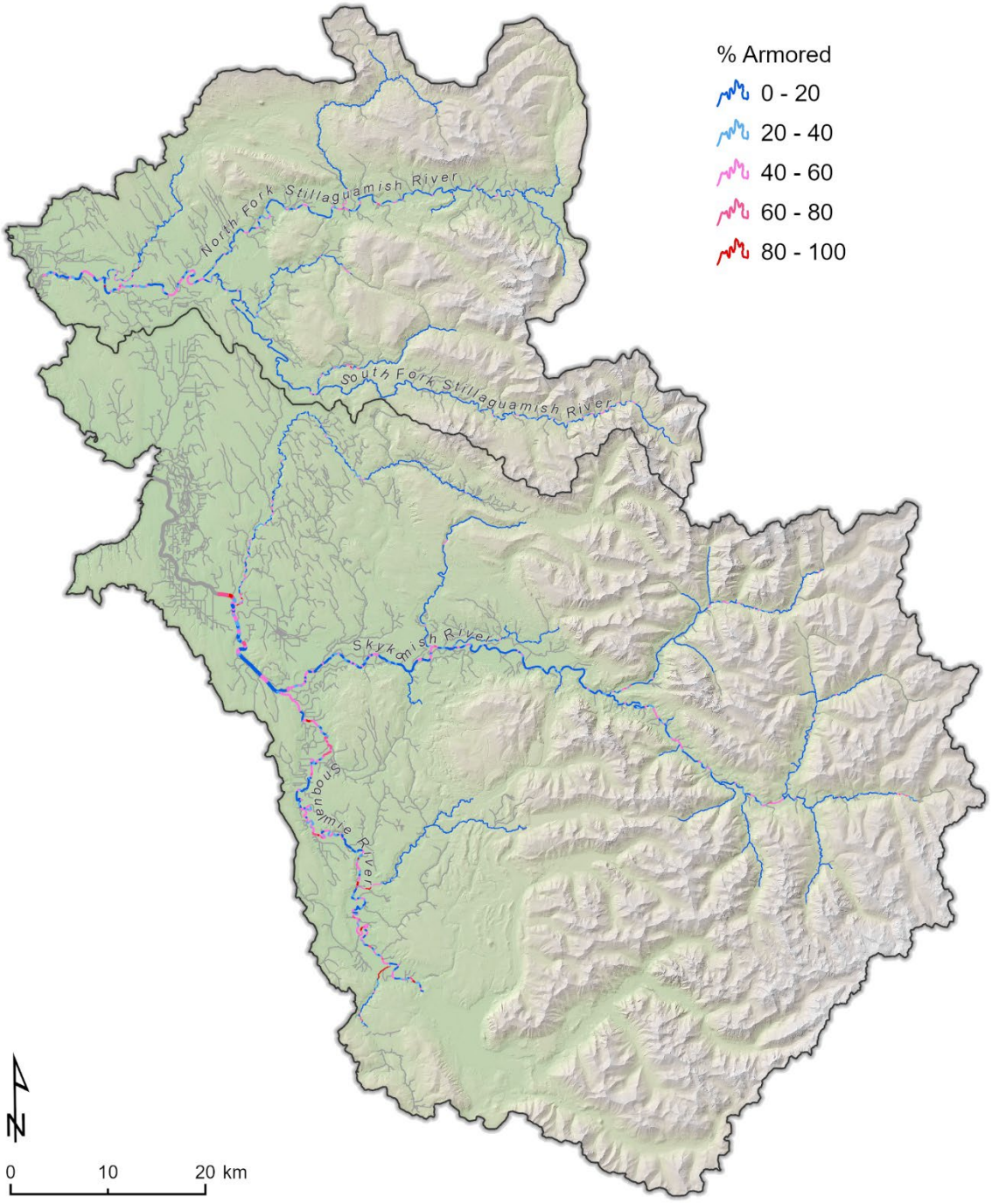

Figure 4-12. Percent of edge habitat classified as armored bank edge for each reach in the Stillaguamish and Snohomish River basins.

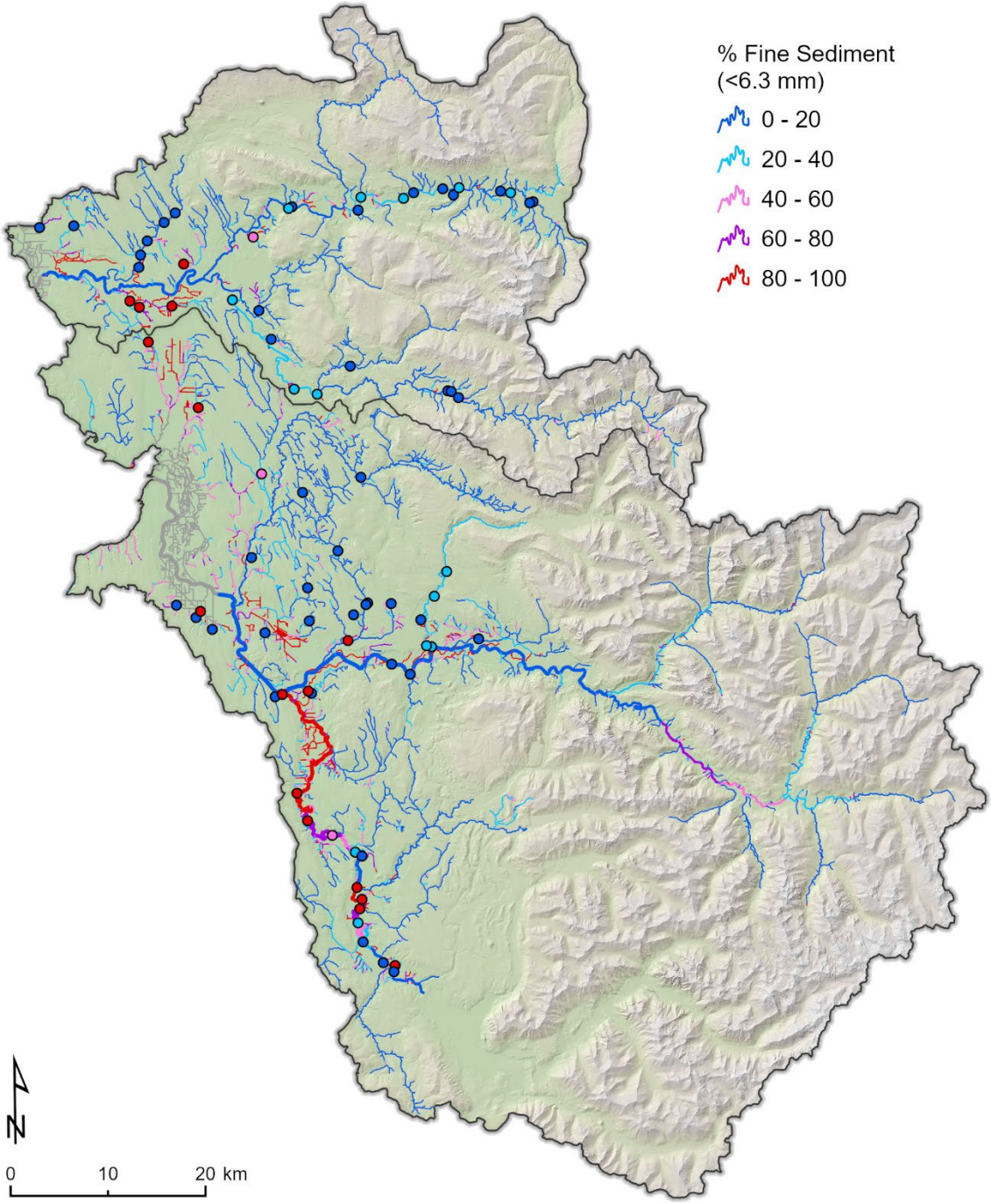

Figure 4-13. Modeled fine sediment levels in the Stillaguamish and Snohomish River basins (lines), and data used to develop the models (points).

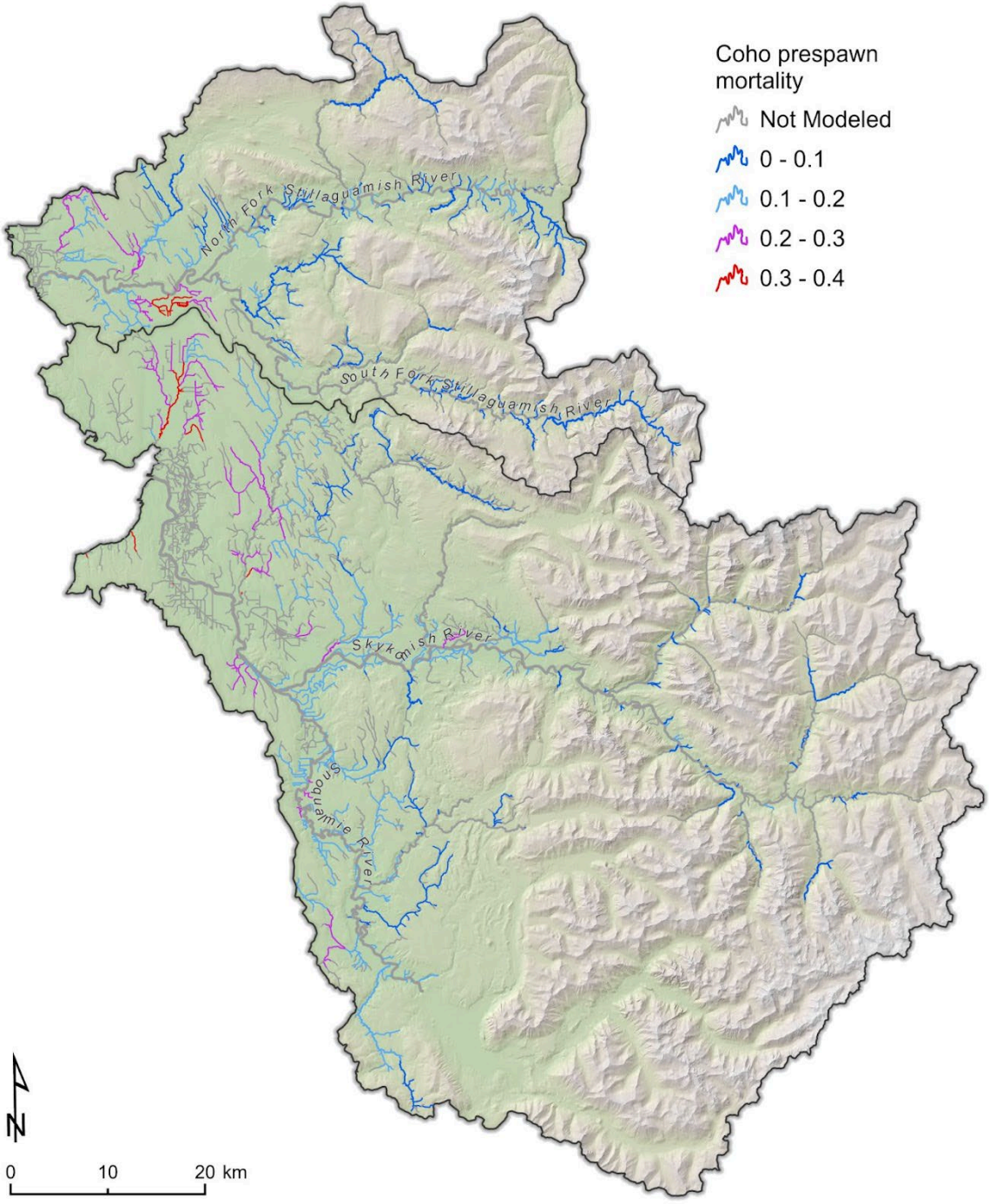

Figure 4-14. Modeled coho prespawn mortality levels in the Stillaguamish and Snohomish River basins. Data from Feist et al. 2017.

4.1.9 Estuary Habitat

In the Stillaguamish estuary, the main channel has shifted from the Old Mainstem historically to Hat Slough currently (Figure 4-15). As a result the delta front has eroded in the northern half and prograded in the southern half, and the connectivity values of most habitats have changed. In the current configuration, juvenile Chinook migrate down Hat Slough, and for most of the outmigration season they can only access the Old Mainstem habitats from the lower delta. Therefore, we modeled connectivity for the dominant migration route only. Under the historical configuration juveniles would have migrated

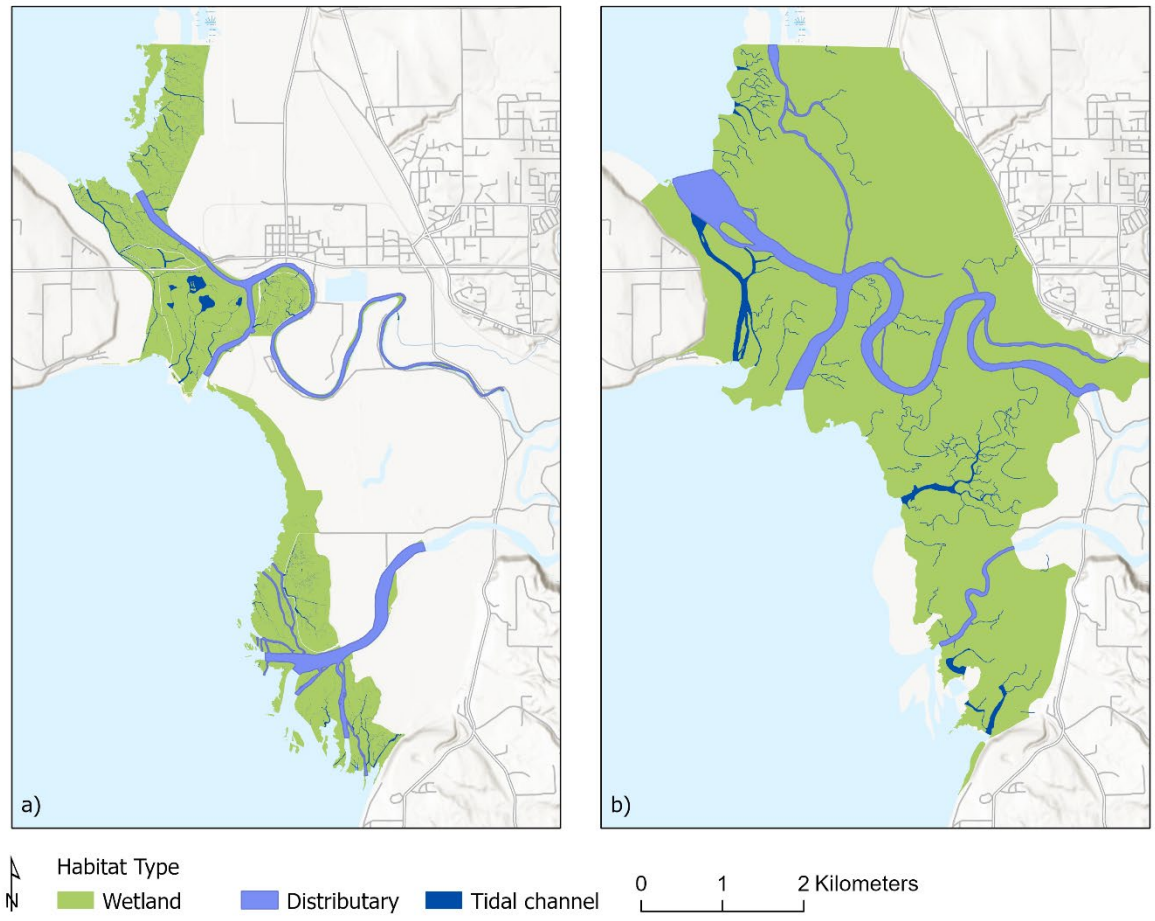

Figure 4-15. Current (a) and historical (b) estuary wetland area in the Stillaguamish River basin. Wetland polygons include estuarine emergent marsh, estuarine forest transition, and forested riverine tidal wetlands. Historically surveyed tidal channels, shown in dark blue in (b), likely only represent a subset of tidal channels present at the time. Therefore, the HARP model uses tidal channel allometry relationships to estimate historical tidal channel area rather than relying on incomplete survey data. Modern roads are shown for reference in both panels. Service layer credits for reference basemap: Island County, WA State Parks, Esri, HERE, Garmin, SafeGraph, GeoTechnologies Inc, METI/NASA, USGS, Bureau of Land Management, EPA, NPS, USDA, NASA, NGA, USGS, FEMA.

down the Old Mainstem, and we use this routing for the diagnostic scenario even though potential restoration actions are not likely to shift the main stem back into the Old Mainstem. Most of the estuarine emergent marsh, estuarine forest transition, and forested riverine tidal habitats have been blocked by levees (80%) (Figure 4-15). Distributary edge habitat areas were quite small both historically and currently, and there has been an increase in the estimated usable area (+4%) (Table 4-4). Tidal channel areas have been reduced by 50% (Table 4-4).

In the Snohomish estuary, the main channel and distributaries are essentially in the same locations as they were historically, so estimated current and historical areas of those habitat types are very similar, and connectivity of habitat also was unchanged (Figure 4-16). Most of the estuarine emergent marsh, estuarine forest transition, and forested riverine tidal habitats have been blocked by levees (81%). Distributary edge habitats have decreased by 1%, and tidal channel areas have been reduced by 92% (Table 4-4).

Note that percent marsh loss is similar in the two estuaries, but we predict less tidal channel loss in the Stillaguamish because the allometry predicts higher drainage density in smaller wetland "islands" and the historical Snohomish estuary was made up of more separate islands than the Stillaguamish estuary. That is, the estimated historical tidal channel density is smaller in the Stillaguamish estuary than in the Snohomish Estuary, which produces a smaller estimate of estuary tidal channel loss.

Table 4-4. Changes in estuary habitat areas for distributary edges (2-m width on each side of the channel) and tidal channels in the Stillaguamish and Snohomish River estuaries.

	Useable Habitat Area (ha)		
Estuary Habitat Type	**Historical**	**Current**	**Percent Change**
Stillaguamish			
Distributary Edge	8.6	8.9	+4%
Tidal Channel	71.2	35.8	-50%
Total	79.8	44.7	-44%
Snohomish			
Distributary Edge	25.7	25.5	-1%
Tidal Channel	1008.3	79.5	-92%
Total	1034.0	105.0	-90%

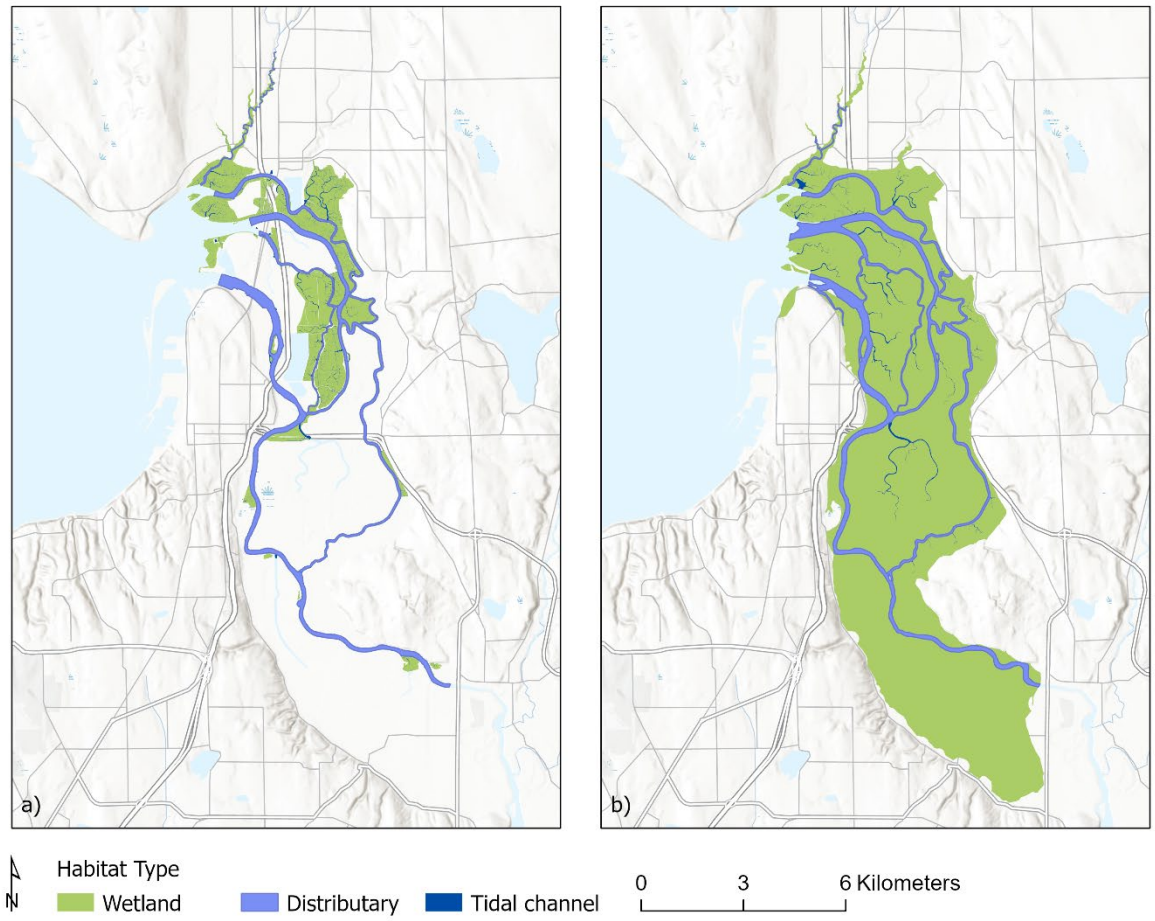

Figure 4-16. Current (a) and historical (b) estuary wetland area in the Snohomish River basin. Wetland polygons include estuarine emergent marsh, estuarine forest transition, and forested riverine tidal wetlands. Historically surveyed tidal channels, shown in dark blue in (b), likely only represent a subset of tidal channels present at the time. For this reason, the HaRP model uses tidal channel allometry relationships to estimate historical tidal channel area rather than relying on incomplete survey data. Modern roads are shown for reference in both panels. Service layer credits for reference basemap: Esri, NASA, NGA, USGS, FEMA, Everett Community College, WA State Parks, HERE, Garmin, SafeGraph, GeoTechnologies Ince, METI/NASA, Bureau of Land Management, EPA, NPS, USDA.

4.2 Changes in Life-Stage Capacity and Productivity

The HARP model indicates that spawning and rearing capacities have been reduced in both basins for all capacity-limited life stages of all populations (Table 4-5). The greatest basin-wide capacity reduction was for Chinook salmon in the Snohomish estuary (98% capacity

loss), and the greatest freshwater capacity loss was in the winter rearing capacity for coho (78% and 80% loss in the Stillaguamish and Snohomish basins, respectively). Other capacity losses were less than 50%, except for coho spawning, coho summer rearing, and Chinook summer rearing.

Capacity-weighted averages of life-stage productivities show basin-wide reductions in the Beverton-Holt density-independent productivity parameter for most life stages in most populations. Rearing life stages for coho showed 12-21% reduction relative to historical conditions (Table 4-6). Both basins show a 14% decrease in prespawn productivity for Chinook salmon, and the Snohomish basin shows relatively higher reductions in summer and winter rearing productivities for yearling-type fish. Modeled declines in the life-stage productivity parameters are generally smaller for steelhead than for either coho or Chinook salmon.

Table 4-5. Change in modeled life-stage capacities in the Snohomish and Stillaguamish River basins.

		Capacity Loss	
Population	**Life Stage**	**Snohomish**	**Stillaguamish**
Coho	Spawning	-74%	-64%
	Summer rearing	-54%	-49%
	Winter rearing	-80%	-78%
Summer- and Fall-Run Chinook	Spawning	-33%	-35%
	Colonization	-28%	-20%
	Subyearling rearing	-28%	-20%
	Summer rearing	-55%	-48%
	Winter rearing	-33%	-10%
	Estuary rearing	-98%	-80%
Winter-run Steelhead	Spawning	-36%	-39%
	1st Summer rearing	-21%	-19%
	1st Winter rearing	-17%	-14%
	2nd/3rd Summer rearing	-19%	-19%
	2nd/3rd Winter rearing	-17%	-20%
Summer-run Steelhead	Spawning	-35%	-41%
	1st Summer rearing	-21%	-21%
	1st Winter rearing	-17%	-14%
	2nd/3rd Summer rearing	-18%	-19%
	2nd/3rd Winter rearing	-18%	-21%

Table 4-6. Modeled change in density-independent productivity parameters for each life-stage in the Snohomish and Stillaguamish River basins.

		Productivity Reduction	
Population	**Life Stage**	**Snohomish**	**Stillaguamish**
Coho	Prespawn	-10%	-4%
	Incubation	-10%	-10%
	Summer rearing	-14%	-10%
	Winter rearing	-12%	-19%
Summer- and Fall-Run Chinook	Prespawn	-14%	-14%
	Incubation	-3%	-4%
	Colonization	-12%	-7%
	Subyearling rearing	-12%	-7%
	Summer rearing	-17%	NA
	Winter rearing	-26%	NA
Winter-run Steelhead	Prespawn	0%	0%
	Incubation	-1%	-1%
	1st Summer	-5%	-7%
	1st Winter	-7%	-7%
	2nd/3rd Summer rearing	-5%	-8%
	2nd/3rd Winter rearing	-8%	-11%
Summer-run Steelhead	Prespawn	0%	0%
	Incubation	-1%	0%
	1st Summer rearing	-5%	-7%
	1st Winter rearing	-7%	-7%
	2nd/3rd Summer rearing	-5%	-7%
	2nd/3rd Winter rearing	-8%	-12%

4.3 Diagnostic Scenarios

The diagnostic scenarios compare modeled spawner abundance under each diagnostic scenario against the modeled current spawner abundance, and the difference between the two is the *restoration potential* for that action type (Figure 4-17). The model was run deterministically for this project, so there is no annual variation around the modeled spawner abundances. The diagnostic scenarios suggest that restoration actions to improve coho salmon populations should focus on restoration of beaver pond and floodplain habitats in both River basins (Figure 4-17), which are important overwintering habitats for juvenile coho. Modeled restoration potentials for beaver ponds are 66% and 43% in the Stillaguamish and Snohomish basins, respectively, and 87% and 55%, for floodplain reconnection in the Stillaguamish and Snohomish basins, respectively. Restoring wood also

has a significant effect on coho salmon abundance, although a substantially smaller one than for beaver pond restoration or floodplain reconnection (25% and 30% in the Stillaguamish and Snohomish basins, respectively). Migration barrier removal has a relatively small effect in both basins (13% and 14% in the Stillaguamish and Snohomish, respectively). These relatively small effects reflect the fact that 20-22% of the coho spawning and rearing habitat length is above any type of barrier, and that many of those barriers are partially passable. Beaver pond restoration potential for coho salmon is widespread throughout the Stillaguamish and Snohomish River basins, whereas floodplain and wood restoration potentials are more localized (Figure 4-18). Not surprisingly, floodplain restoration potential is greatest along the larger mainstem rivers. In general the effect of wood on coho salmon habitat capacity and productivity is much greater in small streams, so subbasins with a greater proportion of small streams have greater modeled restoration potential.

The diagnostic scenarios suggest that summer- and fall-run Chinook salmon will likely benefit from wood augmentation, bank armor removal, and floodplain reconnection in both basins (restoration potentials ranging from 17% to 22% in the Stillaguamish basin and 13% to 18% in the Snohomish basin) (Figure 4-17). Each of these actions address subyearling and yearling rearing capacity and productivity, which decreased in both basins (Table 4-5 and Table 4-6). Modeled restoration potential for the shade scenario is lower in both basins (8-11%). The modeled estuary restoration potential is +4% in the Stillaguamish basin and +45% in the Snohomish basin. The low potential benefit for estuary restoration in the Stillaguamish basin is a result very low numbers of fry leaving freshwater, and the number of fry is far below estuary capacity. Therefore, increasing estuary capacity has little effect on Chinook spawner abundance. Chinook salmon show relatively widespread responses to bank armor removal, wood augmentation, and floodplain reconnection (Figure 4-18). However, the modeled restoration potentials for bank armor and floodplain reconnection are highest in the lower Snoqualmie and lower Stillaguamish Rivers where bank armor is most extensive, and slightly lower in the mainstem Skykomish and North Fork Stillaguamish Rivers (Figure 4-18).

Steelhead will likely be most responsive to wood augmentation in both basins (restoration potential = 34%) (Figure 4-17), although shade restoration and floodplain reconnection also benefit steelhead (14% and 31% in the Stillaguamish basin, and 7% and 20% in the Snohomish River basin). The mechanisms underlying the steelhead restoration potentials are likely (1) an increase in rearing habitat capacities and productivities due to wood addition, and (2) reduction in summer rearing temperatures due to increased shade and increased hyporheic exchange through floodplain reconnection. For steelhead, the restoration potential for wood augmentation is widespread throughout both river basins. In contrast, the restoration potential for floodplain reconnection is mostly in the lower mainstem rivers where winter steelhead subpopulations are dominant. Shade restoration potential is generally low for steelhead, except in a few lower mainstem segments where increasing shade could increase summer rearing capacity and productivity.

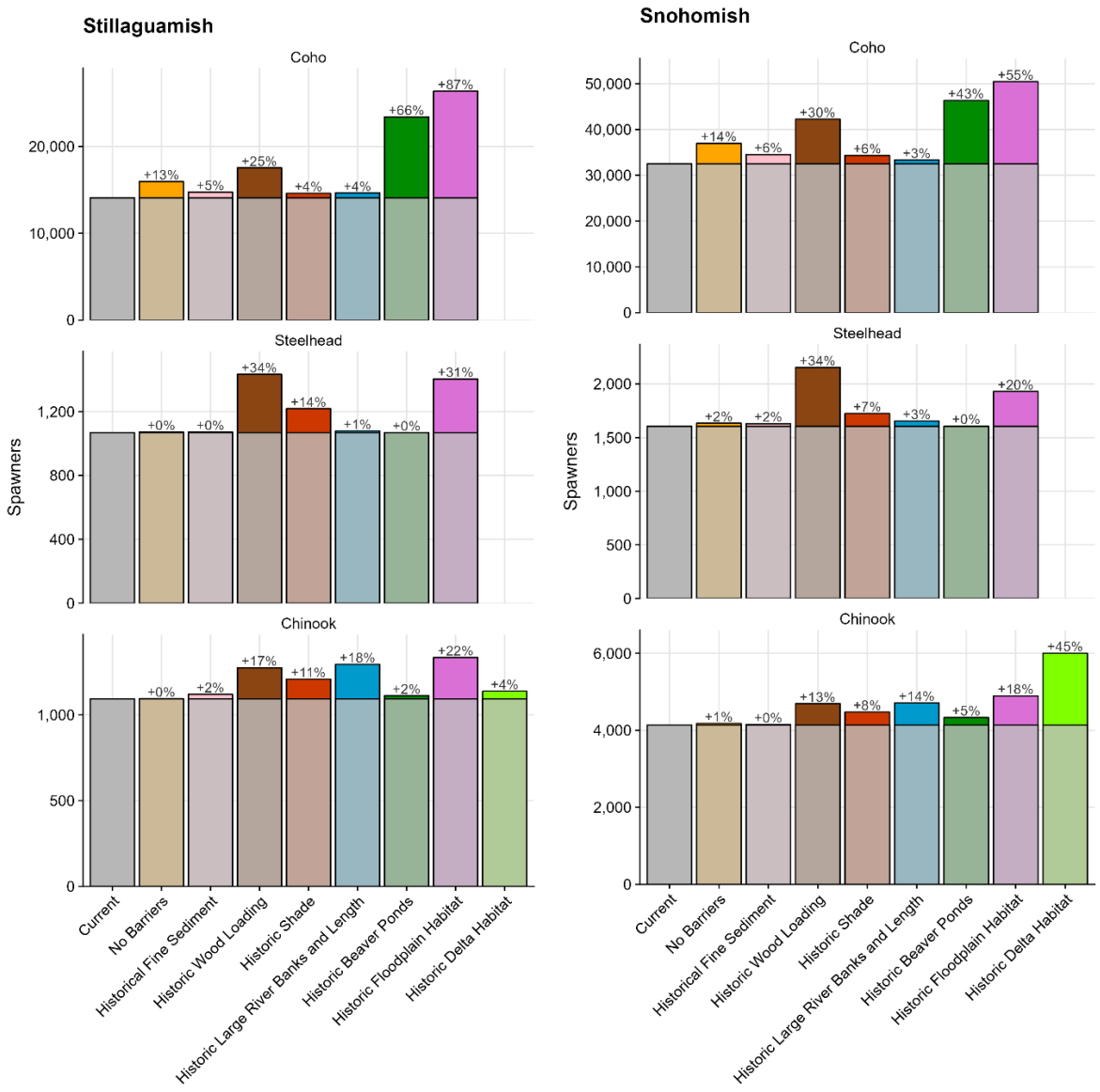

Figure 4-17. Modeled spawner abundances for each basin and species under each diagnostic scenario. Steelhead is the total of summer and winter steelhead combined.

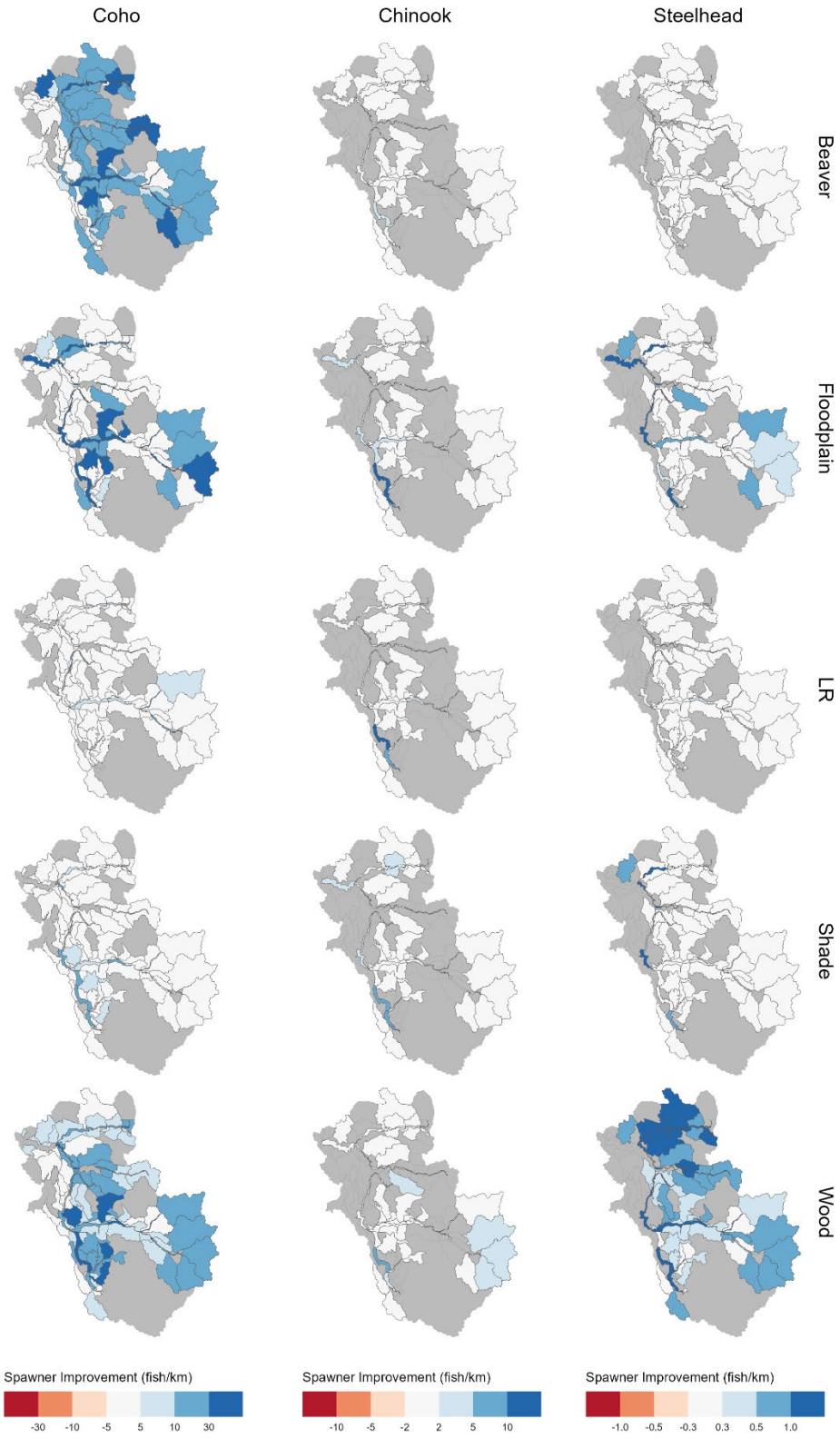

Figure 4-18. Modeled change in spawner density (number of spawners per kilometer of spawning habitat) by subbasin for the five most responsive diagnostic scenarios. Note different color scales for each column.

4.4 Sensitivity Analysis

The one-at-a-time sensitivity analysis shows relatively similar patterns among the two basins for the freshwater life-stage parameters (Figure 4-19). In these plots, steeper slope of a line indicates greater sensitivity to that parameter per increment of change, and greater length of a line indicates greater restoration potential. In their freshwater life stages, coho salmon are most sensitive to changes in prespawn mortality, but at the population level there is little restoration potential because prespawn morality has not increased substantially across either basin. However, changes in prespawn mortality are spatially heterogeneous (Fig 4-14), and in streams where prespawn mortality is locally high, restoration actions to filter road runoff may be beneficial. Most of the restoration potential in both basins is in winter rearing habitat capacity, followed by summer rearing habitat capacity. These results reinforce the diagnostic scenarios, which indicated that the greatest restoration potential is in restoring floodplain connectivity and beaver pond habitat. However, selecting actions that improve the most sensitive capacities or productivities may still be relatively cost-effective because the subpopulation response can be high relative to the restoration effort.

Chinook salmon are most responsive to subyearling parr rearing capacity during their freshwater stages, followed by prespawn productivity (Figure 4-19). Increasing parr rearing capacity increases the number of parr migrants, which have greater survival to adult return. This supports the diagnostic results, which indicate that actions that increase rearing habitat capacity and productivity (floodplain reconnection, bank armor removal, wood augmentation) are likely to be most beneficial. Chinook salmon are also very sensitive to prespawn productivity, which is largely a response to change in summer temperature. Therefore, restoration actions to reduce summer stream temperature (floodplain reconnection and increasing shade) may help reduce prespawn mortality for Chinook salmon.

In freshwater, steelhead are most sensitive to summer and winter rearing productivities in both basins, and less sensitive to rearing capacities (Figure 4-19). However, steelhead are more sensitive to life-stage capacities in the Snohomish basin than in the Stillaguamish River basin. The productivities are influenced largely by wood abundance and stream temperature, suggesting that a habitat restoration strategy including wood augmentation, floodplain reconnection, and shade restoration may be most beneficial for steelhead, which is consistent with the diagnostic scenarios.

There are very few data on Chinook fry survival in estuaries, so we conducted a simple sensitivity analysis to evaluate (1) how much the estuary productivity parameter changes the modeled response in spawner abundance, and (2) whether increasing the number of fry reaching the delta influences the response. Under current freshwater habitat conditions in the Snohomish estuary, at low estuary productivity value of 0.10, the model predicts a minimal response of Chinook to restoring the full estuary (~3% increase in spawner abundance), but at a high estuary productivity value of 0.5, the model predicts a very large response (~80% increase in spawner abundance) (Figure 4-20). Increasing the number of fry reaching the estuary (via freshwater restoration in this example) also increases the

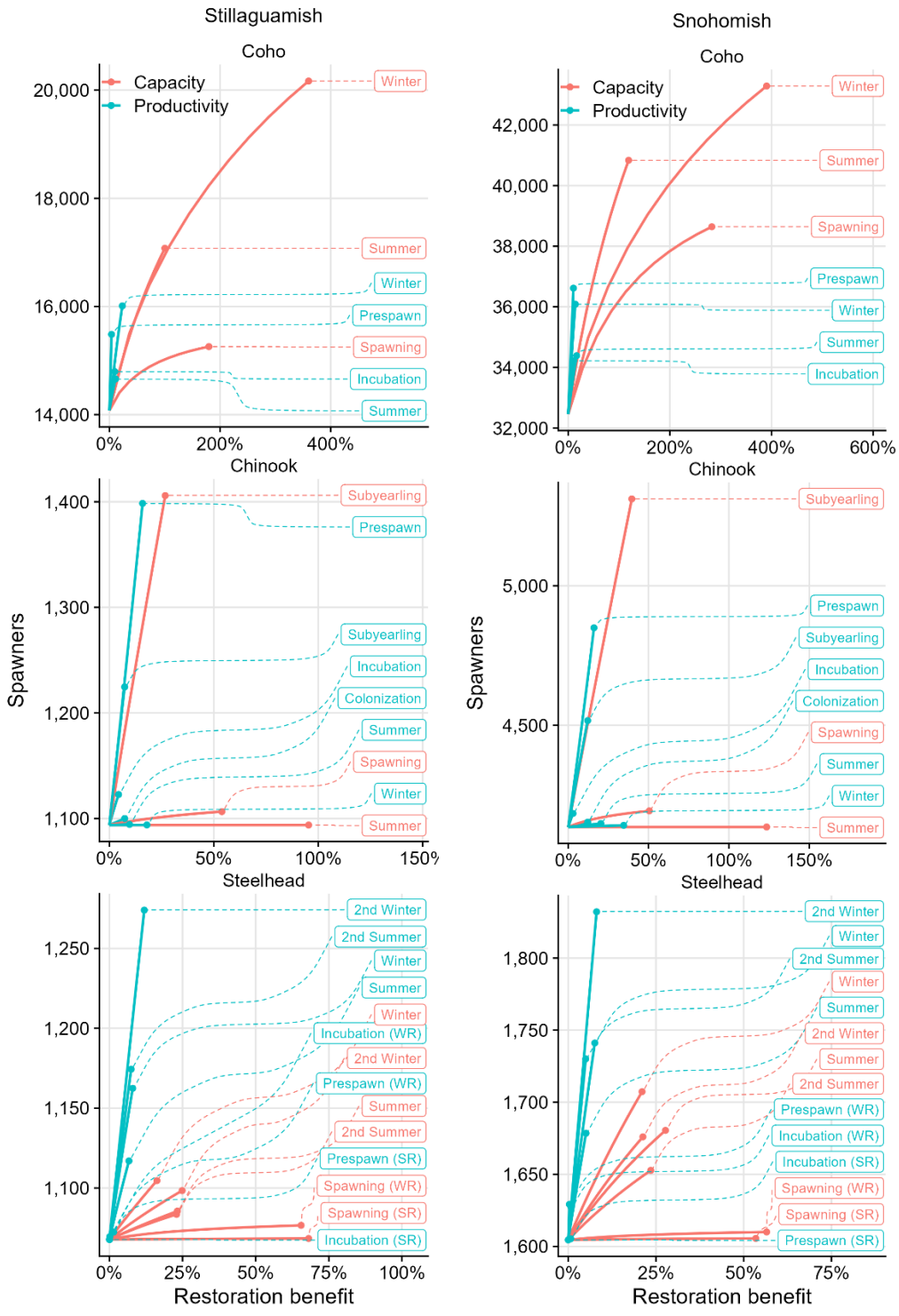

Figure 4-19. One-at-a-time sensitivity analysis of life stage parameters for each species/run in the Stillaguamish and Snohomish basins. The baseline (0% on the x-axis) is the modeled spawner abundance with current habitat conditions. The x axis is percent increase in a capacity or productivity parameter from the current condition up to the maximum value of the parameter, and the y axis is modeled spawner abundance (note different y-axis scales).

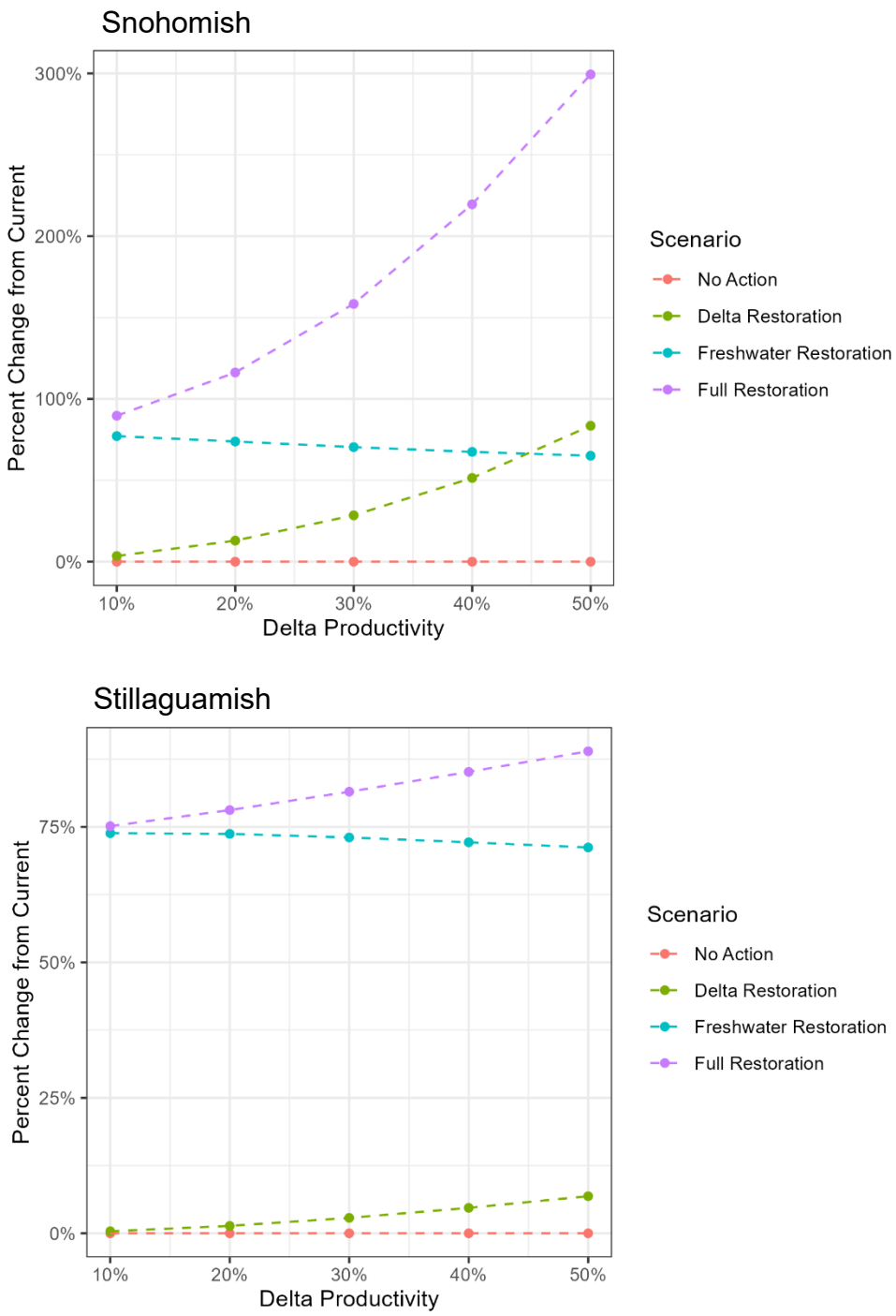

Figure 4-20. Modeled change in spawner abundance as a function of the estuary productivity parameter chosen for the model, for the Snohomish and Stillaguamish River basins. No action is current habitat conditions for freshwater habitats and the estuary, estuary restoration is current habitat conditions for freshwater habitats and historical conditions for the estuary, freshwater restoration is historical conditions for freshwater habitats and current conditions for the estuary, and full restoration is historical conditions for both freshwater habitats and the estuary.

population response to estuary restoration. At the low productivity value of 0.10, the model predicts an increase of ~10% (compared to ~3%) in modeled spawner abundance when more juveniles reach the estuary, and at the high productivity value of 0.50 the model predicts an increase of ~235% (compared to ~80%).

In the Stillaguamish estuary, estuary restoration potential is considerably less than that of the Snohomish under current freshwater habitat conditions, ranging from an increase of ~1% with a productivity of 0.1 to an increase of ~6% with a productivity of 0.50. While there is still a synergistic effect when combined with freshwater restoration, the model does not suggest that a fully restored delta at high productivity will have a large effect on Chinook salmon spawner abundance (up to ~35%). The small response is due to the low number of fry reaching the delta, which we calibrated to match the ratio of fry to parr passing the smolt trap. Even though the modeled number fry migrants exceeds the observed number of fry passing the smolt trap, the low numbers of fry reaching the delta are far below the estuary rearing capacity and increases in rearing capacity have little influence on the modeled spawner abundance.

5. Discussion

5.1 Potential Restoration Options

The HARP Model results indicate that the most important habitat restoration actions vary by species, but that the most important actions for each species are similar in the Stillaguamish and Snohomish River basins (except for estuary restoration). For example, coho salmon in both basins will likely respond most to beaver pond restoration and floodplain reconnection, both of which primarily influence juvenile overwinter capacity and survival. However, the modeled restoration potential for both actions is higher in the Stillaguamish basin than in the Snohomish basin. Beaver restoration potential is widespread in small streams of both basins, while floodplain restoration potential is mostly along large rivers. We have relatively high confidence in this result because increasing availability of slow-water winter rearing habitat has been shown to increase coho salmon abundance in other studies (Solazzi et al. 2000, Ogston et al. 2015). Wood augmentation and barrier removal may also benefit coho salmon populations, although the total restoration potential is lower for those actions. Wood restoration potential is also widespread, but barrier removal restoration potential is more localized. Fine sediment reduction, shade restoration, and bank armor removal appear to have lower restoration potential for coho salmon in either basin.

For Chinook salmon, estuary restoration appears to have the greatest restoration potential in the Snohomish basin, but much lower potential in the Stillaguamish River basin. The primary difference between the two basins is that the current number of outmigrating Chinook fry is far below the modeled Stillaguamish delta capacity, so they are less responsive to additional increases in delta capacity. However, this model does not account for non-natal fish (i.e., Skagit-origin fish) rearing in either estuary. The combined populations of natal and non-natal Chinook juveniles using a particular estuary could create a more capacity-limited rearing stage than what is currently predicted by the HARP Model. In this more capacity-limited context, estuary restoration would have a greater potential to reduce capacity limitation and improve overall estuarine survival. Other potential restoration actions for Chinook salmon include bank armor removal, floodplain restoration, and wood augmentation, which have restoration potentials ranging from +12% to +18% in both basins. Floodplain and bank armor removal restoration potentials are highest in the Snoqualmie main stem and Stillaguamish main stem. Shade restoration potential is lower in both basins, and restoration potential is concentrated in the Snoqualmie mainstem and smaller tributaries within the Chinook spawning range.

Wood augmentation and floodplain restoration have the greatest restoration potential for steelhead, followed by shade restoration. Floodplain and shade restoration both reduce summer stream temperature, which increases summer rearing capacity and productivity (Section 2.1.7). Wood restoration potential is widespread in steelhead spawning and rearing reaches, whereas floodplain restoration potential is concentrated along the large mainstem reaches. Shade restoration potential is localized in a few reaches of the lower

Snohomish River and lower North and South forks of the Stillaguamish River. The remaining restoration action types have lower restoration potential for steelhead.

It is worth noting that many restoration actions such as floodplain reconnection may involve other actions such as bank armor removal or wood augmentation. Those combinations of actions would likely achieve the cumulative benefit of all included actions, increasing the restoration potential at individual sites. Moreover, some actions such as riparian restoration provide multiple benefits. For example, riparian restoration not only provides shade, it also provides wood recruitment to streams, root reinforcement of stream banks, and leaf litter subsidies to support aquatic food webs. Similarly, bank armor removal can lead to channel widening and increased rearing habitat areas in addition to altering the cover type of bank edge units.

The HARP Model results for the Stillaguamish and Snohomish River basins are generally similar to HARP Model results in the Chehalis River basin, except that fine sediment reduction appears to afford little restoration opportunity in the Stillaguamish and Snohomish River basins compared to the Chehalis River basin. This difference is primarily due to differences in the fine sediment models for the two locations, resulting in the predicted increase in fine sediment levels from historical to current conditions in the Stillaguamish and Snohomish basins being much smaller than in the Chehalis basin. We have relatively high confidence in the predicted current fine sediment levels in the Stillaguamish and Snohomish basins because we had a large number of sample sites with which to construct fine sediment models. However, we only detected a land use influence on fine sediment levels in channels less than 30 m bankfull width, and the predicted restoration potential is low. There are almost certainly some streams and reaches where fine sediment restoration potential may be higher due to localized sediment sources that can be effectively reduced through restoration or changes in land use practices.

5.2 Uncertainties

Modeled current spawner abundances are low compared to the most recent 10 years of observed escapements for coho salmon and steelhead, and closed to observed values for Chinook salmon (Table 5-1). The model is not calibrated to run size or escapement, so differences between modeled and observed spawners are likely due to under- or over-estimates of certain model parameters (e.g., one or more life-stage productivity values). While we have no way to determine which parameters are most responsible for the differences, we can describe uncertainties in the model that warrant future investigation.

There are two primary sources of uncertainty in the habitat assessment and life-cycle model outputs: parameter uncertainty and model form uncertainty (Jorgensen et al. 2021, Beechie et al. 2021a). Parameter uncertainty refers to the accuracy of input data and model parameters, including measurement error and extrapolation error. Model form uncertainty refers to the accuracy of the model structure, including choices of model components to include or exclude and accuracy of the functional relationships in the model.

Table 5-1. Comparison of modeled spawner abundance to the most recent 10 years of observed escapements. Annual escapements for each species/run are summarized in Appendix F. The model is run with no harvest.

Species/run	Stillaguamish		Snohomish	
	Modeled spawners	Observed escapement	Modeled spawners	Observed escapement
Coho salmon	14,100	19,495	32,500	45,913
Chinook salmon	1,090	982	4,100	3,917
Steelhead	1,070	425[a]	1,600	2,441[b]

a. Steelhead escapement estimates are not expanded and only represent spawners within an index area in the North Fork Stillaguamish.

b. Summer-run steelhead are not included in the escapement estimate.

5.2.1 Parameter Uncertainty

Uncertainty in the parameter estimates used in the life-cycle models can arise from natural spatial and temporal variation, extrapolation errors, and measurement errors, all of which influence the accuracy of parameters such as fish densities or productivity estimates. In most cases, there is substantial variation in the data underpinning the parameters and functions used in the models, and selection of any parameter value or function aims to capture a "typical" value or response function (Beechie et al. 2021b).

The reach-level habitat values used in the model contain varying types and levels of uncertainty. For measured parameters such as large river bank habitat or canopy opening angle, the main source of uncertainty is measurement error. Bank habitats are digitized from aerial imagery, so there may be errors in identification of habitat types where canopy cover obscures the bank. Canopy opening angles are calculated from lidar data, so measurement error may be smaller. Other habitat attributes such as percent pool area in small streams are extrapolated from a sample of field surveys. We stratified the data by channel slope and adjacent land cover and then extrapolated data to reaches in the same slope and land cover class to reduce extrapolation error. However, extrapolating mean values to other reaches still includes some unknown error. Finally, some habitat parameters are produced from other models, and prediction errors are a source of uncertainty. For example, there is prediction uncertainty in the reach-level fine sediment or temperature values because we built models to predict those values from a sample of field sites.

An important geospatial dataset that influences uncertainty in many habitat parameters is the National Hydrography Dataset. This dataset has many spatial inaccuracies in small streams, creating challenges in assigning accurate attributes from other geospatial data. For example, spatial inaccuracies in the stream location create inaccurate adjacent land cover attributes because the stream is in the wrong location. Similarly, assigning attributes

from barrier data and lidar-derived datasets (which are spatially more accurate) to the correct reaches is also challenging. For the HARP Model analyses, using various means of transferring data from accurate locations to the hydrography line has been an acceptable solution, but a more accurate hydrography data set would streamline the analysis.

In the life-cycle models we use data on current spawning and rearing densities or productivities to parameterize the models for current habitat conditions (Jorgensen et al. 2021). For capacities, we used published densities for estimating capacity when data were available (e.g., juvenile coho density data from Nickelson 1998). Where published data were not available, we used density data from the Snohomish, Stillaguamish, and Skagit basins. Because all data are from locations where run sizes are low compared to historical levels, we reanalyzed raw density data and chose the 95th percentile of observed densities to calculate capacity.

For Chinook salmon, we did not use most of the density data from two recent studies in the Snohomish and Skagit basins because the 95th percentile or maximum densities in both recent studies were lower than the densities we currently use for fry colonization in the HARP Model (95th percentile of densities from Beamer and Henderson 1998). This suggests that habitats are not occupied to capacity, so we chose to retain the higher densities to avoid underestimating rearing capacity. Nonetheless, after discussion with project partners we adjusted the armored bank density down to 0.14 to reflect the lower densities in a recent Snohomish River study.

To estimate density-independent productivity for each species and life stage, we also used published survival estimates where possible. Where a range of observations was available, we chose values from the high end of the observed range because the observations include density-dependent effects on survival, and the density independent productivity parameters should be higher than observed survival rates. We note that the productivity estimates likely to have high uncertainty because (1) they are more difficult to measure and (2) there are fewer studies documenting survival rates than studies documenting fish density by habitat type. Moreover, the data on rearing life-stage survivals are observed density-dependent survival rates, and the productivity estimate for a Beverton-Holt function should be higher than the observed density-dependent survival. In light of these uncertainties, it is perhaps not surprising that the coho and steelhead models tend to produce equilibrium spawner abundance estimates that are in the low end of the observed spawner abundance range for the last 10 years.

5.2.2 Model Form Uncertainty

Model form uncertainties in the life-cycle models include (1) which aspects of life histories are represented or omitted, (2) which habitat effects are represented or omitted, and (3) the accuracy of equations used to represent habitat effects on life stage parameters (Beechie et al. 2021b). The HARP model includes life stages for which we were able to find sufficient data, but some life history types such as coho salmon age-0 nomads (Koski 2009, Bennett et al. 2015) are not included due to insufficient data. Omitting certain life history types will, of course, change the behavior of the models. The model also includes simple

movement rules that govern migration of juveniles to downstream locations during rearing, but there is little data available to estimate what proportion of each species/life stage should migrate or how far they should move. We also do not know the extent to which model results are affected by inter- and intra-species interactions in the subbasins, estuary, and Puget Sound (Jorgensen et al. 2021), or by predation by native and non-native species. We did not model variable ocean conditions or the effects they might have on fish of different ages and sizes, nor did we include hatchery supplementation or the influence of hatchery fish on the survival of wild fish.

The HARP Model includes a number of habitat change effects on fish density or survival, but there are some effects that we were not able to include. For example, food availability and growth are not modeled, so the effects of increased growth on survival in later life stages is not included. We also did not have sufficient data to model pollutant effects on juveniles of any species. For habitat relationships included in the model, we used single equations that represent the typical density or survival response of fish to habitat changes, but there is considerable variation in the data used to generate those equations. Therefore, each function may under- or over-estimate fish responses to habitat changes.

5.3 Next Steps

Results of the HARP Model in these basins can be used to inform restoration strategies or salmon recovery plans. However, model results should only be one source of information used, and they should be considered in light of model uncertainties. The diagnostic scenarios indicate which restoration actions have the greatest restoration potential, as well as which subbasins are likely to provide the greatest response. While we cannot estimate potential error in the modeled percent changes, we suggest that scenarios with somewhat similar restoration potentials be considered as having similar priority (e.g., bank armor removal, wood augmentation, and floodplain reconnection would be ranked similarly for Chinook salmon). Moreover, the sensitivity analyses indicate that some life-stage parameters have large influences on spawner abundance even when there is low overall restoration potential. This suggests that some restoration actions may be very cost-effective contributions to recovery within certain subbasins even though they make small contributions at the basin scale.

Climate change scenarios were not included in this project, and it is important to recognize that climate change will alter habitat conditions and will likely reduce spawner abundances in the future (Nicol et al. 2022, Fogel et al. 2022). Such habitat changes may shift restoration priorities (Beechie et al. 2021b), but many restoration actions that are high priorities today are likely to remain high priority in the future because they can ameliorate climate change effects and have high restoration potential (e.g., floodplain reconnection). The HARP Model has the capability of modeling climate change and complex restoration scenarios (Beechie et al. 2023), which can be used to evaluate the types and level of restoration needed to increase resilience against climate change. Such model results may help set current restoration priorities, especially for actions with long lag times between the restoration action and the habitat response (e.g., riparian restoration).

References

Anderson, J. H., and P. C. Topping. 2018. Juvenile life history diversity and freshwater productivity of Chinook salmon in the Green River, Washington. North American Journal of Fisheries Management 38:180–193.

Arrigoni, A. S., G. C. Poole, L. A. K. Mertes, S. J. O'Daniel, W. W. Woessner, and S. A. Thomas. 2008. Buffered, lagged, or cooled? Disentangling hyporheic influences on temperature cycles in stream channels. Water Resources Research 44:W0948.

Beamer, E., and R. Henderson. 1998. Juvenile salmonid use of natural and hydromodified stream bank habitat in the mainstem Skagit River, northwest Washington. Skagit River System Cooperative, La Conner, WA.

Beamer, E., A. McBride, C. Greene, R. Henderson, W. G. Hood, K. Wolf, K. Larsen, C. Rice, and K. Fresh. 2005. Delta and Nearshore Restoration for the Recovery of Wild Skagit River Chinook Salmon: Linking Estuary Restoration to Wild Chinook Salmon Populations. Appendix D of the Skagit Chinook Recovery Plan. Skagit River System Cooperative, La Conner, WA.

Bear, E. A., T. E. McMahon, and A. V. Zale. 2007. Comparative thermal requirements of westslope cutthroat trout and rainbow trout: implications for species interactions and development of thermal protection standards. Transactions of the American Fisheries Society 136:1113–1121.

Beck, S. M., and D. W. Reiser. 2006. Spatial and Temporal Comparison of Spawning Gravel Quality in the Sultan River, Washington. R2 Resources Consultants, Inc., Redmond, WA.

Beechie, T., E. Beamer, and L. Wasserman. 1994. Estimating coho salmon rearing habitat and smolt production losses in a large river basin, and implications for habitat restoration. North American Journal of Fisheries Management 14:797–811.

Beechie, T. J. 1990. Evaluation of the TFW stream classification system: stratification of physical habitat area and distribution. Master of Science, University of Washington, Seattle, WA.

Beechie, T. J., B. D. Collins, and G. R. Pess. 2001. Holocene and recent geomorphic processes, land use, and salmonid habitat in two north Puget Sound river basins. Pages 37–54 *in* J. M. Dorava, D. R. Montgomery, B. B. Palcsak, and F. A. Fitzpatrick, editors. Geomorphic Processes and Riverine Habitat. American Geophysical Union, Washington, D. C.

Beechie, T. J., C. Fogel, C. Nicol, J. C. Jorgensen, B. L. Timpane-Padgham, and P. M. Kiffney. 2023. How does habitat restoration increase salmon population resilience to climate change? Ecosphere.

Beechie, T. J., C. Fogel, C. Nicol, and B. Timpane-Padgham. 2021a. A process-based assessment of landscape change and salmon habitat losses in the Chehalis River basin, USA. PLOS ONE 16:e0258251.

Beechie, T. J., C. M. Greene, L. Holsinger, and E. M. Beamer. 2006a. Incorporating parameter uncertainty into evaluation of spawning habitat limitations on Chinook salmon (Oncorhynchus tshawytscha) populations. Canadian Journal of Fisheries and Aquatic Sciences 63:1242–1250.

Beechie, T. J., M. Liermann, E. M. Beamer, and R. Henderson. 2005. A classification of habitat types in a large river and their use by juvenile salmonids. Transactions of the American Fisheries Society 134:717–729.

Beechie, T. J., M. Liermann, M. M. Pollock, S. Baker, and J. Davies. 2006b. Channel pattern and river-floodplain dynamics in forested mountain river systems. Geomorphology 78:124–141.

Beechie, T. J., C. Nicol, C. Fogel, J. Jorgensen, J. Thompson, G. Seixas, J. Chamberlin, J. Hall, B. Timpane-Padgham, P. Kiffney, S. Kubo, and J. Keaton. 2021b. Modeling effects of habitat change and restoration alternatives on salmon in the Chehalis River basin using a salmonid life-cycle model. NOAA Contract Report NMFS-NWFSC-CR-2021-01, Seattle, WA.

Beechie, T. J., and T. H. Sibley. 1997. Relationships between channel characteristics, woody debris, and fish habitat in northwestern Washington streams. Transactions of the American Fisheries Society 126:217–229.

Bennett, T. R., P. Roni, K. Denton, M. McHenry, and R. Moses. 2015. Nomads no more: early juvenile coho salmon migrants contribute to the adult return. Ecology of Freshwater Fish 24:264–275.

Bisson, P. A., K. Sullivan, and J. L. Nielsen. 1988. Channel hydraulics, habitat use, and body form of juvenile coho salmon, steelhead, and cutthroat trout in streams. Transactions of the American Fisheries Society 117:262–273.

Bjornn, T. C. 1969. Embryo survival and emergence studies. Salmon and steelhead investigations. Job Completion Report, Project F-49-R-7, Idaho Fish and Game Department, Boise, ID.

Booth, D. B., K. Bell, and K. X. Whipple. 1991. Sediment Transport Along the South Fork and Mainstem of the Snoqualmie River. King County Surface Water Management Division, Seattle, WA.

Brandes, P. L., and J. S. McLain. 2000. Juvenile Chinook Salmon Abundance, Distribution, and Survival in the Sacramento-San Joaquin Estuary. Fish Bulletin 179, Volume 2, California Department of Fish and Game, Sacramento, CA.

Campbell, L. A., and A. M. Claiborne. 2017. Salish Sea Marine Survival Project (4): Successful juvenile life History Strategies in Returning Adult Chinook from Five Puget Sound Populations (4.1). Annual Report:44.

Chamberlin, J. W., W. T. Zackey, and O. Stefankiv. 2022. Estimating Rearing Capacity for Juvenile Chinook Salmon in Tidal Deltas: Implications for Recovery Planning in the Snohomish Delta. National Marine Fisheries Service, Seattle, WA.

Collins, B. D., and D. R. Montgomery. 2011. The legacy of Pleistocene glaciation and the organization of lowland alluvial process domains in the Puget Sound region. Geomorphology 126:174–185.

Collins, B. D., and A. J. Sheikh. 2003. Historical aquatic habitat in river valleys and estuaries of the Nooksack, Skagit, Stillaguamish, and Snohomish watersheds. Department of Earth and Space Sciences, University of Washington, Seattle, WA.

Dittbrenner, B. J., M. M. Pollock, J. W. Schilling, J. D. Olden, J. J. Lawler, and C. E. Torgersen. 2018. Modeling intrinsic potential for beaver (Castor canadensis) habitat to inform restoration and climate change adaptation. PLOS ONE 13:e0192538.

Feist, B. E., E. R. Buhle, P. Arnold, J. W. Davis, and N. L. Scholz. 2011. Landscape Ecotoxicology of Coho Salmon Spawner Mortality in Urban Streams. PLOS ONE 6:e23424.

Feist, B. E., E. R. Buhle, D. H. Baldwin, J. A. Spromberg, S. E. Damm, J. W. Davis, and N. L. Scholz. 2017. Roads to ruin: conservation threats to a sentinel species across an urban gradient. Ecological Applications 27:2382–2396.

Fogel, C. B., C. L. Nicol, J. C. Jorgensen, T. J. Beechie, B. Timpane-Padgham, P. Kiffney, G. Seixas, and J. Winkowski. 2022. How riparian and floodplain restoration modify the effects of increasing temperature on adult salmon spawner abundance in the Chehalis River, WA. PLOS ONE 17:e0268813.

Gablonsky, J. M., and C. T. Kelley. 2001. A Locally-Biased form of the DIRECT Algorithm. Journal of Global Optimization 21:27–37.

Gallagher, S. P., and C. M. Gallagher. 2005. Discrimination of Chinook Salmon, Coho Salmon, and Steelhead Redds and Evaluation of the Use of Redd Data for Estimating Escapement in Several Unregulated Streams in Northern California. North American Journal of Fisheries Management 25:284–300.

Grantham, T. E., D. A. Newburn, M. A. McCarthy, and A. M. Merenlender. 2012. The Role of Streamflow and Land Use in Limiting Oversummer Survival of Juvenile Steelhead in California Streams. Transactions of the American Fisheries Society 141:585–598.

Greene, C., E. Beamer, J. Chamberlin, G. Hood, M. Davis, K. Larsen, J. Anderson, R. Henderson, J. Hall, M. Pouley, T. Zackey, S. Hodgson, C. Ellings, and I. Woo. 2021. Landscape, density-dependent, and bioenergetic influences upon Chinook salmon in tidal delta habitats: Comparison of four Puget Sound estuaries. Page 165. ESRP Report 13-1508.

Greene, C. M., and T. J. Beechie. 2004. Consequences of potential density-dependent mechanisms on recovery of ocean-type Chinook salmon (Oncorhynchus tshawytscha). Canadian Journal of Fisheries and Aquatic Sciences 61:590–602.

Harvey, B. C., J. L. White, and R. J. Nakamoto. 2005. Habitat-specific biomass, survival, and growth of rainbow trout (Oncorhynchus mykiss) during summer in a small coastal stream. Canadian Journal of Fisheries and Aquatic Sciences 62:650–658.

Hood, W. G. 2015. Geographic variation in Puget Sound tidal channel planform geometry. Geomorphology 230:98–108.

Isaak, D. J., S. J. Wenger, E. E. Peterson, J. M. V. Hoef, D. E. Nagel, C. H. Luce, S. W. Hostetler, J. B. Dunham, B. B. Roper, S. P. Wollrab, G. L. Chandler, D. L. Horan, and S. Parkes-Payne. 2017. The NorWeST summer stream temperature model and scenarios for the Western U.S.: a crowd-sourced database and new geospatial tools foster a user community and predict broad climate warming of rivers and streams. Water Resources Research 53:9181–9205.

Jensen, D. W., E. A. Steel, A. H. Fullerton, and G. R. Pess. 2009. Impact of fine sediment on egg-to-fry survival of Pacific salmon: a meta-analysis of published studies. Reviews in Fisheries Science 17:348–359.

Johnson, S. G. 2022, July 19. stevengj/nlopt. C.

Johnson, S., J. D. Rodgers, and M. Solazzi. 1993. Development and evaluation of techniques to rehabilitate Oregon's wild salmonids. Fish Research Project F-125-R-5, Annual Progress Report, Oregon Department of Fish and Wildlife, Portland, OR.

Jorgensen, J. C., C. Nicol, C. Fogel, and T. J. Beechie. 2021. Identifying the potential of anadromous salmonid habitat restoration with life cycle models. PLOS ONE 16:e0256792.
Kareiva, P., M. Marvier, and M. McClure. 2000. Recovery and management options for spring/summer Chinook salmon in the Columbia River basin. Science 290:977–979.
Koski, K. V. 2009. The fate of coho salmon nomads: the story of an estuarine-rearing strategy promoting resilience. Ecology and Society 14.
Martens, K. D., and P. J. Connolly. 2014. Juvenile Anadromous Salmonid Production in Upper Columbia River Side Channels with Different Levels of Hydrological Connection. Transactions of the American Fisheries Society 143:757–767.
McHugh, P. A., W. C. Saunders, N. Bouwes, C. E. Wall, S. Bangen, J. M. Wheaton, M. Nahorniak, J. R. Ruzycki, I. A. Tattam, and C. E. Jordan. 2017. Linking models across scales to assess the viability and restoration potential of a threatened population of steelhead (Oncorhynchus mykiss) in the Middle Fork John Day River, Oregon, USA. Ecological Modelling 355:24–38.
McIntyre, J. K., J. W. Davis, C. Hinman, K. H. Macneale, B. F. Anulacion, N. L. Scholz, and J. D. Stark. 2015. Soil bioretention protects juvenile salmon and their prey from the toxic impacts of urban stormwater runoff. Chemosphere 132:213–219.
Montgomery, D. R., J. M. Buffington, R. D. Smith, K. M. Schmidt, and G. Pess. 1995. Pool spacing in forest channels. Water Resources Research 31:1097–1105.
Moussalli, E., and R. Hilborn. 1986. Optimal stock size and harvest rate in multistage life history models. Canadian Journal of Fisheries and Aquatic Sciences 43:135–141.
Nelson, L. M. 1971. Sediment Transport by Streams in the Snohomish River Basin, Washington: October 1967-June 1969. Open File Report, Washington Department of Ecology, Olympia, WA.
Nickelson, T. E. 1998. A habitat-based assessment of coho salmon production potential and spawner escapement needs for Oregon coastal streams. Page 17. Information Reports Number 98-4, Oregon Department of Fish and Wildlife, Portland, OR.
Nicol, C. L., J. C. Jorgensen, C. B. Fogel, B. Timpane-Padgham, and T. J. Beechie. 2022. Spatially overlapping salmon species have varied population response to early life history mortality from increased peak flows. Canadian Journal of Fisheries and Aquatic Sciences 79:342–351.
Ogston, L., S. Gidora, M. Foy, and J. Rosenfeld. 2015. Watershed-scale effectiveness of floodplain habitat restoration for juvenile coho salmon in the Chilliwack River, British Columbia. Canadian Journal of Fisheries and Aquatic Sciences 72:479–490.
Orcutt, D. R., B. R. Pulliam, and A. Arp. 1968. Characteristics of Steelhead Trout Redds in Idaho Streams. Transactions of the American Fisheries Society 97:42–45.
Pollock, M. M., G. R. Pess, T. J. Beechie, and D. R. Montgomery. 2004. The importance of beaver ponds to coho salmon production in the Stillaguamish River basin, Washington, USA. North American Journal of Fisheries Management 24:749–760.
Poole, G. C., S. J. O'Daniel, K. L. Jones, W. W. Woessner, E. S. Bernhardt, A. M. Helton, J. A. Stanford, B. R. Boer, and T. J. Beechie. 2008. Hydrologic spiralling: the role of multiple interactive flow paths in stream ecosystems. River Research and Applications 24:1018–1031.
Powell, M. J. D. 1994. A Direct Search Optimization Method That Models the Objective and Constraint Functions by Linear Interpolation. Pages 51–67 *in* S. Gomez and J.-P.

Hennart, editors. Advances in Optimization and Numerical Analysis. Springer Netherlands, Dordrecht.
Purser, M. D., B. Gaddis, and J. J. Rhodes. 2009. Primary Sources of Fine Sediment in the South Fork of the Stillaguamish River. Snohomish County Public Works, Surface Water Management, Everett, WA.
Purser, M. D., and W. Leif. 2013. Pilchuck Creek Low Flow Assessment and Projects (08-1617). Snohomish County Public Works Surface Water Management.
Quinn, T. P., and N. P. Peterson. 1996. The influence of habitat complexity and fish size on over-winter survival and growth of individually marked juvenile coho salmon (Oncorhynchus kisutch) in Big Beef Creek, Washington. Canadian Journal of Fisheries and Aquatic Sciences 53:1555–1564.
R2 Resource Consultants, Inc. 2008. Snohomish Basin Steelhead Trout (Oncorhynchus mykiss) "State of the Knowledge." Technical Memorandum, Redmond, WA.
Reeves, G. H., F. H. Everest, and T. E. Nickelson. 1989. Identification of Physical Habitats Limiting the Production of Coho Salmon in Western Oregon and Washington. General Technical Report PNW-GTR-245, U.S. Department of Agriculture, Forest Service, Pacific Northwest Research Station, Portland, OR.
Ricker, W. E. 1976. Review of the Rate of Growth and Mortality of Pacific Salmon in Salt Water, and Noncatch Mortality Caused by Fishing. Journal of the Fisheries Research Board of Canada 33:1483–1524.
Salo, E. O., and W. H. Bayliff. 1958. Artificial and natural production of silver salmon, Oncorhynchus kisutch, at Minter Creek, Washington 4.
Seedang, S., A. G. Fernald, R. M. Adams, and D. H. Landers. 2008. Economic analysis of water temperature reduction practices in a large river floodplain: an exploratory study of the Willamette River, Oregon. River Research and Applications 24:941–959.
Seixas, G. B., T. J. Beechie, C. Fogel, and P. M. Kiffney. 2018. Historical and future stream temperature change predicted by a lidar-based assessment of riparian condition and channel width. Journal of the American Water Resources Association 54:974–991.
Solazzi, M. F., T. E. Nickelson, S. L. Johnson, and J. D. Rodgers. 2000. Effects of increasing winter rearing habitat on abundance of salmonids in two coastal Oregon streams. Canadian Journal of Fisheries and Aquatic Sciences 57:906–914.
Spromberg, J. A., D. H. Baldwin, S. E. Damm, J. K. McIntyre, M. Huff, C. A. Sloan, B. F. Anulacion, J. W. Davis, and N. L. Scholz. 2016. Coho salmon spawner mortality in western US urban watersheds: bioinfiltration prevents lethal storm water impacts. Journal of Applied Ecology 53:398–407.
Stefankiv, O., T. J. Beechie, J. E. Hall, G. R. Pess, and B. Timpane-Padgham. 2019. Influences of valley form and land use on large river and floodplain habitats in Puget Sound. River Research and Applications 35:133–145.
Stillaguamish Tribe Natural Resources Department. 2011. The Impact of Fine Sediment Pollution on Chinook Survival to Emergence in the North Fork Stillaguamish River. Stillaguamish Tribe, Arlington, WA.
Stober, Q. J., C. R. Steward, and F. Winchell. 1983. Tolt River Fisheries and Instream Flow Analysis. University of Washington, School of Fisheries, Fisheries Research Institute.
Tian, Z., H. Zhao, K. T. Peter, M. Gonzalez, J. Wetzel, C. Wu, X. Hu, J. Prat, E. Mudrock, R. Hettinger, A. E. Cortina, R. G. Biswas, F. V. C. Kock, R. Soong, A. Jenne, B. Du, F. Hou, H.

He, R. Lundeen, A. Gilbreath, R. Sutton, N. L. Scholz, J. W. Davis, M. C. Dodd, A. Simpson, J. K. McIntyre, and E. P. Kolodziej. 2020. A ubiquitous tire rubber–derived chemical induces acute mortality in coho salmon. Science.

Zimmerman, M. S., C. Kinsel, E. Beamer, E. J. Connor, and D. E. Pflug. 2015. Abundance, survival, and life history strategies of juvenile Chinook salmon in the Skagit River, Washington. Transactions of the American Fisheries Society 144:627–641.

Appendix A. Model Spatial Structure

A.1 Subbasin Boundaries

Subbasin numbers are shown in Figure A-1 and subbasin names are in Tables A-1 and A-2. Subbasin boundaries were based on Endangered Species Act subbasins, then modified to add mainstem floodplain subbasins and remove areas without anadromous salmonids.

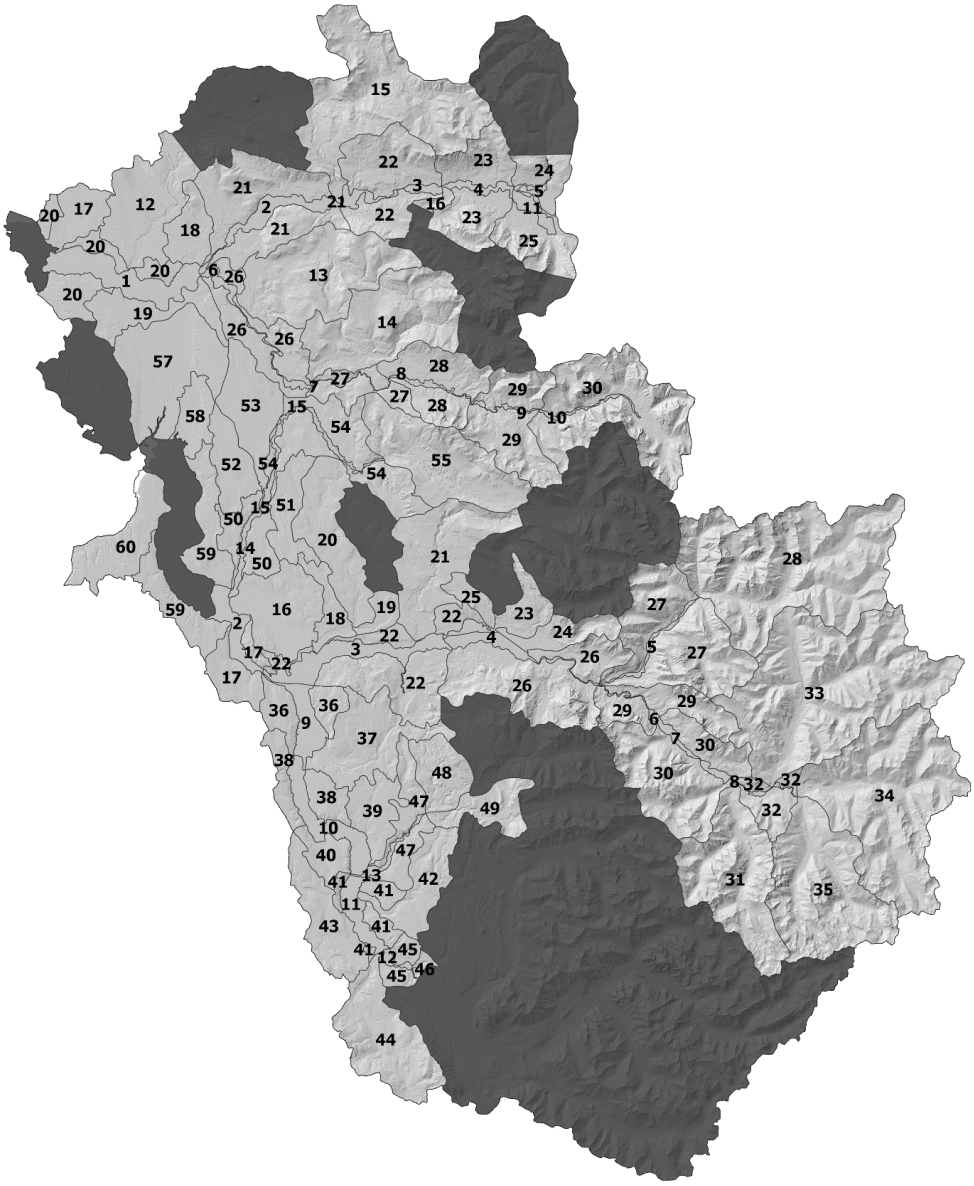

Figure A-1. Freshwater subbasin boundaries used in the HARP model analysis. Dark gray areas are subbasins without anadromous salmonids, and the Snohomish and Stillaguamish deltas. Note that each basin is numbered separately.

Table A-1. List of basin numbers and names for the Stillaguamish River basin.

Subbasin number	Subbasin Name	Location
1	Lower Mainstem Stillaguamish	Norman Rd. to confluence of NF and SF
2	Mainstem North Fork Stillaguamish 1	Confluence to Deer Creek
3	Mainstem North Fork Stillaguamish 2	Deer Creek to Boulder River
4	Mainstem North Fork Stillaguamish 3	Boulder River to Squire Creek
5	Mainstem North Fork Stillaguamish 4	Above Squire Creek
6	Mainstem South Fork Stillaguamish 1	Confluence to Canyon Creek
7	Mainstem South Fork Stillaguamish 2	Robe Canyon
8	Mainstem South Fork Stillaguamish 3	Robe Canyon to Twenty–two Creek
9	Mainstem South Fork Stillaguamish 4	Twenty–two Creek to Mallardy Creek
10	Mainstem South Fork Stillaguamish 5	Above Mallardy Creek
11	Squire Creek	Mouth to end of Squire Creek Rd.
12	Pilchuck Creek	Lower Pilchuck Creek
13	Jim Creek	Entire subbasin
14	Canyon Creek	Entire subbasin
15	Deer Creek	Entire subbasin
16	Boulder River	Confluence to NW-SE bend
17	Church Creek	
18	Harvey Armstrong Creek	
19	Upland Portage Creek	
20	Upland Lower Stillaguamish	
21	NF Stillaguamish 1 tribs	Confluence to Deer Creek
22	NF Stillaguamish 2 tribs	Deer Creek to Boulder River
23	NF Stillaguamish 3 tribs	Boulder River to Squire Creek
24	NF Stillaguamish 4 tribs	Above Squire Creek
25	Squire Creek	Upland Squire Creek
26	SF Stillaguamish 1 tribs	Confluence to Canyon Creek
27	SF Stillaguamish 2 tribs	Robe Canyon
28	SF Stillaguamish 3 tribs	Robe Canyon to Twenty–two Creek
29	SF Stillaguamish 4 tribs	Twenty–two Creek to Mallardy Creek
30	SF Stillaguamish 5 tribs	Above Mallardy Creek

Table A-2. List of basin numbers and names for the Snohomish River basin.

Subbasin number	Subbasin Name	Location
2	Mainstem Snohomish	Snohomish River from Hwy 9 to Confluence
3	Lower Mainstem Skykomish	Confluence with Snoqualmie to Sultan
4	Upper Mainstem Skykomish	Sultan to confluence of N. and S. Fork
5	Lower North Fork Skykomish	Confluence of N. and S. Fork to Silver Creek
6	Lower South Fork Skykomish	Confluence of N. and S. Fork to County Line
7	South Fork Skykomish	County Line to Miller River
8	Upper South Fork Skykomish	Miller River to Foss River
9	Snoqualmie Mouth	Skykomish River to Duvall
10	Mid-Mainstem Snoqualmie	Duvall to Tolt River
11	Upper Mainstem Snoqualmie 1	Tolt River to Raging River
12	Upper Mainstem Snoqualmie 2	Raging River to Snoqualmie Falls
13	Lower Tolt River	Snoqualmie to Confluence of NF and SF Tolt
14	Lower Pilchuck River	Snohomish River to Dubuque Creek
15	Middle Pilchuck River	Dubuque Creek to Worthy Creek
16	French Creek	
17	Upland Cathcart Drainages	
18	Lower Woods Creek	
19	Woods Creek	
20	West Fork Woods Creek	
21	Lower Sultan River	Skykomish River to end of Diversion
22	Upland Lower Mainstem Skykomish	
23	Wallace River	Skykomish River to Headwaters
24	May Creek	
25	Bear Creek	
26	Upland Upper Mainstem Skykomish	
27	Upland Lower North Fork Skykomish	
28	Upper North Fork Skykomish	Silver Creek to Headwaters
29	Upland Lower South Fork Skykomish	
30	Upland South Fork Skykomish	
31	Miller River	SF Skykomish to Headwaters
32	Upland Upper South Fork Skykomish	
33	Beckler River	SF Skykomish to Headwaters
34	Tye River	Foss River to Headwaters
35	Foss River	SF Skykomish to Headwaters
36	Upland Snoqualmie Mouth	
37	Cherry Creek	
38	Upland Mid-Mainstem Snoqualmie	
39	Harris Creek	
40	Ames Creek	
41	Upland Upper Mainstem Snoqualmie	
42	Griffin Creek	

Table A-2 (cont.). List of basin numbers and names for the Snohomish River basin.

Subbasin number	Subbasin Name	Location
43	Patterson Creek	
44	Raging River	Snoqualmie River to Headwaters
45	Upland Coal Creek Lower	
46	Tokul Creek	
47	Upland Lower Tolt River	
48	North Fork Tolt River	Confluence to Headwaters
49	South Fork Tolt River	Confluence to Dam
50	Upland Lower Pilchuck River	
51	Dubuque Creek	
52	Lake Stevens	
53	Little Pilchuck Creek	
54	Upland Middle Pilchuck River	
55	Upper Pilchuck River	Worthy Creek to Headwaters
57	Quilceda Creek	
58	Allen Creek	
59	Upland Lower Snohomish	
60	Everett Drainages	

A.2 Spawning and Rearing Ranges

Spawning and rearing distributions for each species are in Figure A-2 (coho), Figure A-3 (Chinook), Figure A-4 (winter-run steelhead), and Figure A-5 (summer-run steelhead). Species distributions were reviewed by local biologists, and all suggested changes were incorporated into the final distribution maps.

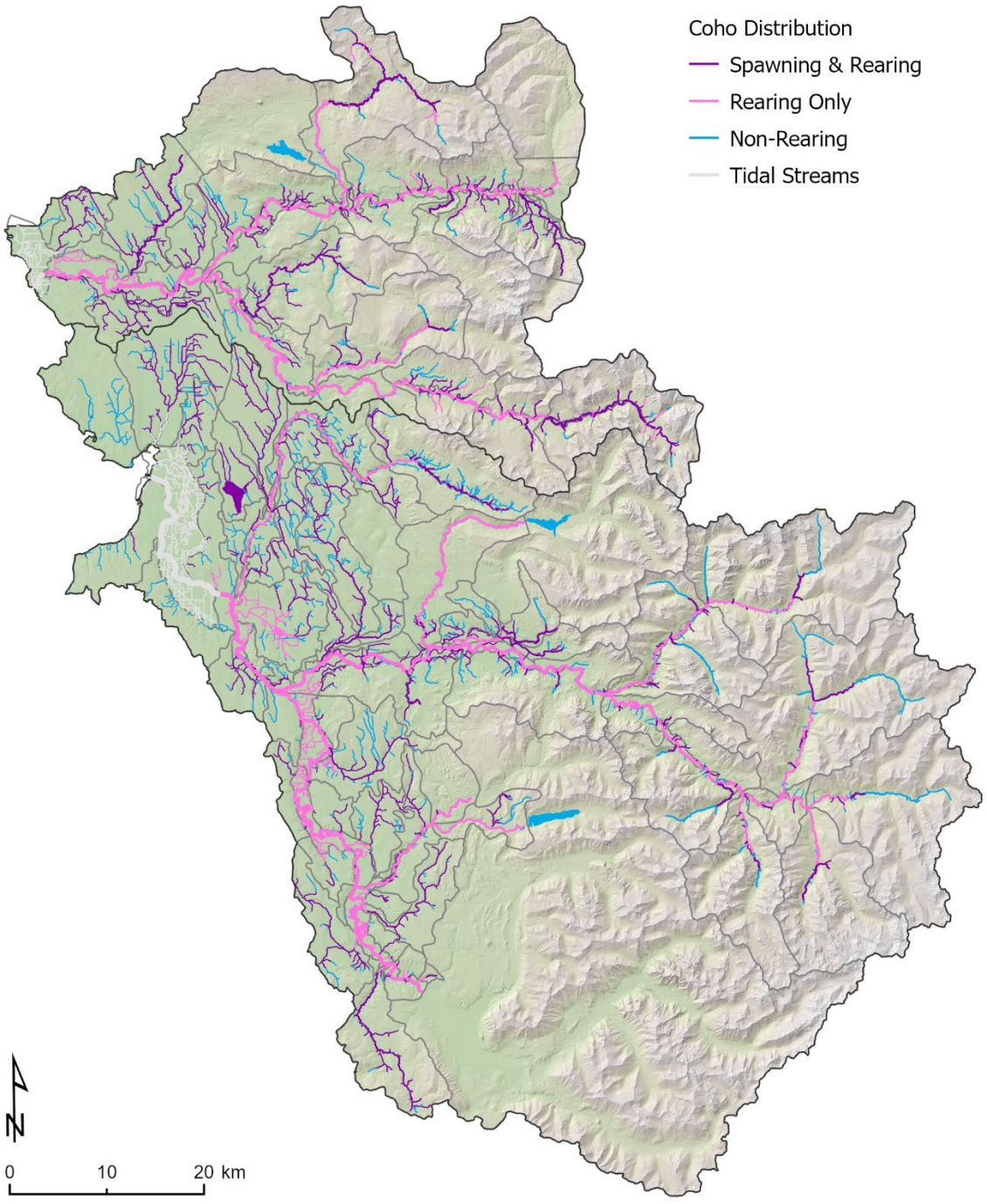

Figure A-2. Spawning and rearing distribution of coho salmon used in the HARP model analysis. Tidally-influenced streams are shown in light gray. Subbasins boundaries are shown in dark gray. The HARP model allows coho to spawn in suitable side channels in any reaches described as “Spawning & Rearing” or “Rearing Only,” but it only allows primary channel spawning in reaches described as “Spawning & Rearing.” Several large lakes are shown for reference purposes. The widths of the stream lines on the map do not represent the true widths of the streams and are not to scale with the size of the reference lakes.

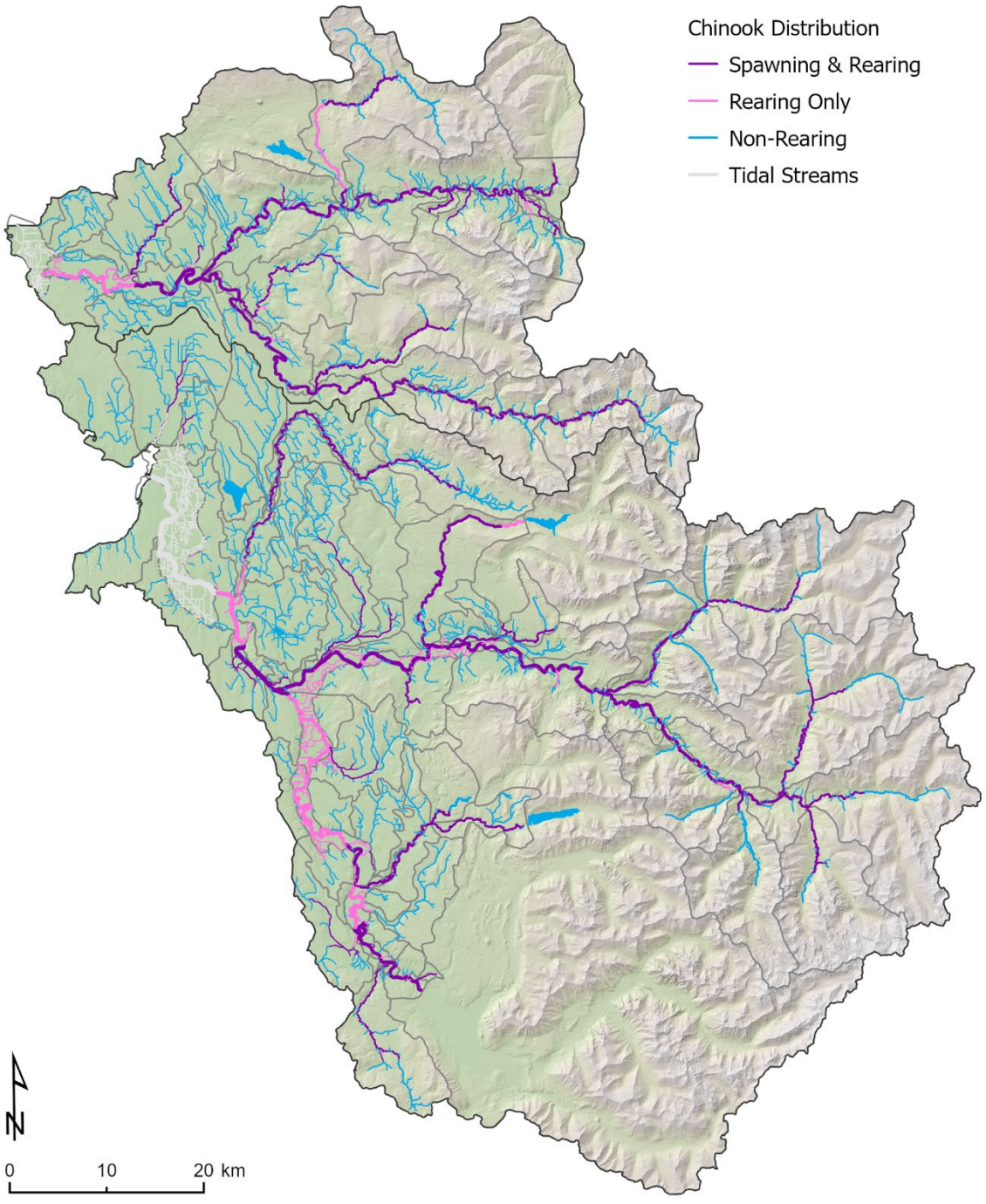

Figure A-3. Spawning and rearing distribution of Chinook salmon used in the HARP model analysis. Tidally-influenced streams are shown in light gray. Subbasins boundaries are shown in dark gray. Several large lakes are shown for reference purposes. The widths of the stream lines on the map do not represent the true widths of the streams and are not to scale with the size of the reference lakes.

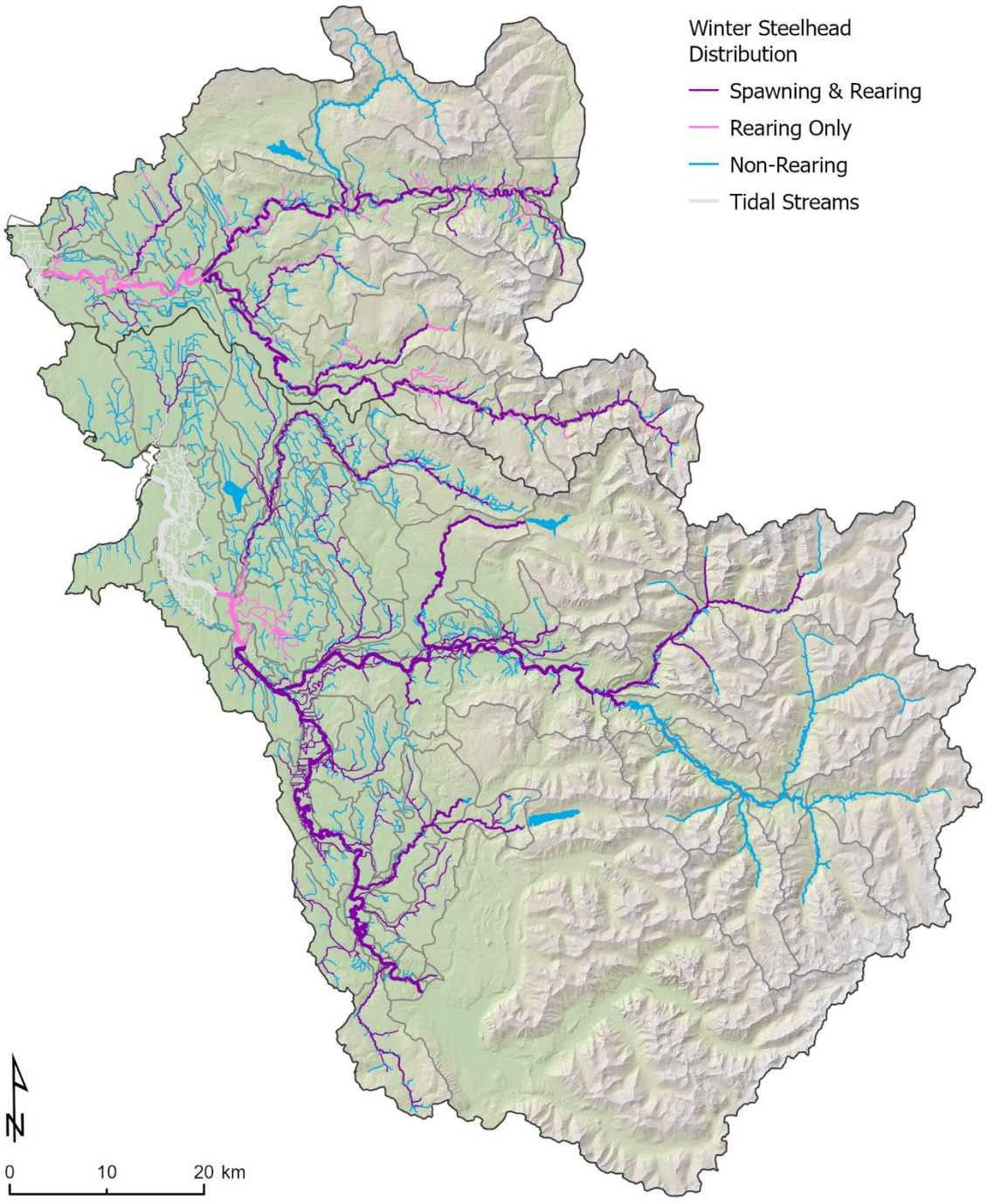

Figure A-4. Spawning and rearing distribution of winter-run steelhead used in the HARP model analysis. Tidally-influenced streams are shown in light gray. Subbasins boundaries are shown in gray. The HARP model allows winter-run steelhead to spawn in suitable side channels in any reaches described as "Spawning & Rearing" or "Rearing Only," but it only allows primary channel spawning in reaches described as "Spawning & Rearing." Several large lakes are shown for reference purposes. The widths of the stream lines on the map do not represent the true widths of the streams and are not to scale with the size of the reference lakes.

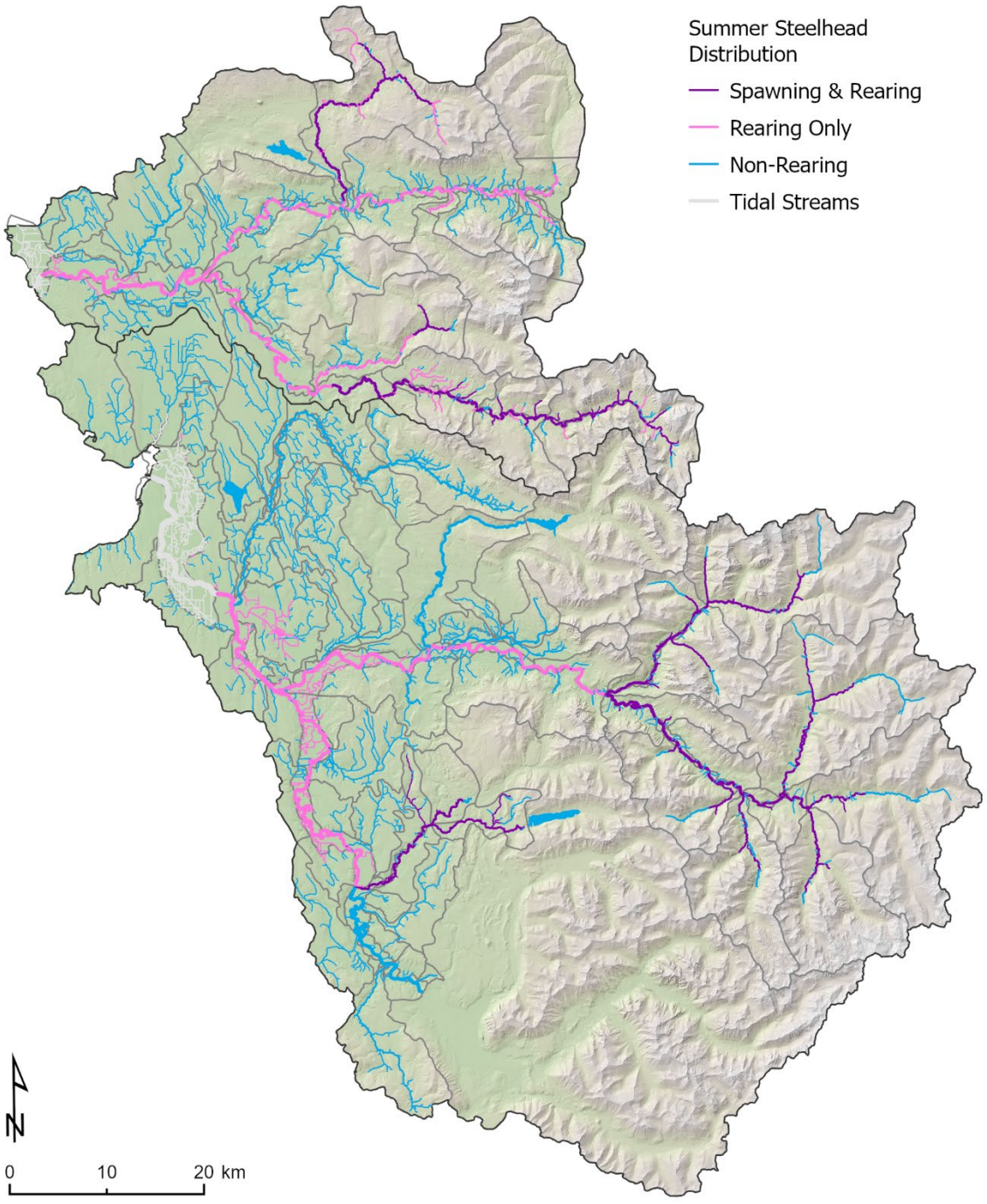

Figure A-5. Spawning and rearing distribution of summer-run steelhead used in the HARP model analysis. Tidally-influenced streams are shown in light gray. Subbasins boundaries are shown in gray. Several large lakes are shown for reference purposes. The widths of the stream lines on the map do not represent the true widths of the streams and are not to scale with the size of the reference lakes.

Appendix B. Estimating Chinook Estuary and Marine Productivity Values

Following (Greene et al. 2021), we conceptualize four main groups of subyearling Chinook salmon leaving the freshwater to the estuary and nearshore (Figure B-1):

1. **Delta-rearing parr**: Parr-sized fish that leave freshwater and rear for a time in the delta.
2. **Nearshore-rearing parr**: Parr-sized fish that leave freshwater and enter the nearshore after spending very little time in the delta.
3. **Delta-rearing fry**: Fry that leave freshwater and spend a substantial amount of time rearing in the delta to become parr-sized fish.
4. **Nearshore-rearing fry**: Fry that leave freshwater and enter the nearshore after spending very little time in the delta (still fry sized). One Skagit basin study indicates that less than 0.2% of nearshore rearing fry survive to be adult returns (Beamer et al. 2005).

As a simplification, we assume that the first three groups all begin their migration from the nearshore to the ocean as "parr-sized" fish and have similar, density-independent survivals from that point forward. The fourth group (nearshore-rearing fry) have very low survival and we currently assume it is zero.

B.1 Filling the Delta

We have estimates of the total number of fry- and parr- sized outmigrants from each freshwater system via smolt trap data. We also have instantaneous density measurements of fish in the delta and nearshore (Greene et al. 2021, Chamberlin et al. 2022). However, we do not know the total number of fish from each size class using the delta each year.

Given a delta capacity, and delta productivity, we could model annual delta use with a Beverton-Holt equation:

$$N_{s,delta} = \frac{N_{s,river} * p}{1 + \frac{N_{s,river} * p}{c_s}} \quad (1)$$

where $N_{s,delta}$ is the number of fish of size class s able to survive in the delta, $N_{s,river}$ is the annual number of freshwater outmigrant fish of a given size class, p is the density-independent survival within the delta, and c_s is the total annual capacity for fish in that size class. When c_s is very large, relative to $N_{s,river}$ (that is, when delta capacity, is very high compared to the number of fish passing the smolt trap), the number of fish in the delta approaches $N_{s,river}\cdot p$. When c_s is very small, relative to $N_{s,river}$, the number of fish in the delta approaches c_s. For the HARP model, we assumed that for each size class, the number of fish that would be supported by the delta ($N_{s,delta}$) rear in the delta, and the rest of the fish in that size class ($N_{s,river}$ - $N_{s,delta}$) migrate out to the nearshore and rear there.

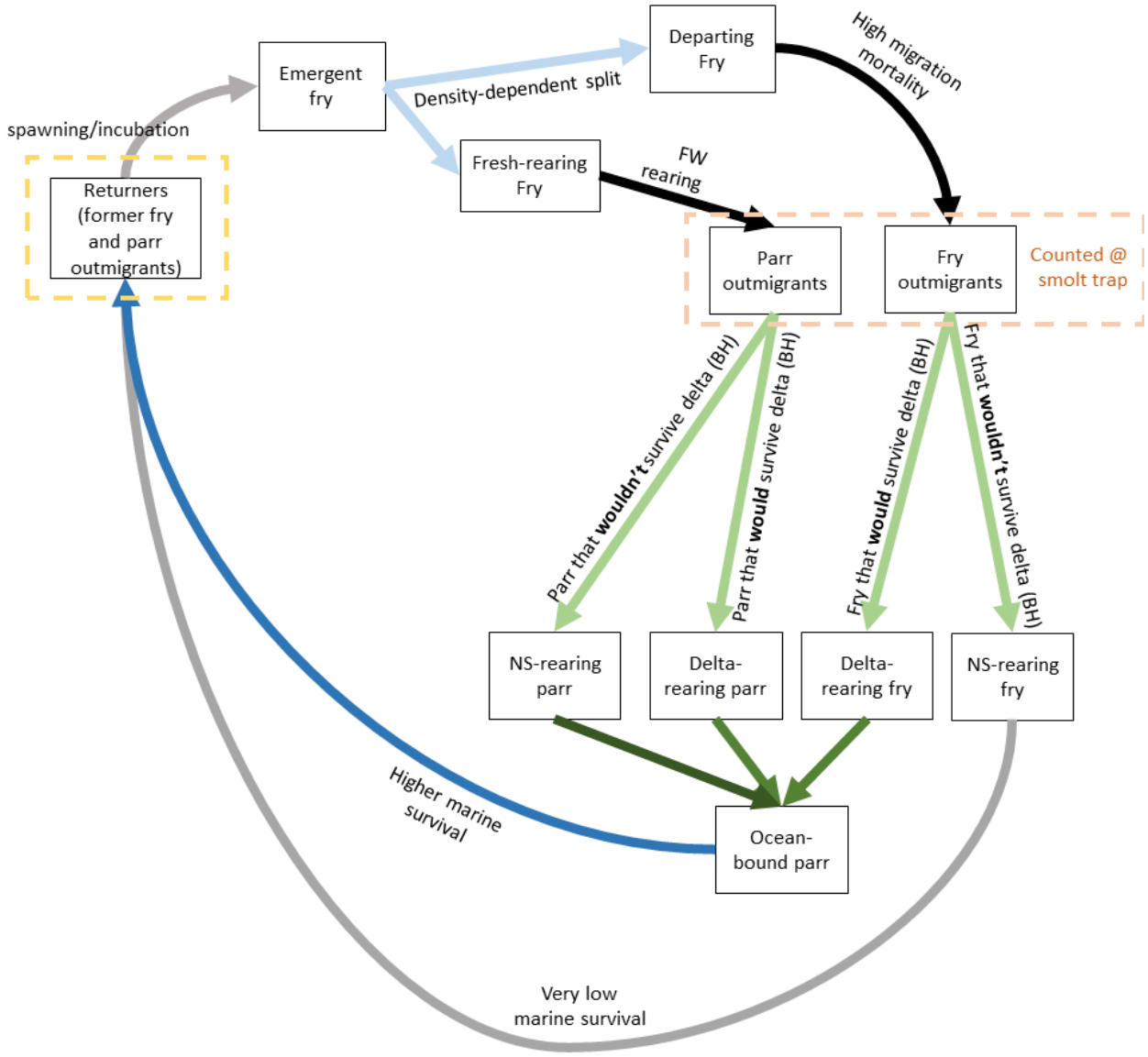

Figure B-1. Conceptual diagram of Chinook salmon fry and parr outmigrant life history types and data sources (yellow and orange dashed boxes).

B.2 Nearshore and Marine Survival Estimates

We expect that overall survival from outmigration to adult return (the ratio of the yellow box to the orange box in Figure B.1) to vary between fry and parr outmigrants. From otolith data (Campbell and Claiborne 2017), we know that 36% of returning Skagit basin fish in

2015 had fry-outmigrant type life history strategies, or alternately the ratio of surviving fry-outmigrants to surviving parr-outmigrants was 36/64. Using age-structure-weighted Skagit outmigrant data, we estimated that the cohort contributing to the 2015 return had a ratio of approximately 5.2/1 outmigrating fry to outmigrating parr passing the Skagit smolt trap. This suggests a survival ratio (fry survival/parr survival) of 0.108.

The following equations describe survival ratios (S), where N_s is the number of freshwater outmigrant fish of a given size class and R_s is the number of returning adults that left freshwater at a given size class.

$$S_{parr} = \frac{R_{parr}}{N_{parr}} \quad (2)$$

$$S_{fry} = \frac{R_{fry}}{N_{fry}} \quad (3)$$

We do not have individual estimates of S_{parr} or S_{fry}, but we have values corresponding to the overall survival and the ratio between them:

$$S_{total} = \frac{R_{parr} + R_{fry}}{N_{parr} + N_{fry}} \quad (4)$$

$$S_{ratio} = \frac{S_{fry}}{S_{parr}} \quad (5)$$

Using these pieces of information, we solved for delta survival and post-delta survival in Skagit, then transferred the estimates to other basins.

B.3 Post-delta Fry Survival

We expect there to be a density-independent survival associated with passage through the nearshore, Puget Sound, and the ocean for both fry (m_{fry}) and parr (m_{parr}) (dark blue and gray arrows in Figure B-1).

We modeled fry occupancy in the estuary and post-delta survival, so that the resulting overall parr survival is density independent and equal to m_{parr}:

$$S_{parr} = \frac{R_{parr}}{N_{parr}} = \frac{N_{parr} * m_{parr}}{N_{parr}} = m_{parr} \quad (6)$$

Fry are more complicated since they have two different post-delta survivals, depending on whether they rear in the delta or nearshore:

$$DeltaRearing\ fry = \frac{N_{fry} * p}{1 + \frac{N_{fry} * p}{c}} \tag{7}$$

$$NearshoreRearing\ fry = N_{fry} - \frac{N_{fry} * p}{1 + \frac{N_{fry} * p}{c}} \tag{8}$$

We can express the total number of the returners using these equations:

$$R_{fry} = \left(N_{fry} - \frac{N_{fry} * p}{1 + \frac{N_{fry} * p}{c}} \right) m_{fry} + \left(\frac{N_{fry} * p}{1 + \frac{N_{fry} * p}{c}} \right) m_{parr}$$

If we assume m_{fry} is very close to 0, we can simplify this equation by removing the first term.

$$R_{fry} = \left(\frac{N_{fry} * p}{1 + \frac{N_{fry} * p}{c}} \right) m_{parr} \tag{9}$$

We can then calculate overall fry survival using this this term in the numerator:

$$S_{fry} = \frac{\left(\frac{N_{fry} * p}{1 + \frac{N_{fry} * p}{c}} \right) m_{parr}}{N_{fry}} \tag{10}$$

Which simplifies to:

$$S_{fry} = \frac{m_{parr} * p}{1 + \frac{N_{fry} * p}{c}} \tag{11}$$

We can insert this expression into equation 5:

$$S_{ratio} = \frac{\frac{m_{parr} * p}{1 + \frac{N_{fry} * p}{c}}}{m_{parr}} \tag{12}$$

$$S_{ratio} = \frac{p}{1 + \frac{N_{fry} * p}{c}} \tag{13}$$

B.4 Delta Rearing Productivity

Estimates for survival of fry and parr outmigrants through estuaries vary greatly and are subject to a number of sources of uncertainty. Previous estimates range from 0.017 in the Columbia River basin (Kareiva et al. 2000) to 0.62 in the Skagit River basin (Greene and Beechie 2004). Estimated fry (<70 mm) survivals through the Sacramento-San Joaquin delta ranged from 0.10 to 0.51 among years for fry released below Red Bluff Diversion Dam and 0.03 to 0.33 among years for fry released in various delta locations (Brandes and McLain 2000). Median values were 0.29 (n=7) and 0. 19 (n = 5), respectively. Some lower estimates (e.g., 0.017 in the Columbia) are combined estuary and nearshore productivities, whereas higher estimates (e.g., 0.62 in the Skagit) have separate estuary and nearshore estimates. Estimates from the Sacramento-San Joaquin are measured estimates, and therefore are density-dependent survival estimates. Fish sizes also differ within and among studies, and larger fish tend to have higher survival.

For the HARP Model, we rearranged the equation above to get productivity (p) as function of capacity (c) and the survival ratio:

$$p = \frac{c}{-N_{fry} + c * S_{ratio}{}^{-1}}$$

In the Skagit River basin, using mean fry outmigrant numbers from 2010-2020 the equation is:

$$p = \frac{c}{-2{,}451{,}815 + c * 0.108^{-1}}$$

We had four widely ranging estimates of delta capacity (Table B-1), which produced estimates of estuary p ranging from 0.11 to 0.49. This is within the broad range of values we found in the literature (0.03 to 0.62). For this model we chose to use a mid- to upper-range value of p = 0.35 for the Chinook fry and parr migrant estuary rearing life stage, which is weighted toward the Skagit River estimate because the life stages modeled and fish sizes are more similar to the HARP Model for the Stillaguamish and Snohomish River basins.

Table B-1. Summary of estuary capacity and productivity estimates for the Skagit river basin.

Capacity estimate (fry/year)	Source	Productivity estimate
2.2×10^{6}	Tidal delta rearing capacity (Beamer et al. 2005)	0.12
6.4×10^{6}	Instantaneous 95th percentile capacity × ~140 days of fry dominance (Greene et al. 2021)/ ~35 day residence time (Chamberlin et al. 2022)	0.11
3.4×10^{5}	Instantaneous Beverton-Holt capacity × ~140 days of fry dominance (Greene et al. 2021)/ ~35 day residence time (Chamberlin et al. 2022)	0.49
6.6×10^{5}	Annual Snohomish capacity × the ratio of instantaneous capacities between the Skagit and Snohomish (1.6 × 10^6/7.4 × 10^5) (Greene et al. 2021, Chamberlin et al. 2022)	0.18

Appendix C. Calibration of Movement and Survival Parameters to Age Structure Data

The steelhead and Chinook lifecycle models contain several parameters for which we do not have literature values and that cannot be derived from a system of linear equations. We used a nonlinear optimization method to estimate the value of these parameters so that the model would produce known (target) values for certain life stages or ratios between life stages. During model development, we recalibrated the model after any major change to the habitat model inputs, habitat model mechanics, or lifecycle model mechanics.

For the Chinook model, there were three unknown parameters and three target life-stage values (Table C-1). For the steelhead model, there were six unknown parameters and eight life-stage target values (Table C-2). For each species and basin, we created a custom objective function calculating the root mean square difference between the modeled target life-stage values and the observed target life stage values in the deterministic model under current habitat conditions. We then minimized each objective function for each basin using the locally biased dividing rectangles algorithm, “NLOPT_GN_DIRECT_L” (Gablonsky and Kelley 2001) followed by the constrained optimization by linear approximations "NLOPT_LN_COBYLA" algorithm (Powell 1994) via the “nloptr” package in R, an interface to Nlopt (Johnson 2022). We provided a best-guess starting value for each parameter and allowed them to range between 0 and 1. In the interest of time, we allowed each algorithm to run for 2,000 iterations. The outputs of the algorithm were the “best estimate” of values for the three unknown Chinook parameters and the six unknown steelhead parameters.

Table C-1. Unknown parameters and known parameter target values for the Chinook salmon life-cycle model.

Parameter or Target Value	Description
Unknown Parameter	
Outmigrant survival	The survival rate of fry migrants traveling between their natal basins and the delta
Percent outmigrating parr	The percent of parr-sized fish that smolt after 12 weeks rather than remaining in the freshwater to become yearlings
Parr survival in Puget Sound	The survival rate of parr-sized fish in the Puget Sound (between estuary and the ocean)
Known Parameter Target Value	
Ratio of fry to parr outmigrants	The ratio of fry-sized fish to parr-sized fish passing the smolt trap on the way to the estuary
Ratio of sub-yearling-origin spawners to yearling-origin spawners	The ratio of spawners that had outmigrated as subyearling-aged fish to spawners that had outmigrated as yearling-aged fish
Subyearling Smolt-to-Adult-Return rate (SAR)	SAR calculated as the ratio between the total age 0.1 ocean fish and total number of outmigrants at the trap

Table C-2. Unknown parameters and known parameter target values for the steelhead life-cycle model.

Parameter or Target Value	Description
Unknown Parameter	
Percent of winter-run age-1 juveniles that smolt	Percent of total age-1 juvenile winter-run steelhead that smolt each year rather than remaining in the river
Percent of winter-run age-2 juveniles that smolt	Percent of total age-2 juvenile winter-run steelhead that smolt each year rather than remaining in the river
Winter-run survival in estuary and Puget Sound	The survival rate of winter-run steelhead in the Puget Sound (between freshwater and the ocean)
Percent of summer-run age-1 juveniles that smolt	Percent of total age-1 juvenile summer-run steelhead that smolt each year rather than remaining in the river
Percent of summer-run age-2 juveniles that smolt	Percent of total age-2 juvenile summer-run steelhead that smolt each year rather than remaining in the river
Summer-run survival in estuary and Puget Sound	The survival rate of summer-run steelhead in the Puget Sound (between freshwater and the ocean)
Known Parameter Target Value	
Parameters 1-3. Percent age-1, 2, and 3 winter-run smolt survivors	Percent of adult winter-run returners that had outmigrated as age-1, age-2, and age-3 smolts, respectively
Parameters 4-6. Percent age-1, 2, and 3 summer-run smolt survivors	Percent of adult summer-run returners that had outmigrated as age-1, age-2, and age-3 smolts, respectively
Parameters 7-8. Winter- and summer-run Smolt-to-Adult-Return rates (SAR)	SARs of winter-run and summer-run steelhead, calculated as the ratio between the total return and total number of outmigrants for each run

Appendix D. Smolt-to-Adult Return Estimates

In the Habitat Assessment and Restoration Planning (HARP) Model we use empirical estimates of Smolt-to-Adult Return SAR and fixed ocean year survivals to back calculate estuary and nearshore survival for each species and life history type. Data for SAR for each species were obtained from the co-managers in an Excel spreadsheet, with data summaries conducted by NOAA (Updated SARs 2.xls). Final selected SAR values are shown in Table D-1, and the following sections lay out the data and logic for SAR selection for each species.

Table D-1. Final selected Smolt-to-Adult Return (SAR) values for each species and life history type in each basin.

	Smolt-to-Adult Return	
Species/life history type	**Stillaguamish**	**Snohomish**
Chinook subyearling	1.2%	1.1%
Chinook yearling	2.6%	2.6%
Summer-run steelhead	1.6%	1.6%
Winter-run steelhead	1.6%	1.6%
Coho	4.1%	4.1%

Coho Salmon

For coho salmon there were five data sets, but only three with long records (Skykomish hatchery, Tulalip Bay hatchery, and Baker wild), and only two had complete data in the last 10 years. The Skykomish wild coho data were only available for the period 1978-1986 when SARs were generally higher than in recent years (Figure D-1), so we did not consider those data. Of the three hatchery data sets, the Stillaguamish hatchery only had three years of data and SARs were extremely low, we also omitted that data set. For the most recent 10-yer period (2009-2018), the Skykomish hatchery had 10 years of data and a mean SAR of 3.6%. Baker wild had 10 years of data and a mean SAR of 4.1%, whereas the Tulalip Bay hatchery had only 5 years of data and a mean SAR of 3.0% (Table D-2). **Based on the recommendation of Joe Anderson of WDFW, we used the estimate of 4.1% SAR from the Baker River wild population for both basins because it is (1) probably more precise, being a coded wire tag estimate, and (2) it is a wild population.**

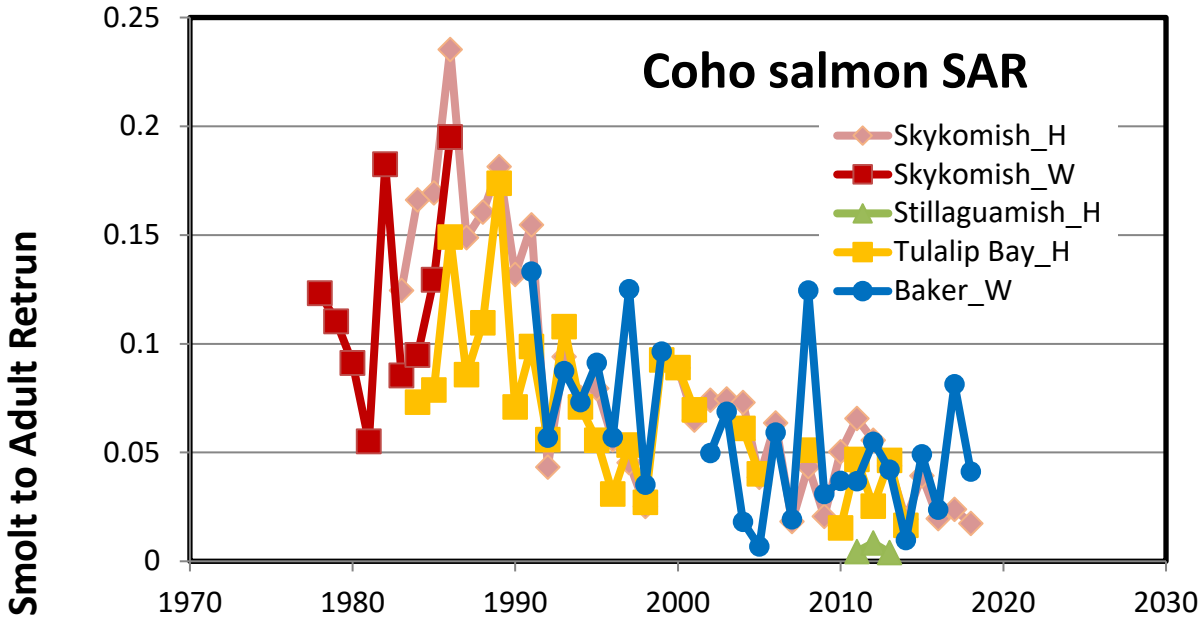

Figure D-1. SAR trends for coho salmon in the Stillaguamish River basin. Note that only the red line is for wild fish, and all others are hatchery fish. Ocean entry year is on the x-axis. "W" indicates wild population and "H" indicates hatchery population.

Table D-2. SAR metrics for coho salmon from five populations in the Skykomish Stillaguamish, and Baker River basins for all years and for the most recent 10 year period. Proposed value of 4.1% for both Snohomish and Stillaguamish coho salmon models highlighted in blue. W indicates wild population and H indicates hatchery population.

Coho salmon	**Average SAR**	
	All years	**2009-2018**
Baker River-W (1991-2018	5.8%	4.1%
Skykomish-W (1978-1986)	11.9%	ND
Skykomish-H (1983-2018)	8.0%	3.6% (n=10)
Stillaguamish-H (2011-2013)	0.6%	0.6% (n=3)
Tulalip Bay-H (1984-2014)	6.9%	3.0% (n=5)

Chinook salmon

For Chinook salmon there were six data sets, five for subyearling Chinook and one for yearling Chinook, all from hatcheries. For most populations the long-term average was similar to the average over the last 10 years. Over the last 10 years, SAR ranged from 1.0 to 1.5% over the five subyearling populations, and was 2.6% for the yearling population (Table D-3). **We used 1.1% for the Snohomish subyearlings, 1.2% for the Stillaguamish subyearlings, and 2.6% for the Snohomish yearlings (highlighted cells).**

Table D-3. SAR metrics for subyearling Chinook salmon from the Skykomish and Stillaguamish basins, as well as the Skagit River basin.

Chinook salmon	Average SAR	
	All years	Last 10 years
Subyearling		
Skykomish (2000-2013)	1.0%	1.1% (n=10)
Stillaguamish (1980-2013, 5 years missing)	1.8%	1.2% (n=10)
Skagit fall-run (1999-2008)	0.8%	1.0% (n=5)
Skagit summer-run (1994-2013)	1.2%	1.0% (n=10)
Skagit spring-run (1993-2013)	1.5%	1.5% (n=10)
Yearling		
Skagit spring-run (1981-2010, 4 years missing)	2.7%	2.6% (n=7)

Steelhead

For steelhead there was one data set each for summer-run and winter-run in each basin, and all were from hatcheries (Table D-4). Years of data ranged from ca. 1990 to 2017 (smolt outmigrant year) for all populations. SAR was substantially lower in the Stillaguamish basin than in the Snohomish basin (average SAR = 0.5% and 1.8%, respectively). **Because neither run had consistently higher survival over time than the other, we used the average of the most recent 10 years for both runs combined, which is 1.6%.**

Table D-4. SAR metrics for winter and summer steelhead from the Snohomish and Stillaguamish basins, showing average SAR over all available years and average over the most recent complete 10-year period (2008-2017, smolt outmigrant years).

Steelhead	Average SAR	
	All years	2008-2017
Stillaguamish summer-run (1991-2013)	0.5%	0.2%
Stillaguamish winter-run (1992-2013)	0.6%	0.3%
Snohomish summer-run (1993-2013)	1.9%	1.9%
Snohomish winter-run (1988-2014)	1.7%	1.3%
Snohomish summer + winter (1988-2014)	1.6%	1.6%

Appendix E. Age Structure Data

This appendix summarizes the age structure data and recommended age structure targets for the life-cycle models for each species in the Stillaguamish and Snohomish River basins. Age structure targets are used to calibrate the maturation rates (proportion of fish of each age class in the ocean that return to spawn) and proportions of juveniles that emigrate at different ages (e.g., age 1, 2, or 3 smolts for steelhead or subyearling and yearling migrants for Chinook salmon).

E.1 Stillaguamish Age Structures

The Chinook salmon data were provided by the Stillaguamish Tribe. We did not have steelhead data for the Stillaguamish River, so we used steelhead data from the Snohomish River basin.

Steelhead

Winter steelhead

For winter steelhead age structure, we used age summaries from Michaela Lowe of WDFW; data and summaries are in "Snohomish_Steelhead age_2013-2021_Lowe.xslm" (WDFW, unpublished data). Data analyzed include only first time spawners (categories: 1.1+, 2.1+, 2.2+, 2.3+, 3.1+, 3.2+, 4.1+, W1.1+, W1.2+, W2.2+).

For life history variation, ages are expressed as fw.sw, in years. That is, 1.2 indicates a 3 year old fish that spent 1 year in fresh water and 2 years in salt water. Table E-1 reflects age at first spawning for winter-run steelhead (repeat spawners not included). It is clear that most adult returns are age 2.1 and 2.2 (total age 3 and 4). Table E-2 summarizes freshwater, saltwater, and total ages separately.

Table E-1. Age at first spawning for winter-run steelhead in the Snohomish River basin.

Total first spawners	1.1	1.2	2.1	2.2	2.3	3.1	3.2
354	4%	6%	39%	38%	1%	4%	7%

Table E-2. Freshwater and saltwater age proportions in adult returns for the winter-run steelhead life-cycle model in the Snohomish River basin, and proportion of repeat spawners.

	Age (years)				
	1	2	3	4	5
Freshwater age	10%	78%	12%		
Saltwater age	45%	54%	1%		
Total age		4%	46%	42%	8%

Repeat spawners = 4.9%

Summer steelhead

There were fewer data for summer steelhead, but enough to estimate age structure as shown in Tables E-3 and E-4. Summer-run steelhead occupy Deer Creek and South Fork Stillaguamish above Granite Falls. The South Fork population overlaps winter-run steelhead, so we need to estimate the proportion of spawning steelhead that are summer-run in the South Fork.

Table E-3. Age at first spawning for winter-run steelhead in the Snohomish River basin.

Total first spawners	1.2	1.3	2.1	2.2	2.3	3.1	3.2
119	1%	1%	2%	74%	3%	1%	18%

Table E-4. Freshwater and saltwater age proportions in adult returns for summer-run steelhead in the Snohomish River basin, and proportion of repeat spawners.

	Age (years)				
	1	2	3	4	5
Freshwater age	2%	80%	18%		
Saltwater age	3%	93%	4%		
Total age			3%	76%	21%

Repeat spawners = Assume same as winters

Summer- and fall-run Chinook salmon

The Stillaguamish Tribe estimated proportions of each total age class of Chinook based on adult spawning ground data from 2007-2020, summarized here in Table E-5. Smolt Trap data records from 2001-2021 indicate that an estimated 1.3% juvenile Chinook of all sampled outmigrants were likely yearlings (>90mm length), and that 27% of outmigrating subyearling Chinook salmon are likely fry (<45mm). Subsequently, spawning ground adult scale data records from 1985-2021 indicate that an estimated 0.3% of adult Chinook of all sampled spawners were yearling outmigrants. The scale samples with 1+ freshwater ages were mostly recorded during mid 80s – late 80s, with only a few records in recent years. Based on these data, we calibrated the Stillaguamish Chinook model to include 1% of yearling outmigrants in the adult returns.

Table E-5. Proportions of freshwater age groups from smolt data and proportions of total age (CWT + Scale) groups in adult natural spawning (HOR +NOR) returns for summer- and fall-run Chinook in the Stillaguamish River basin. We assumed saltwater age equals total age because the majority of out-migrants are age 0. Percentages may not total 100% due to rounding error.

	Age (years)					
	0	**1**	**2**	**3**	**4**	**5**
Freshwater age	~99%	<1%				
Saltwater age (assumed)			8%	36%	52%	4%
Total age			8%	36%	52%	4%

Coho salmon

The Work Group recommended that we assume that all adult returns are age 3 based on understanding of Stillaguamish fall-run coho life cycle. Juveniles are all age-1 outmigrants.

E.2 Snohomish Age Structures

Data sets were provided by the Tulalip Tribes and WDFW.

Steelhead

Winter and summer steelhead have different age distributions in the model. We summarized each below.

Winter steelhead

We used age summaries from Michaela Lowe of WDFW; data and summaries are in "Snohomish_Steelhead age_2013-2021_Lowe.xslm" (WDFW, unpublished data). Data analyzed include only first time spawners (categories: 1.1+, 2.1+, 2.2+, 2.3+, 3.1+, 3.2+, 4.1+, W1.1+, W1.2+, W2.2+).

For life history variation, ages are expressed as fw.sw, in years. That is, 1.2 indicates a 3 year old fish that spent 1 year in fresh water and 2 years in salt water. Table E-6 reflects only age at first spawning for winter-run steelhead (repeat spawners not included). It is clear that most adult returns are age 2.1 and 2.2 (total age 3 and 4). Table E-7 summarizes freshwater, saltwater, and total ages separately.

Table E-6. Age at first spawning for winter-run steelhead in the Snohomish River basin.

Total first spawners	1.1	1.2	2.1	2.2	2.3	3.1	3.2
354	4%	6%	39%	38%	1%	4%	7%

Table E-7. Freshwater and saltwater age proportions in adult returns for the winter-run steelhead life-cycle model in the Snohomish River basin, and proportion of repeat spawners.

	Age (years)				
	1	2	3	4	5
Freshwater age	10%	78%	12%		
Saltwater age	45%	54%	1%		
Total age		4%	46%	42%	8%

Repeat spawners = 4.9%

Summer steelhead

There were fewer data for summer steelhead, but enough to estimate age structure as shown in Tables E-8 and E-9. Tim Beechie summarized these data from the same Excel file as above (Snohomish_Steelhead age_2013-2021_Lowe.xslm). Summer steelhead spawner locations are in NF Skykomish, SF Skykomish, and the Tolt River. All other reaches are winter-run (R2 Resource Consultants, Inc. 2008).

Table E-8. Age at first spawning for winter-run steelhead in the Snohomish River basin.

Total first spawners	1.2	1.3	2.1	2.2	2.3	3.1	3.2
119	1%	1%	2%	74%	3%	1%	18%

Table E-9. Freshwater and saltwater age proportions in adult returns for summer-run steelhead in the Snohomish River basin, and proportion of repeat spawners.

	Age (years)				
	1	2	3	4	5
Freshwater age	2%	80%	18%		
Saltwater age	3%	93%	4%		
Total age			3%	76%	21%

Repeat spawners = Assume same as winters

Summer- and fall-run Chinook salmon

We estimated Chinook age structure based on data from 2006-2020, which are in the file "Snohomish_age_structure_for_hinton_Chinook_TJB.xslx", received from Diego Holmgren, Tulalip Tribes. Note that an age 3 fingerling type has age 0.3 (0+ freshwater and 3 saltwater) and age 3 yearling type has age 1.2 (1 freshwater and 2 saltwater). Data on life-history combinations are in Tables E-10 and E-11 for the Skykomish and Snoqualmie Rivers. Additionally, smolt trap data from WDFW suggest that 62% of outmigrating subyearling Chinook salmon are <45mm in length. Tables E-12 and E-13 show the age structure data we will use to set parameters that influence percent of juveniles that leave as yearlings and proportions of each adult age in the Chinook life-cycle model.

Table E-10. Skykomish average age structure from 2006-2020. Percentages may not total 100% due to rounding.

	Age (fw.sw)						
	0.2	**0.3**	**0.4**	**0.5**	**1.2**	**1.3**	**1.4**
Percent of total run	3%	14%	54%	9%	3%	9%	7%

Table E-11. Snoqualmie average age structure from 2006-2020. Percentages may not total 100% due to rounding.

	Age (fw.sw)						
	0.2	**0.3**	**0.4**	**0.5**	**1.2**	**1.3**	**1.4**
Percent of total run	3%	18%	56%	8%	1%	7%	7%

Table E-12. Freshwater and saltwater age proportions in adult returns for summer- and fall-run Chinook in the Skykomish River basin. Percentages may not total 100% due to rounding.

	Age (years)					
	0	**1**	**2**	**3**	**4**	**5**
Freshwater age	81%	19%				
Saltwater age			6%	23%	61%	8%
Total age			3%	17%	63%	16%

Table E-13. Freshwater and saltwater age proportions in adult returns for summer- and fall-run Chinook in the Snoqualmie River basin. Percentages may not total 100% due to rounding.

	Age (years)					
	0	**1**	**2**	**3**	**4**	**5**
Freshwater age	85%	15%				
Saltwater age			4%	25%	63%	9%
Total age			3%	19%	63%	15%

Coho salmon

The Work Group recommended that we assume that all smolts are age 1, and all adult returns are age 3.

Appendix F. Escapement Estimates

We use recent escapement estimates from the co-managers only as a gage for model performance, and the model is not calibrated to observed escapements.

F.1 Stillaguamish Basin

Escapements in the Stillaguamish Basin have varied considerably from year to year, but escapements for all species have been low since about 2015 (Figure F-1). Coho salmon escapements were generally high between 2000 and 2015, but have dropped since. Steelhead abundance has declined steadily since the 1980s, while Chinook abundance has declined since the higher runs of 2000 to 2005. Median abundances over the last 10 years are slightly lower than the long term abundance for Chinook and steelhead, and slightly higher for coho (Table F-1). Maximum escapements are considerably lower over the last 10 years for steelhead.

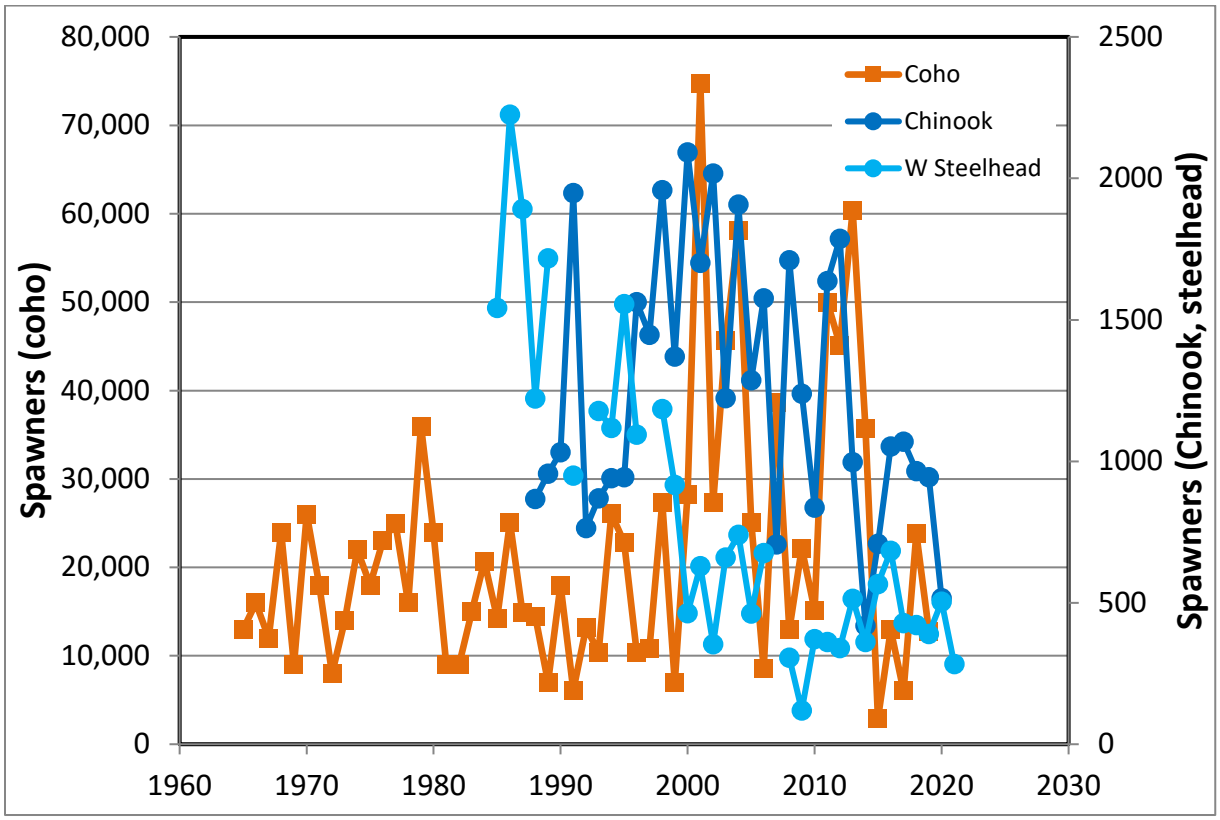

Figure F-1. Escapement trends for coho, Chinook, and winter steelhead in the Stillaguamish River basin. Coho abundance on left axis. Chinook and winter steelhead abundances on right axis. Data from WDFW. There were no data for summer steelhead (https://fortress.wa.gov/dfw/score/score/species/species.jsp). Chinook data includes both NOR and HOR spawners. Steelhead escapement is for index areas only (mainly NF Stillaguamish above Deer Creek), without expansion factor for a full–basin estimate. Harvested fish are not included in the escapement estimates.

Table F-1. Escapement metrics for three species/runs in the Stillaguamish River basin. Data from WDFW (https://fortress.wa.gov/dfw/score/score/species/species.jsp). Chinook data includes both NOR and HOR spawners. Steelhead escapement estimates are not expanded and only represent spawners within an index area in the North Fork Stillaguamish. Harvested fish are not included in the escapement estimates.

Stillaguamish River basin	**Coho**	**Chinook**	**W Steelhead**
All years			
Low	2,909	419	120
25th	12,198	941	390
Median	18,000	1,070	630
75th	25,785	1,637	1,118
High	74,773	2,092	2,226
Last 10 years			
Low	2,909	419	284
25th	12,827	864	369
Median	19,495	982	425
75th	42,808	1,066	512
High	60,387	1,787	684

F.2 Snohomish Basin

Escapements in the Snohomish Basin have varied considerably from year to year, but escapements for all species have been low since about 2010 (Figure F-2). Median abundances over the last 10 years are slightly lower than the long term abundance for Chinook (1965-2020) and coho (1965-2020) (Table F-2), but substantially lower than long-term abundance for winter steelhead (1981-2021) and summer steelhead (1985-2021).

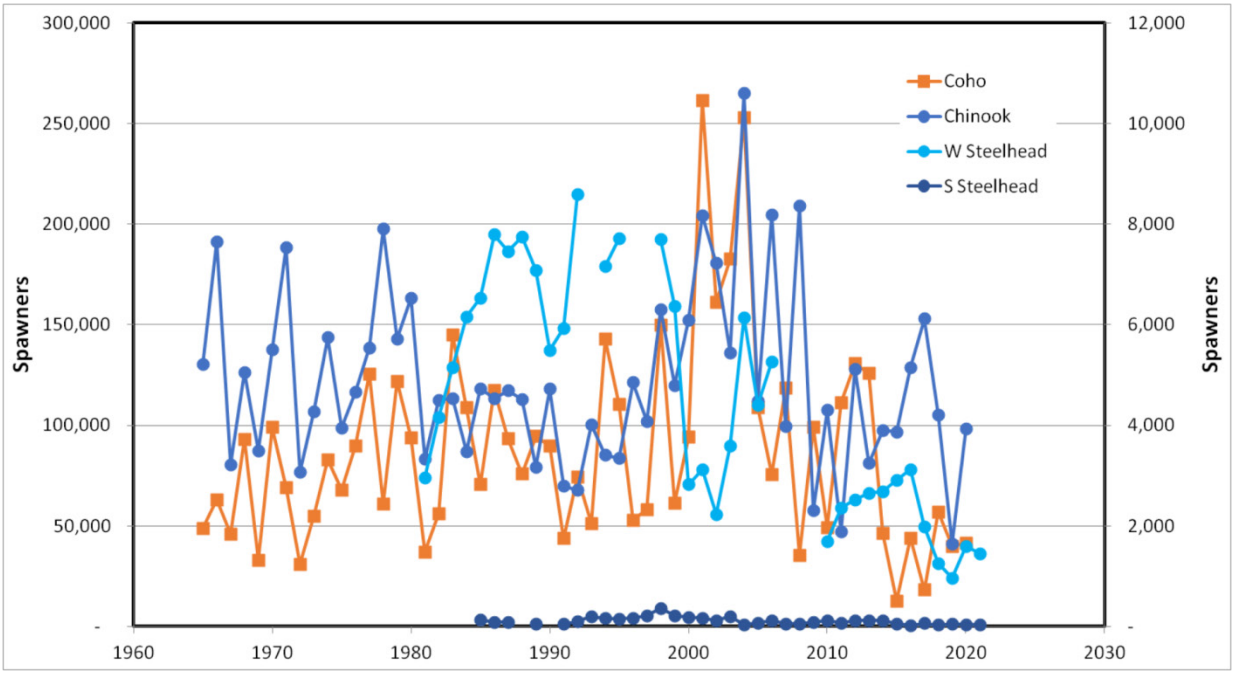

Figure F-2. Escapement trends for coho, Chinook, winter steelhead, and summer steelhead in the Snohomish River basin. Coho abundance on left axis. Chinook, winter steelhead, and summer steelhead abundances on right axis. Data from WDFW. (Snohomish_co-managers_Agreed_to_Salmon_Escapements_12-17-21). Harvested fish are not included in the escapement estimates.

Table F-2. Abundance metrics for four species/runs in the Snohomish River basin. Data from WDFW (Snohomish_co-managers_Agreed_to_Salmon_Escapements_12-17-21). Summer steelhead numbers are not expanded and represent spawners only within an index area on the South Fork Tolt River.

Snohomish River basin	Coho	Chinook	W Steelhead	S Steelhead
All years				
Low	12,804	1,642	959	16
25th Percentile	52,085	3,676	2,587	57
Median	75,739	4,536	4,160	108
75th Percentile	110,847	5,634	6,454	156
High	261,550	10,602	8,588	366
Last 10 years				
Low	12,804	1,642	959	16
25th Percentile	43,496	3,892	1,992	52
Median	45,193	3,917	2,441	60
75th Percentile	97,808	4,895	2,679	109
High	130,637	6,119	3,120	126

U.S. Secretary of Commerce
Gina M. Raimondo

Under Secretary of Commerce for
Oceans and Atmosphere
Dr. Richard W. Spinrad

Assistant Administrator for Fisheries
Janet Coit

February 2023

fisheries.noaa.gov

OFFICIAL BUSINESS

National Marine
Fisheries Service
Northwest Fisheries Science Center
2725 Montlake Boulevard East
Seattle, Washington 98112